

ADAMAS TECHNICAL REVIEW

**Vol: 2 Issue: 2
December- 2025**

Editor(s) in Chief

**Prof. Ujjwal Kumar Nyogi
Prof. Moumita Mukherjee**

ADAMAS TECHNICAL REVIEW
(ISSN: 2348-3385)

VOL 2 ISSUE 2 DECEMBER 2025

Editors in Chief:

Prof. Ujjwal Kumar Neogi,
Director, School of Smart Agriculture

Prof. Moumita Mukherjee,
Dean, Research and Development

Journal Committee for Adamas Technical Review (ISSN: 2348-3385)

Editors-in-Chief:

- **Prof. Ujjwal Kumar Neogi**, Director, School of Smart Agriculture, Adamas University
- **Prof. Moumita Mukherjee**, Dean, Research & Development, Adamas University

Managing Editor:

- Prof. Debdutta Pal, Adamas University

Associate Editors:

- **Prof. Sajal Saha**, Department of Computer Science
- **Prof. Sushanta Kumar Mandal**, Department of Electronics and Communication
- **Prof. Rudraprasad Saha**, Dean, Department of Biotechnology
- **Prof. Bharat Chandra Saha**, Dean, School of Smart Agriculture
- **Dr. Mohammad Zubair**, Department of Mechanical Engineering
- **Dr. Hasim Ali Khan**, Department of Civil Engineering

Advisory Board (National & International Experts):

- **Prof. Suranjan Das**, Vice-Chancellor, Adamas University, India
- **Prof. Radha Tamal Goswami**, Pro-Vice-Chancellor, Adamas University, India
- **Prof. Amlan Chakraborty**, Director of the A.K.Choudhury School of Information Technology at the University of Calcutta, India
- **Prof. Priyanka Raha**, Professor at Banaras University
- **Dr. Gauri Modwel**, Director, New Delhi Institute of Management
- **Dr. Deepshikha Kalra**, Dean, in the department of Management at Management Education and Research Institute, India
- **Dr. Vijayalaxmi Biradar**, Professor, Kalinga University
- **Dr. Santu Sardar**, Director DYSLQT-PUNA, DRDO
- **Dr. P. K Khosla**, Chancellor Shoolini University
- **Dr. Madhumita Chakravarty**, Head R&D, N- Space Take
- **Dr. Sadia Samar Ali**, Professor, Department of Industrial Engineering, King Abdulaziz University
- **Alison P. McGuigan**, Associate Professor, University of Toronto
- **Peter Friedl**, Professor, Department of Genitourinary
- **Joan Montero Boronat**, Senior Researcher, Institute of Bioengineering in Catalunya
- **Dr. Xuebin Yang**, Head of Tissue Engineering Research, University of Lee

Publication & Editorial Support Team:

- **Mr. Prabir Roy**, Samit Ray Publications
- **Prof. Sandip Banerjee**, Department of Smart Agriculture
- **Ms. Keya Ghosh**, Deputy Librarian, Adamas University
- **Ms. Puja Biswas**, Section Officer, R & D Cell
- **Mr. Soumyadip Dey**, Secretary, R & D Cell

INDEX

Sl No.	Title	Page No.
Research Paper		
1.	Strategy Development for the Management of Iodine Deficiency Disorders in human- an Intervention of Agriculture <i>Priyanka Raha</i>	8
2.	Biostimulation of Dormant Seeds Using Plant Growth-Promoting Rhizobia: A Path to Eco Friendly Agriculture <i>Umesh Laha, Amit Ghosh</i>	12
3.	Lowland Saffron Cultivation at Adamas Smart Green House <i>Pritwee Chakraborty, Sreoshi Kar, Arnish Das, Soham Ghosh, Archit Mondal, Sudip Barman, Suprativ Sengupta</i>	17
4.	Incorporation of Moringa powder for making value added Beverages and evaluation of nutritional properties <i>Umra Khan, Devraj Singh, Shravan Kumar, Rida Khan, Anuj Shakya, Vivek Padey</i>	21
5.	Assessment and Impact of Green Synthesized ZnO Nanoparticles against Soil Borne Fungal Pathogens, <i>Swapnila Roy</i>	26
6.	An Insight on Core-shell Morphology on the Functionality of Solid Oxide Fuel Cell <i>Madhumita Mukhopadhyay, Jayanta Mukhopadhyay</i>	39
7.	Child-Friendly Smart Glasses with Eye-Blink Monitoring and Spectacle Locator Mechanism-Aishi Mahapatra, Debdutta Pal	49
Article		
1.	A HEED-Inspired Hybrid-Score Clustering Protocol for Energy-Efficient Border Surveillance in Wireless Sensor Networks <i>Bhudeb Chakravarti^{1*}, Santanu Chatterjee²</i>	54
2.	Development of various drug delivery system for semaglutide: a wonder drug for diabetes <i>Sayan Biswas, Sonali Rudra</i>	61
3.	A Sustainable Impact of NEP 2020 on Indian Education System with Future Prospects: A Perspective of Teachers in Higher Education <i>Sarita Yadav, Deepshikha Kalra, Dalip Raina</i>	65
Review		
1.	Fork Index: A Quantitative Dermatoglyphic Marker for Human Sex Identification <i>Prerana Roy, D Piyali Das, Diptendu Chatterjee. Biswarup Dey</i>	75
2.	Comparative Evaluation of Antioxidant and Free Radical Scavenging Activities of <i>Alocasia indica</i> , <i>Colocasia esculenta</i> , and <i>Amorphophallus campanulatus</i> <i>Rameshwar Mukhopadhyay, Swagata Roy Chowdhury, Sanmitra Ghosh, Arpita Das, Rajib Majumder</i>	80
Informative		
1.	Student Research Initiative	90

Editorial



Welcome to Vol. 2, Issue 2 (July - December ,2025) of the Adamas Technical Review. This bi-annual publication showcases the forefront of technological and interdisciplinary exploration. Within these pages, our peer-reviewed journal stands as a beacon of research and innovation, offering a rich and diverse collection of research papers, insightful articles, illuminating case studies, comprehensive reviews, and promising student research contributions, each meticulously selected to reflect the dynamic landscape of modern advancements.

Adamas Technical Review serves as a vital conduit for knowledge dissemination and collaborative discourse. We provide a platform where academics, researchers, students, and industry professionals converge to share groundbreaking insights and foster a collective understanding of the challenges and opportunities that lie ahead. The contributions featured in this edition address critical issues within science, engineering, and technology, offering innovative solutions and theoretical frameworks that push the boundaries of current knowledge.

We extend our deepest gratitude to our esteemed contributors, whose dedication and intellectual rigor have enriched this issue with invaluable scholarship. Their commitment to excellence is the cornerstone of our journal's success. We also acknowledge the tireless efforts of our distinguished editorial board and meticulous reviewers, whose unwavering commitment to academic integrity ensures the highest standards of quality and rigor.

To our valued readers, we express our sincere appreciation for your continued support and engagement. Your interest fuels our pursuit of scholarly advancement and inspires us to continually strive for excellence.

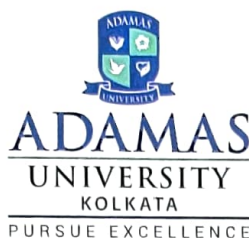
It is our earnest hope that this edition of the Adamas Technical Review will serve as a catalyst for further research, igniting meaningful discussions and fostering a spirit of intellectual curiosity. We remain steadfast in our dedication to promoting scholarly excellence and cultivating a culture of innovation as we collectively navigate the ever-expanding frontiers of knowledge.

Happy reading.

A handwritten signature in blue ink, reading "U. K. Neogi".

Dr. U. K. Neogi
Editor-in-Chief
Adamas Technical Review

Dean (Research & Development)
Office of the Dean (R & D)
Adamas University Campus
Kolkata - 700126, WB, India



Adamas Knowledge City
Barasat - Barrackpore Road,
P.O. - Jagannathpur,
North 24 Parganas,
Kolkata - 700126,
West Bengal, India

(Established by the WB Act IV of 2014, passed by the WB Legislative Assembly and Recognized by UGC & AICTE)

☎ +91 1800 419 7423 @ dean_rd@adamasuniversity.ac.in 🌐 www.adamasuniversity.ac.in



Foreword from the Editor-in-Chief

It is with great pride and anticipation that we present the latest edition of the Adamas Technical Review, the bi-annual research journal of Adamas University, Kolkata. This publication stands as a testament to our unwavering commitment to fostering a culture of inquiry, innovation, and interdisciplinary dialogue across the scientific and technological landscape.

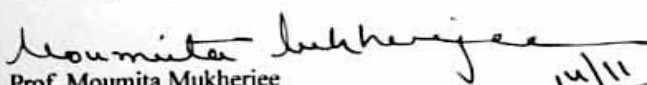
In a world increasingly driven by data, research, and rapid technological advancement, the role of academic institutions as hubs of original thought and rigorous experimentation becomes more vital than ever. Adamas Technical Review serves as a platform where scholars, researchers, and practitioners can converge to share insights, challenge conventional boundaries, and inspire new avenues of exploration.

This issue encapsulates a diverse range of contributions- from applied sciences and engineering breakthroughs to novel interdisciplinary studies- that reflect the vibrant intellectual ecosystem nurtured at Adamas University. Each article has undergone a meticulous review process, ensuring academic rigor and relevance to both academia and industry.

We are deeply grateful to our contributors for their valuable work, to our reviewers for their discerning assessments, and to the editorial board for their unwavering dedication in bringing this journal to life. Their collective efforts continue to elevate the standards of scholarship and underscore the university's mission to advance knowledge that serves both local and global communities.

As you delve into these pages, we invite you to engage with the ideas presented, question assumptions, and perhaps, find inspiration for your own research journey. May this journal be a catalyst for conversation, collaboration, and continued discovery.

Warm Regards,



Prof. Moumita Mukherjee
Professor & Dean (Research & Development)
Editor-in-Chief

Adamas Technical Review
Adamas University, Kolkata- 700126

Prof. (Dr.) Moumita Mukherjee
Professor, Department of Physics
Dean (Research and Development)
Adamas University- Kolkata- 700126
Ex Scientist - DRDO Centre, Govt. of India
Chief Investigator, DRDO Project, Govt. of India
Mail : drmmukherjee@outlook.com



RESEARCH PAPERS

Strategy Development for the Management of Iodine Deficiency Disorders in human- an Intervention of Agriculture

PRIYANKAR RAHA

*Department of Soil Science and Agricultural Chemistry, Institute of Agricultural Sciences,
Banaras Hindu University, Varanasi-221 005
Email: rahapriyankar@gmail.com*

Abstract—Essential trace elements such as iron, iodine, fluorine, copper, zinc, chromium, selenium, manganese and molybdenum are vital for maintaining health, although require in small amounts. They are called trace elements because of their body concentration, which are few milligrams per kg or less. It is also referred to as micronutrients and these trace elements are part of enzymes, hormones and cells in the body. Insufficient intake of trace minerals can cause symptoms of nutritional deficiency.

Keywords: Iodine deficiency, Agriculture, Minerals

I. INTRODUCTION

Since each trace element is related to so many enzymes, deficiency of a single trace element is often not associated with any specific clinical manifestations, but rather manifests as a combination of various symptoms. Iodine is an essential micronutrient element, occupies a prominent place in human health.

Essential trace elements such as iron, iodine, fluorine, copper, zinc, chromium, selenium, manganese and molybdenum are vital for maintaining health, although require in small amounts. They are called trace elements because of their body concentration, which are few milligrams per kg or less. It is also referred to as micronutrients and these trace elements are part of enzymes, hormones and cells in the body. Insufficient intake of trace minerals can cause symptoms of nutritional deficiency. Iodine is one of the essential elements in the Earth's crust and its estimated mean concentration varied from 0.25 mg kg⁻¹ (Fuge, 1988) and 0.3 mg kg⁻¹ (Muramatsu and Wedepohl, 1998). It is required for the synthesis of thyroid hormones, thyroxine (T₄) and triiodothyronine (T₃), which is iodinated molecules of the amino acid, tyrosine. The thyroid hormones regulate a variety of important physiological processes including the cellular oxidation. Adolescents and adults need iodine (average) in amounts of 150 µg per day (WHO, 1996). Therefore, once the human body is deficient in iodine, it can lead to physiological malfunctioning and health problems (Liao, 1992) generally regarded as Iodine Deficiency Disorders (IDD). Deficiency can lead to a broad spectrum of symptoms of which the most spectacular is goitre, well

known in humans as well as in domestic animals. There are other diseases related to iodine deficiency such as abortion, stillbirth, infant mortality, cretinism, impaired mental function and hypothyroidism. Cretinism is a serious disease related to children, who appear to be normal at birth, but become physically and mentally retarded when they are 6 months old (Pharoah, 1985). These effects are seen at all stages of development and particularly in the foetus, the neonate and the infant, i.e. during periods of rapid growth. Foetal survival and development are both sensitive to iodine deficiency. Brain development in the foetus and neonate is particularly affected and increasing in proportion to the severity of the iodine deficiency. The offsprings of mothers who are iodine deficient in early pregnancy has lower than average IQ scores (Bath and Raymen, 2015).

The human body needs 50-200 µg iodine every day as per World Health Organization recommendation for infants to adults (Hetzel, 1983), about 75-80% of which comes from foods viz., vegetables, fish and meat (Liao, 1992). The concentration of iodine in vegetables and indirectly other food materials is mainly determined by two factors; background content of iodine in soil and their biological assimilation. The background content of iodine in soil largely depends on the parent material, texture and geographic distribution in soil. The content of iodine in soil is relatively lower in interior and mountainous due to precipitation eluviations, which results in the deficiency of iodine in vegetables and the prevalence of IDD. Human population and livestock that only depend on the food grown in iodine deficient soil cannot obtain sufficient iodine for their body requirement (Hetzel, 1997). Thus,

IDD in human and animals are predominant in the areas where vegetation is poor in iodine. Oceanic deposition through atmospheric wet and dry precipitation on lands is the principal source of iodine (Goldschmidt, 1954). Thus, distribution of iodine in soils is depended on topography of land, amount and intensity of rainfall as well as wind flow and direction. Due to these facts, iodine contents are varied widely in soil, i.e. < 0.1 to 150 mg kg^{-1} (Johnson, 2003). The principal natural source of iodine is seawater (average value $58 \text{ } \mu\text{g/L}$). Iodine in rainfall in coastal areas is therefore generally higher than over continental areas and hence recharge of water to soils and aquifers will be higher generally in coastal areas. In coastal areas, sea spray is the major contributor of iodine (Englund et al., 2010) to the terrestrial environment. This correlates with the fact that goitre and related endemic disorders are often concentrated in inland areas remote from the sea, with some exception. Thus iodine content of surface soils decreases rapidly with increasing distance from sea. Since, about 98% of the human food is produced on the land, soil is a primary source of iodine, which gets into the human food chain via plants that absorb iodine from the soil and are consumed directly as vegetative material or indirectly as animal products (milk, meat, fish etc.) via animals using the vegetation as fodder. Intake of iodine from drinking water represents only a small fraction (10%) of the total intake (Decker et al., 2000). Thus human and animals severely affected with IDD where iodine content in soil and groundwater is poor. Moreover, glaciations, flooding, river changing course and deforestation, iodine present in crop grown surface soil is continuously leached.

Iodine deficiency disorders (IDD) are now significant global health problems affecting 145 countries including India. Approximately 1.9 billion people around the world have been estimated to be at risk of IDD. WHO estimates that 740 million people are currently affected only by goiter (Delange, 2002). Recent studies indicate that about 30% of world's population show iodine deficiency (White and Broadley, 2005; Abrahams, 2006). In general, regions most affected by iodine deficiency are the developing areas of Africa, South America, and Southeast Asia. Interestingly, this disorder is beginning to be detected in developed countries such as the USA, Germany, Great Britain and Australia (Kersting et al., 2001; Fields et al., 2005). In Europe, a strong contrast exists between the Scandinavian countries, where almost no goitre occurs (due to iodine additions to animal feed) versus south and east Europe, where the number of goitre cases seems to increase (Meltzer and Ghattre, 1992). Iodine deficiency is still quite common in sea-locked remote areas of sub-Saharan Africa such as the Ethiopian Highlands, mountainous zones in China, in the inter-Andine Depression in South America.

Globally, India has the largest number of children born vulnerable to iodine deficiency (Iodine Global Network, 2011). Iodine deficiency disorder constitutes a major nutrition deficiency disorder in India. In India, out of

587 districts in the country, a nation-wide goitre survey revealed that out of 283 studied districts of 29 states and 4 union territories, 235 districts have prevalence of endemic goitre (National Iodine Deficiency Disorders Control Programme, 2003). The total number of IDD suffers in India is estimated to be more than 63 million.

Iodine deficiency in soil is found in almost all part of the developed and developing world due to its irregular distribution over the earth crusts. The problem is aggravated by accelerated deforestation and soil erosion and flood plains (Goldschmidt, 1958). The regions with heavy rainfall or snowfall and frequent flooding are likely to be iodine deficient as the surface layer of soil (in which iodine is present) gets washed. Goldschmidt (1958) reported that its content generally decreased with increasing distance from sea. Its deficiency in the Indian soils is generally confined to the Himalayan mountain areas (Sharma et al., 1999) over the lower plain. In Uttar Pradesh, IDD is a serious nutritional problem. Out of 83 districts of Uttar Pradesh, 34 districts have been surveyed for IDD and 29 districts have been found to be endemic. The severe occurrence of goitre, hypothyroidism, women pre- and post pregnancy problems, mental retardation have been found in endemic in the Himalayan tarai region of Uttar Pradesh (Kapil and Singh, 2003) particularly Deoria, Kushinagar and Gorakhpur districts (Raha, 2022). Its content in the cultivated soil of Pantnagar, Bilaspur, Kaladungi and Varanasi were reported in range from $3.65\text{--}7.54$, $5.45\text{--}9.82$, $4.23\text{--}8.08$ and $1.14\text{--}2.54 \text{ mg kg}^{-1}$, respectively (Singh et al., 2002; Nath et al., 2010), whereas, $0.05\text{--}0.75 \text{ mg kg}^{-1}$ in the Himalayan tarai region (Raha, 2022) of Uttar Pradesh.

Iodine in ground water in specific geographical location is also a serious concern of IDDs, as iodine is essential to health and so, is required to be present at certain concentrations in drinking water or food. The principal sources of iodine in groundwater are aquifers, soils and the atmosphere. The range of iodine was noticed $3.5\text{--}7.5 \text{ } \mu\text{g L}^{-1}$ in the Himalayan tarai (Raha, 2022) region of Uttar Pradesh, the most sensitive IDDs prone area of India. Considering the geological condition, limestone aquifers are the most likely to have low iodine concentrations. The identified soil association (Pathak and Sharma, 1985) in the north-eastern tarai region of Uttar Pradesh is recent alluvium-calcium soils with a large reserve of soft lime (limestones). Thus, due to limestone aquifers in the tarai region of Uttar Pradesh, iodine content in ground water is poor. Iodine deficiency (i.e. goitre prevalence) has often been noted in people inhabiting limestone areas (Fuge, 1989). But, no strict regulations or recommendations are placed on iodine in drinking water in respect of IDDs. According to the studies on correlation of iodine in portable water and goitre incidence in different countries, viz. Sri Lanka (Mahadeva and Senthe Shanmuanathan, 1967), UK (McClendon and Williams, 1923), Ghana (Smedley et al., 1995), $5 \text{ } \mu\text{g L}^{-1}$ or less in drinking water should be considered as goitrogenic. In normal human diets, plant materials provide the major

source of iodine (Weng et al., 2014), particularly leafy vegetables, viz., lettuce, spinach and amaranthus. Marine fish (viz. Hilsa fish) and shellfish are the richest sources (Risher and Keith, 2009) of human dietary iodine. Edible brown sea algae (viz. *Laminaria digitata*) are also the common dietary iodine source in many countries (Yeh et al., 2014) which contains iodine up to 1.92 g kg⁻¹. In general, vegetables contain only limited dietary iodine (Dahl et al., 2004). Thus, for iodine enrichment or fortification of vegetables, potassium iodide and iodate salts (Nath et al., 2010) or iodine rich algae fertilizers (Weng et al., 2014) are added to the soils. Milk is also considered as the good source of iodine, where animals are fed iodine enriched fodder or cattle grazing iodine rich pasture. Iodization of edible salts has been recommended by World Health Organization as a means of IDD's elimination by increasing dietary iodine in the world population, particularly during cooking of vegetable (Longvah et al., 2013). But, high volatilization of iodine during cooking by heating is serious drawback of this programme. Moreover, another demerit of the random exposure of iodised salt to any geographical location is the high-iodine induced goitre, where drinking waters containing high iodine (> 150 µg L⁻¹). The combined effect of iodine in iodised salt and high iodine intake from drinking water has resulted (Li, W. et al., 2012) in high iodine induced goitre. The topography of geographical areas, iodine content in soil, water, plant and dietary habits (i.e. vegetarian or non-vegetarian) should be taken into consideration for irradiation of IDD's. In addition to exposure of iodised salt, food fortification (milk, oil etc.), vegetable fortification through soil amendment of iodine salts (KI or KIO₃) or sea algae fertilizers, inclusion of iodine rich edible brown sea algae in diet or marine fish/shell fish. High iodine uptake or high accumulation capable varieties of rice were identified in Japan (Yuita, 1994). Thus, geographical location specific programme will be successful for elimination of IDD's from the world. Edible crop fortification (Nath et al., 2018) is one of the most important strategies for this purpose after analysis of the status of iodine in soil and water of the specific geographical regions.

References

Abrahams, P. W. (2006). Soil, geography and human disease: a critical review of the importance of medical cartography. *Progress in Physical Geography*, 30: 490-512.

Bath, S. C. and Rayman, M. P. (2015). A review of the iodine status of UK pregnant women and its implications for the offspring. *Environmental Geochemistry and Health*. <http://dx.doi.org/10.1007/s10653-015-9682-3>.

Deckers, J., Laker, M., Van Herreweghe, S., Vanclooster, M., Swenner, R. and Cappuyus, V. (2000). State of art on soil-related geomedicinal issues in the world. In "Geomedical problems in Developing Countries" (Ed. J. Låg), pp. 23-42. The Norwegian Academy of Science and

Letters, Oslo.

Dahl, L., Johansson, L., Julshamn, K. and Meltzer, H. M. (2004). The iodine content of Norwegian foods and diets. *Public Health and Nutrition*, 7: 569-576.

Delange, F. (2002). Iodine deficiency in Europe. *Thyroid International Journal*, 5: 3-18.

Englund, E., Aldahan, A., Hou, X., Possnert, G. and Soderstrom, C. (2010). Iodine (I-129 and I-127) in aerosols from northern Europe. *Nucl. Instrum. Math. Phys. Res. Sect. B Beam Interact. Mater. Atoms* 268: 1139-1141.

Fields, C., Dourson, M. and Borak, J. (2005). Iodine deficient vegetarians: a hypothetical perchlorate-susceptible population. *Regulatory Toxicology and Pharmacology*, 42: 37-46.

Fuge, R. (1988). Sources of halogens in the environment, influences on human and animal health. *Environmental Geochemistry and Health*, 10: 51-61.

Fuge, R. (1989). Iodine in waters: possible links with endemic goitre. *Applied Geochemistry*, 4: 203-208.

Goldschmidt, V.M., 1954. *Geochemistry*. Oxford University Press.

Goldschmidt, V.M. (1958). *Geochemistry*. pp. 602-620. Clarendon Press, Oxford.

Hetzel, B. S. (1983). Iodine deficiency disorders (IDD) and their eradication. *The Lancet*, 322(8359): 1126-1129.

Hetzel, B.S. (1997). SOS for a billion-the nature and magnitude of iodine deficiency disorders. In SOS for a billion the conquest of iodine deficiency disorder. 2nd Edn. Eds. Hetzel, B.S. and Pandav, C.V. Oxford University Press, pp: 1-29. Iodine Network Global scorecard (2010). [accessed on July 1, 2011]. Available from: <http://www.iodinenetwork.net/documents/scorecard-2010.pdf>.

Johnson, C.C. (2003). Database of the Iodine Content of Soils Populated with Data from Published Literature. British Geological Survey, Report CR/03/004N.

Kapil, U. and Singh, P. (2003). Status of iodine content of salt and winery iodine extraction level in India. *Pakistan Journal of Nutrition*, 2 (6): 269-270

Kersting, M., Alexy, U. and Sichert-Hellert, W. (2001). Dietary intakes and food sources of minerals in 1 to 18 year old German children and adolescents. *Nutrition Research*, 21: 607-616.

Liao, Z. J. (1992). *Environmental chemistry of trace element and biochemical effect*. Beijing: Chinese Environmental Science Press, 56: 50-52.

Li, W., Dong, B., Li, P., Li, Y., (2012). Benefits and risks from the national strategy for improvement of iodine nutrition: a community-based epidemiologic survey in Chinese school children. *Nutrition*, 28: 1142-1145.

Longvah, T., Toteja, G.S., Upadhyay, A., (2013). Iodine content in bread, milk and the retention of inherent iodine in commonly used Indian recipes. *Food Chemistry*, 136: 384-388. Mahadeva, K. and Senth Shanmuganathan, S. (1967). The problem of goiter in Ceylon. *British Journal of Nutrition*, 21: 341-352.

McClendon, J. E. and Williams, A. (1923). Simple goitre as

- a result of iodine deficiency. *Journal of American Medical Association*, 80: 600-601.
- Meltzer, M. H. and Glattre, E. (1992). Geographical distribution of iodine and selenium deficiency. In "Chemical Climatology and Geomedical Problems" (Ed. J. Låg), pp. 23-31. The Norwegian Academy of Science and Letters, Oslo.
- Muramatsu, Y. and Wedepohl, K. H. (1998). The distribution of iodine in the earth's crust. *Chemical Geology*, 147: 201-216.
- Nath, T., Raha, P. and Rakshit, A. (2010). Sorption and desorption behaviour of iodine in alluvial soils of Varanasi, India. *Agricultura*, 7: 9-14.
- Nath, T., Raha, P., Singh, O. P. and Tiwari, P. (2018). Iodine fortification of vegetables. *International Journal of Current Microbiology and Applied Sciences*, SP-7: 4991-5001.
- New Delhi: DGHS, Ministry of Health & Family Welfare, Government of India; 2003. Directorate General of Health Services (DGHS). Policy guidelines on national iodine deficiency disorders control programme; pp. 1–10.
- Pathak, A. N. and Sharma, A. K. (1985). Soils of Uttar Pradesh and their management. In *Soils of India and their management* (Ed. Biswas, B. C., Yadav, D. S. and Maheshwari, S.), pp. 405-426.
- Pharoah, P.O.D. (1985). The epidemiology of endemic cretinism. In "The Endocrine System and the Environment" (Eds. B.K. Follet, S. Ishi and A. Chandola), pp. 315-355, Springer, Berlin.
- Raha, P. (2022). UGC Major Research Project, Final Report, Status of iodine in cultivated soil and drinking water of iodine deficiency disorders prevalent tarai region of Uttar Pradesh.
- Risher, J. F. and Keith, L. S. (2009). Iodine and Inorganic Iodides: Human Health Aspects. *Concise International Chemical Assessment Document 72*. World Health Organization.
- Sharma, S. K., Chelleng, P. K., Gogoi, S. and Mahanta, J. (1999). Iodine status of food and drinking water of a sub-Himalayan zone of India. *International Journal of Food Science and Nutrition*, 50: 95-98.
- Singh, J. L., Sharma, M. E., Prasad, S., Kumar, M., Gupta, G. C. and Patnaik, A. K. (2002). Prevalence of endemic goitre in goats in relation to iodine status of the soil, water and fodder. *Indian Veterinary Journal*, 79 (7): 657-660.
- Smedley, P.L., Edwards, W.M., West, J.M., Gardner, S.J. and K.B. Pelig-Ba. (1995) Health problems related to groundwater in the Obuasi and Bolgatanga areas, Ghana. *British Geological Survey, Technical Report. WC/95/43*, pp122.
- Weng, H. X., Liu, H. P., Li, D. W., Ye, M., Pan, L. and Xia, T. H. (2014). An innovative approach for iodine supplementation using iodine-rich phytogenic food. *Environmental Geochemistry and Health*, 36: 815-828.
- White, P. J. and Broadley, M. R. (2005). Biofortifying crops with essential mineral elements. *Trends in Plant Science*, 10: 586-593.
- WHO, (1996). *Elements in Human Nutrition and Health*. World Health Organization, Geneva.
- Wu, Y., Li, X. and Hipgrave, (2012). Variable iodine intake persists in the context of universal salt iodization in China. *The Journal of Nutrition*, 142 (9): 1728-1734.
- Yeh, T. S., Hung, N. H. and Lin, T. C. (2014). Analysis of iodine content in seaweed by GCECD and estimation of iodine intake. *Journal of Food and Drug Analysis*, 22: 189-196.
- Yuita, K. (1994). Overview and dynamics of iodine and bromine in the environment. 2. Iodine and bromine toxicity and environmental hazards. *Japan Agricultural Research Quarterly*, 28 (2): 100-111.



Biostimulation of Dormant Seeds Using Plant Growth-Promoting Rhizobia: A Path to Eco-Friendly Agriculture

Umesh Laha

*Department of Biological Sciences School of Life Science and Biotechnology,
Adamas University Kolkata, India umesh.laha@stu.adamasuniversity.ac.in
Academy of Scientific and Innovative Research (AcSIR),
Gaziabad-201002, India jayanta_mu@cgcri.res.in, jmukhopadhyay75@gmail.com
<https://orcid.org/0000-0001-7936-5093>*

Amit Ghosh#

*Department of Biological Sciences School of Life Science and Biotechnology, Adamas
University Kolkata, India amit.ghosh1@adamasuniversity.ac.in ORCID ID: 0009-0000-1044-7533
#corresponding author*

Abstract—The survival of plants in tough environments depends heavily on seed dormancy as an essential survival mechanism. Excessive seed dormancy duration causes reduced germination rates which diminishes crop yield. Seed dormancy reduction for better seed germination and seedling development occurs through the establishment of specific rhizobial strains that promote plant growth in the soil. Biostimulation involves placing beneficial microorganisms into soil to enhance plant development through their stimulating effects. Certain rhizobial strains or rhizobial sp. like *Rhizobium leguminosarum* and *Pseudomonas fluorescens* cooperatively with *Bacillus* sp. is responsible to release certain phytohormones especially like - Indole-3-acetic acid (IAA), which helps the plant seed to break the barrier of seed dormancy and trigger the process of sprouting and germination in seeds. It contributes to an overall understanding of microbial biostimulants for sustainable crop production systems by identifying potential roles of particular rhizobial strains that promote seed dormancy alleviation.

Keywords— Biostimulation; Seed Dormancy; Plant Growth promoting Rhizobia; Bioinoculant; Bioremediation and Bioaugmentation

I. INTRODUCTION

Current interests in sustainable agriculture have focused on plant germ interactions and the contribution of rhizobacteria to plant productivity. Of the numerous microbial communities in the rhizosphere, rhizobia are famous in their beneficial effects in the growth of leguminous plants. Nevertheless, they are also promising PGPR that mediate plant growth in various manners (1). One successful strategy has been biostimulation of dormant seeds by means of microbial inoculants that promote seed germination and enhance seed vigour. Rhizobia, typically found in root nodules on legumes, have been demonstrated to promote growth in leguminous and non-leguminous plants. The application of rhizobial inoculants on dormant seeds might induce germination by modifying the hormonal status of the seed, enhancing water absorption and nutrient release (2). Rhizobia may also reduce seed-borne pathogens through competitive exclusion and antimicrobial compounds. This inhibits seed germination in

seed-supportive microenvironment. Together, these effects can activate metabolic pathways that release dormancy and initiate growth.

The objective of the present work was to explore the biostimulation of dormant seeds by PGPR along with the physiological and biochemical alterations of this relevant interaction (3). The underlying molecular mechanism of this biostimulatory effect, and PGPRs, entails complex interactions between PGPRs and seed tissues. This first physical touch is the trigger for a multitude of biochemical processes that continues to feed and foster this vibrant early seedling establishment. For example, treatments with the bacterium *Rhizobium leguminosarum* increase seedling vigor, root proliferation and vegetative growth in legumes. Application of biocontrol agents *Pseudomonas fluorescens* and *Bacillus* species increased sprouting rates and yielded more biomass of wheat, barley, and other vegetables (4). It has been found that with the application of growth induced rhizobia on to the dormant seeds can substantially

increase not only germination but also growth of seedlings. Rhizobial strains in non-leguminous seeds increases survival and successful germination it is due to its symbiotic capacity. As nitrogen fixers and hormone producers and soil nutrient increaser, rhizobial strains aid dormant seeds in breaking dormancy, leading to faster and more complete germination.

II. OVERVIEW OF SEED DORMANCY

Nature uses seed dormancy as a mechanism to prevent seed growth until environmental conditions become optimal (5). Three distinct categories exist: Innate traits which are present from birth, Induced traits that develop due to external environmental conditions, and Enforced traits which are temporary states such as those caused by water scarcity. Two primary plant hormones control this process: ABA maintains seed dormancy while GA activates growth initiation. The initiation of growth depends on genetic factors within the seed and climatic conditions which influence development. Four basic categories: primary dormancy, secondary dormancy, specific dormancy, and organic dormancy further divided, these hibernation forms are impacted by environmental cues. Primary dormancy ensures that seeds only germinate at the correct time by stopping germination even under perfect circumstances at seed maturation (6).

whose operation is not completely known. By contrast, organic quiescence is caused from interior physiological or hormonal elements within the seed that stop germination (8).

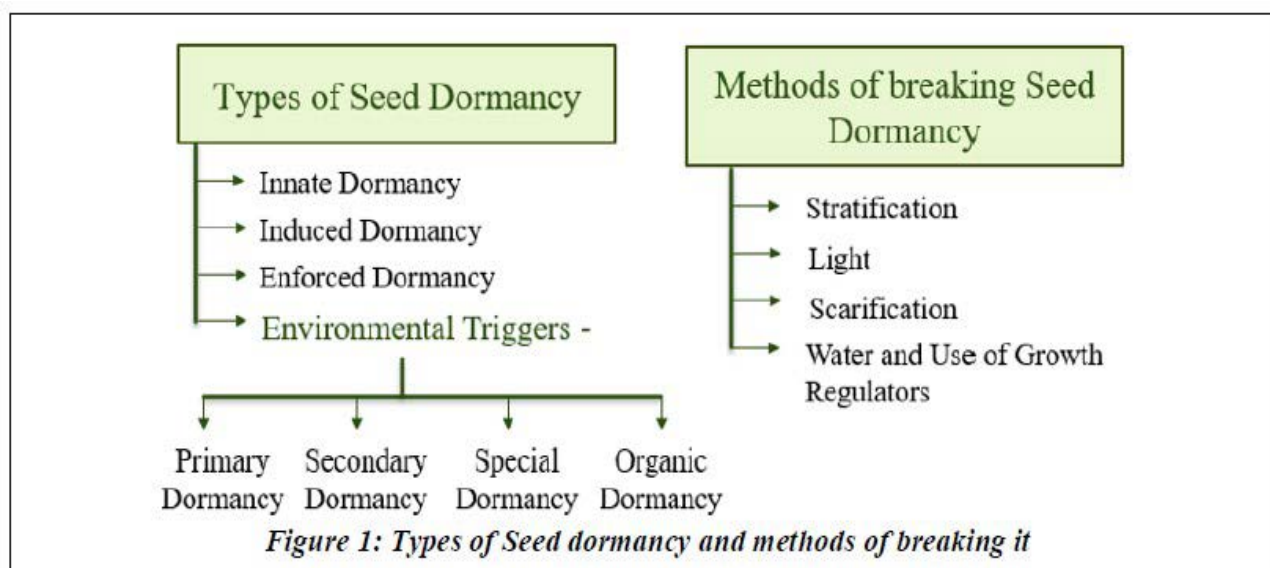
III. CONCEPT OF PGPR TO OVERCOME SEED DORMANCY

Rhizobia are the type of PGPR bacteria that convert atmospheric nitrogen into a form that the plants can use are the main factors of influence for the soil fertility. Besides that, they can also manufacture plant hormones, such as auxins, gibberellins, and cytokinins which are the ones that improve root development and seed germination.

Plants release chemical signals, for example LCOs (lipochito oligosaccharides) to trigger the reaction of genes that are responsible for seed growth.

Besides that, the bacteria also trick the hormones of plants by both increasing the level of gibberellic acid (GA) and decreasing the level of abscisic acid (ABA) (9). Basically, GA is a germination promoting substance, whereas ABA is a germination inhibiting one by providing dormancy to the seed.

The metabolism of the seed is increased which in turn helps the seed to be more receptive to environmental changes thus it becomes capable of germinating more efficiently and it grows more vigorously in the early stages.



Seeds that have lost their first dormancy but go back into a dormant condition as a result of strong environmental factors like heat, insufficient moisture, or darkness cause secondary dormancy (7). Often requiring a combination of internal and outward stimuli, certain plant species exhibit great dormancy and employ sophisticated processes

Through a number of applications, PGPR maintains plant health. This is especially true in the middle of many environmental issues including drought, salinization, hydrocarbon contamination, and significant heavy metal poisoning (10). In the rhizome, the little patch of earth affected by root excretions, these

good bacteria flourish. Participating in many biological processes, they support plant resilience and help growth. PGPR employs several biochemical and physiological processes to assist plants in coping with environmental problems (11). Under difficult situations, the rhizobial bacteria supports and enhances the level of plant survival as well as speeds up growth. PGPR thereby creates

biofilms by assisting plants under severe heavy metal stress from chemicals like lead (Pb), cadmium (Cd), arsenic (As), mercury (Hg), copper (Cu), zinc (Zn), and nickel (Ni) (12). Thick colonies of bacteria encased in an extracellular polymeric matrix make up these biofilms (13). By restricting hazardous metals and promoting root growth, this project lowers plant absorption.

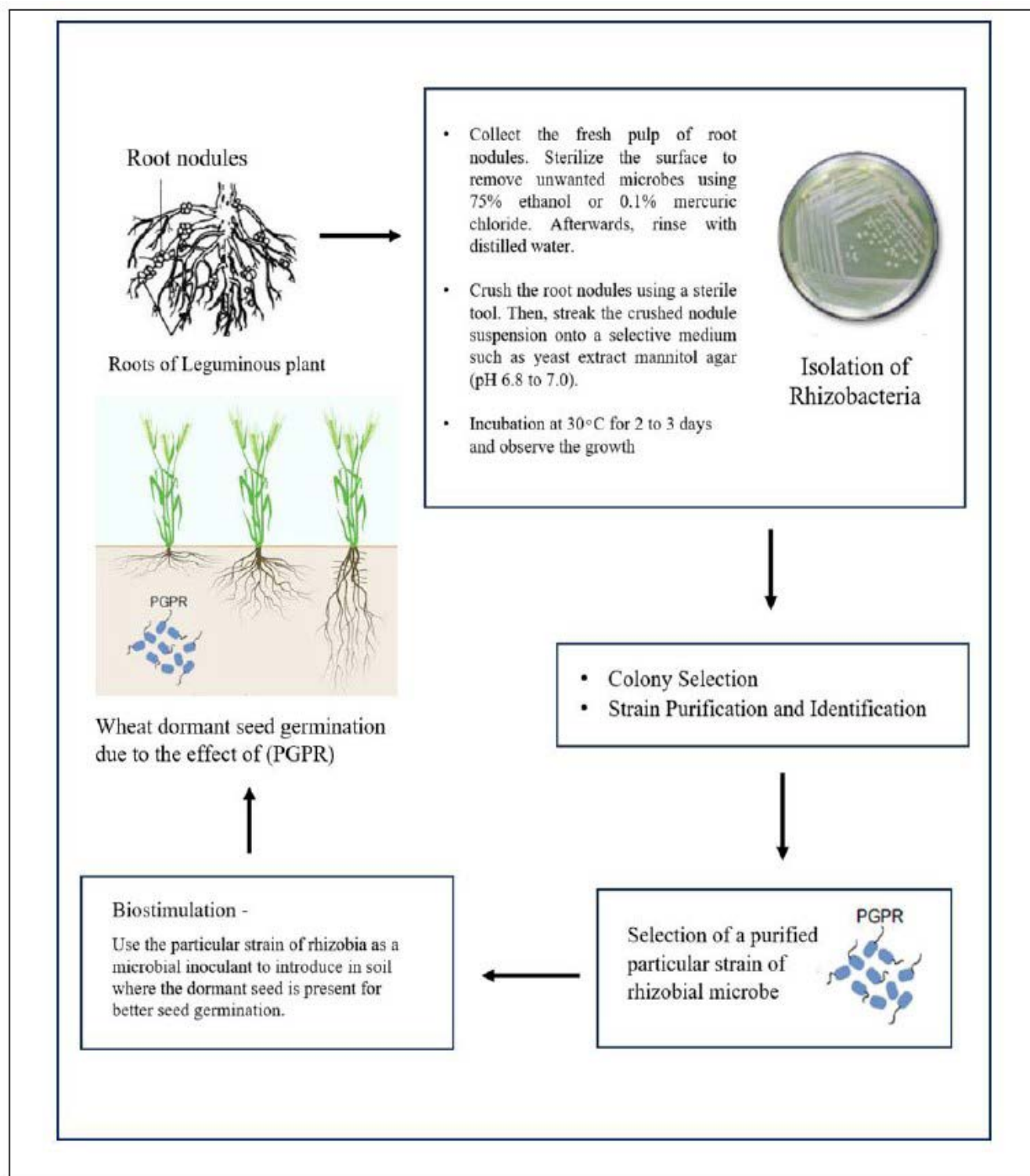


Figure 2: Isolation of soil rhizobacterial strains from leguminous root nodules to improve the germination of dormant wheat seeds through plant growth-promoting mechanisms

PGPR can also help plants grow in the manner of induced systemic resistance (ISR). This helps the plants to more effectively battle stresses and diseases without obviously exhibiting any signs of illness (14). Producing multiple enzymes and metabolic compounds breaking down dangerous hydrocarbons, PGPR lets plants tolerate hydrocarbons in contaminated soils. Furthermore, improving root health and performance via balance of the rhizosphere bacteria. One of the main uses of PGPR in salt conditions is to lessen oxidative stress in plants (15). They achieve this mostly by abscisic acid (ABA), a stress hormone controlling stomatal closure and conserving water. This enables the plant to more actively resist ionic imbalances brought on by salt-induced drying.

Under challenging conditions, PGPR's production of indole-3-acetic acid (IAA) (16), a well-known phytohormone promoting root development, makes it especially significant which helps the plant seed to break the barrier of seed dormancy and trigger the process of sprouting (17). Reaching deeper water reserves helps a plant's drought tolerance by generating longer, more branched roots (18). Additionally known for its antibacterial characteristics, PGPR also produces HCN (19).

This shields the plant against diseases that could aggravate stress reactions and promotes rhizome control of harmful bacteria. Besides allowing plants to manage stress, PGPR directly support their development (20).

For instance, the ACC deaminase enzyme aids plants in managing ethylene levels. Typically caused by stress, high ethylene levels can impede plant development (21). By lowering its concentration, PGPR helps plants to grow naturally even under pressure. PGPR-released volatile organic compounds (VOCs) also support growth and enable species to communicate (22). PGPR also improve soil nutrient availability; they fix atmospheric nitrogen by the nitrogenase enzyme. PGPR release organic acids and decompose phosphate, hence making phosphorus, yet another important component, accessible (23).

This technique converts nitrogen into digestible shapes for plants. These chemicals free iron from the soil, hence releasing it for the plant and so increasing total nutritional intake (24). They produce plant hormones including cytokinins and gibberellins, which then promote various aspects of plant development including seedling germination, leaf expansion, and shoot elongation (25).

The environment is more drought-type with less fertile soils where seed dormancy acts as the chief constraint. Rhizobia activate dormancy and help in better crop establishment and yield (26). And it is a simple, cheap, and eco-safe method (27). So, however certain rhizobial strains can be used as a major biological method to overcome seed dormancy which can also be helpful for seed biostimulation.

IV. CONCLUSION

In conclusion, germination and early seedling growth can be promoted through growth stimulation by rhizobia, which is a very promising sustainable modern method of seed treatment (28). Rhizobia fix nitrogen from the atmosphere, producing certain growth-regulating substances, mainly phytohormones such as auxins and cytokinins. They fix nutrients for plants, cause root elongation, and, along with that, resistance against stresses gets developed. So, if used appropriately, this can reduce chemical fertilizers and thereby promoting a sustainable mode of agriculture (29).

REFERENCES

- [1] R. Gabilondo, J. Sánchez, P. Muñoz, I. Montero-Muñoz, P. V. Mauri, J. Marín, and D. Mostaza-Colado, "Evaluation of Biostimulatory Activity of Commercial Formulations on Three Varieties of Chickpea," *Agriculture*, vol. 13, p. 474, 2023.
- [2] R. Negi, B. Sharma, F. Parastesh, S. Kaur, and A. N. Yadav, "Microbial consortia mediated regulation of plant defense: A promising tool for sustaining crops protection," *Physiol. Mol. Plant Pathol.*, vol. 134, p. 102393, 2024.
- [3] T. Zamljen, S. Lojen, V. Zupanc, and A. Slatnar, "Determination of the yield, enzymatic and metabolic response of two *Capsicum* spp. cultivars to deficit irrigation and fertilization using the stable isotope ^{15}N ," *Chem. Biol. Technol. Agric.*, vol. 10, p. 129, 2023.
- [4] E. Gómez, A. Alonso, J. Sánchez, P. Muñoz, J. Marín, D. Mostaza-Colado, and P. V. Mauri, "Application of Biostimulant in Seeds and Soil on Three Chickpea Varieties: Impacts on Germination, Vegetative Development, and Bacterial Facilitation of Nitrogen and Phosphorus," *Agriculture*, Published online: Jan. 19, 2024.
- [5] M. de los Ángeles Sariñana-Navarrete, A. Benavides-Mendoza, S. González-Morales, A. Juárez-Maldonado, P. Preciado-Rangel, E. Sánchez-Chávez, G. Cadenas-Pliego, A. Antonio-Bautista, and Á. Morelos-Moreno, "Selenium Seed Priming and Biostimulation Influence the Seed Germination and Seedling Morphology of Jalapeño (*Capsicum annuum* L.)," *Horticulturae*, vol. 10, p. 119, 2024.
- [6] M. Ghasemi, M. Zahedi, M. Gheysari, and M. R. Sabzalian, "Effects of Inoculation with Four Mycorrhizal Species on Seed Phenolic and Fatty Acids of Sesame Plants Grown under Different Irrigation Regimes," *Sci. Rep.*, vol. 13, p. 16482, 2023.
- [7] S. Waqar, A. A. Bhat, and A. A. Khan, "Endophytic fungi: Unravelling plant-endophyte interaction and the multifaceted role of fungal endophytes in stress

- amelioration,” *Plant Physiol. Biochem.*, vol. 206, p. 108174, 2024.
- [8] Y. Wen, L. J. Zhou, Y. J. Xu, A. Hashem, E. F. Abd Allah, and Q. S. Wu, “Growth Performance and Osmolyte Regulation of Drought-Stressed Walnut Plants Are Improved by Mycorrhiza,” *Agriculture*, vol. 14, p. 367, 2024.
- [9] S. Fahde, S. Boughribil, B. Sijilmassi, and A. Amri, “Rhizobia: A Promising Source of Plant Growth-Promoting Molecules and Their Non-Legume Interactions: Examining Applications and Mechanisms,” *Agriculture*, vol. 13, no. 7, p. 1279, 2023.
- [10] E. Gómez, A. Alonso, J. Sánchez, P. Muñoz, J. Marín, D. Mostaza-Colado, and P. V. Mauri, “Application of Biostimulant in Seeds and Soil on Three Chickpea Varieties,” *Agriculture*, Published: Jan. 19, 2024.
- [11] P. Guzmán-Guzmán, E. Valencia-Cantero, and G. Santoyo, “Plant growth-promoting bacteria potentiate antifungal and plant-beneficial responses of *Trichoderma atroviride* by upregulating its effector functions,” *PLoS ONE*, vol. 19, p. e0301139, 2024.
- [12] J. Zeng, S. Ma, J. Liu, S. Qin, X. Liu, T. Li, Y. Liao, Y. Shi, and J. Zhang, “Organic Materials and AMF Addition Promote Growth of *Taxodium ‘Zhongshanshan’* by Improving Soil Structure,” *Forests*, vol. 14, p. 731, 2023.
- [13] M. Gong, N. Bai, P. Wang, J. Su, Q. Chang, and Q. Zhang, “Co-Inoculation with Arbuscular Mycorrhizal Fungi and Dark Septate Endophytes under Drought Stress,” *Plants*, vol. 12, p. 2596, 2023.
- [14] M. Añibarro-Ortega, M. I. Dias, J. Petrović, S. Nuñez, R. C. Calhelha, E. M. Costa, M. Machado, M. Pintado, M. D. Soković, and V. López, et al., “Valorization of *Solanum melongena* L. crop by-products: Phenolic composition and in vitro antioxidant, antidiabetic, anti-inflammatory, cytotoxic and antimicrobial properties,” *Process Biochem.*, vol. 153, pp. 315–324, 2025.
- [15] S. K. Mansega, L. S. Kabwe, M. Chakulya, and A. Kirabo, “Mechanisms of Oxidative Stress in Metabolic Syndrome,” *Int. J. Mol. Sci.*, vol. 24, p. 7898, 2023.
- [16] M. Añibarro-Ortega, V. López, S. Nuñez, J. Petrović, F. Mandim, L. Barros, M. Soković, I. C. F. R. Ferreira, M. I. Dias, and J. Pinela, “Phenolic Composition and in Vitro Bioactive and Enzyme Inhibitory Properties of Bell Pepper (*Capsicum annuum* L.) Plant Extracts,” *Ind. Crops Prod.*, vol. 214, p. 118546, 2024.
- [17] R. Ouhaddou, M. Anli, R. Ben-Laouane, A. Boutasknit, M. Baslam, and A. Meddich, “The Importance of the *Glomus* Genus as a Potential Candidate for Sustainable Agriculture Under Arid Environments,” *Int. J. Plant Biol.*, vol. 16, no. 1, p. 32, 2025.
- [18] S. K. Panda, D. Gupta, M. Patel, C. V. D. Vyver, and H. Koyama, “Functionality of Reactive Oxygen Species (ROS) in Plants: Toxicity and Control in Poaceae Crops Exposed to Abiotic Stress,” *Plants*, vol. 13, p. 2071, 2024.
- [19] Y. Hu, H. Zhao, L. Xue, N. Nie, H. Zhang, N. Zhao, S. He, Q. Liu, S. Gao, and H. Zhai, “IbMYC2 Contributes to Salt and Drought Stress Tolerance,” *Int. J. Mol. Sci.*, vol. 25, p. 2096, 2024.
- [20] C. Lu, L. Li, X. Liu, M. Chen, S. Wan, and G. Li, “Salt Stress Inhibits Photosynthesis and Destroys Chloroplast Structure in *Robinia pseudoacacia* Seedlings,” *Plants*, vol. 12, p. 1283, 2023.
- [21] D. Sati, V. Pande, S. C. Pandey, and M. Samant, “Recent advances in PGPR and molecular mechanisms involved in drought stress resistance,” *J. Soil Sci. Plant Nutr.*, vol. 23, pp. 106–124, 2023.
- [22] A. Boutasknit, M. Ait-El-Mokhtar, B. Fassih, R. Ben-Laouane, S. Wahbi, and A. Meddich, “Effect of Arbuscular Mycorrhizal Fungi and Rock Phosphate on Growth of Carob under Water Stress,” *Metabolites*, vol. 14, p. 202, 2024.
- [23] A. S. N. Ribeiro, A. F. C. Junior, L. F. B. Chagas, and M. V. G. Alves, “Efficiency of *Trichoderma* and *Bacillus subtilis* as growth promoters in eucalyptus *Corymbia citriodora*,” *Obs. Econ. Latinoam.*, vol. 21, pp. 20380–20397, 2023.
- [24] L. Buirs and Z. K. Punja, “Endophytes in *Cannabis sativa*: Identifying and Characterizing Microbes with Beneficial and Detrimental Effects on Plant Health,” *Plants*, vol. 14, no. 8, p. 1247, 2025.
- [25] A. Pérez-Piqueres, B. Martínez-Alcántara, R. Canet, R. del Val, and A. Quiñones, “Plant growth-promoting microorganisms as natural stimulators of nitrogen uptake in citrus,” *PLoS ONE*, vol. 20, no. 2, p. e0311400, 2025.
- [26] Z. K. Punja and C. Scott, “Organically grown cannabis (*Cannabis sativa* L.) plants contain a diverse range of culturable epiphytic and endophytic fungi,” *Botany*, vol. 101, pp. 255–269, 2023.
- [27] C. Lobato, J. M. de Freitas, D. Habich, I. Kögl, G. Berg, and T. Cernava, “Wild again: Recovery of a beneficial cannabis seed endophyte from low domestication genotypes,” *Microbiome*, vol. 12, p. 239, 2024.
- [28] I. Jiménez-Guerrero, S. Acosta-Jurad, P. Navarro-Gómez, F. Fuentes-Romero, C. Alías-Villegas, F. J. López-Baena, and J. M. Vinardell, “TtsI: Beyond Type III Secretion System Activation in Rhizobia,” *Appl. Microbiol.*, vol. 5, no. 1, p. 4, 2025.
- [29] A. M. Kumar, G. M. Sandhya, and A. Karthikeyan, “Evaluation of bio-fertiliser (bio-inoculant) consortia and their effect on plant growth performance of sandalwood (*Santalum album*) seedlings,” *J. Trop. For. Sci.*, vol. 35, pp. 311–321, 2023.

Lowland Saffron Cultivation at Adamas Smart Greenhouse

Prithwee Chakraborty, Sreoshi Kar, Arnish Das, Soham Ghosh, Archit Mondal, Sudip Barman, Saprativ Sengupta
School of Smart Agriculture
Adamas University



Abstract—In order to enable precise saffron cultivation in lowland agroclimatic zones, this study gives the insight on the creation of an IoT-enabled Smart Polyhouse that combines conventional polyhouse infrastructure with cutting-edge automated technology. The technology which was put into place by Adamas University's Smart Agriculture Department, addresses the limitations of temperature, humidity, soil moisture, and photoperiod all of which are crucial for saffron production by combining controlled-environment agriculture (CEA) with real-time digital monitoring. GI-frame structural engineering, UV-stabilized cladding, automated ventilation, drip irrigation, fertigation systems, PAR-based light control, and cloud-integrated sensor networks are all features of the polyhouse. ESP32 microcontrollers are used to connect Internet of Things (IoT) devices, including as temperature, RH, soil-moisture, pH, and EC sensors, to a cloud platform. This allows for remote control, predictive decision-making, and automated actuation of fans, pumps, foggers, and shade screens. According to preliminary experiments, compared to traditional lowland farming, microclimate stability increased by 35%, water use efficiency by 42%, and fertiliser delivery precision by 28%.

Through sensitive environmental control, the method shows that saffron, which has historically only been grown in high-altitude settings, can be grown sustainably in lowland places. A feasible, technologically enabled route for high-value crop diversification and climate-resilient agriculture in India is provided by this research, which offers a reproducible model for smart protected cultivation.

Keywords— Smart polyhouse, IoT agriculture, saffron cultivation, automation, precision farming, controlled environment

Background

In order to support next-generation protected cultivation systems designed for precision agriculture, Adamas University in Kolkata recently built a state-of-the-art Smart Agriculture Polyhouse. In order to sustain high-value and climate-sensitive crops like saffron, this infrastructure combines modern Internet of Things (IoT), automation, and climate-control technology with conventional

polyhouse components. The polyhouse has a sturdy Hot Dip Galvanised (GI) structural frame that is designed to withstand local winds exceeding 120 km/h. UV-stabilized, anti-drip polyethylene film offers the best light transmission and thermal insulation. Cooling pads, shading systems, and automated forced and natural ventilation provide precise microclimate control, which is crucial for crops that need specific humidity and temperature ranges.

Sand and disc filters, fertigation injectors, drip irrigation, and Internet of Things-based water quality monitoring are all part of the water management subsystem. Together these solutions improve root-zone conditions for sensitive crops, minimise fertiliser waste, and increase water use efficiency. Reliable, sustainable water sources are offered by rainwater collection and treated water storage.

A network of sensors (temperature, RH, soil moisture, PAR, pH, and EC) connected to ESP32 controllers and a cloud-based platform enables smart automation. Continuous monitoring, automated actuation and threshold-based interventions are made possible via real-time data transmission. The web-based and mobile interfaces enable alarm notifications, data analytics, and remote access.

By simulating the optimal temperature triggers for flowering (23–27°C during the day and 15–18°C at night), this updated polyhouse seeks to show that saffron, a high-altitude, cold-climate crop, can be grown in regulated lowland conditions. The system functions as a paradigm for climate-resilient crop diversification, improving productivity, sustainability, and technological capabilities within the agricultural ecosystem by integrating smart sensing, automated decision-making, and precise resource delivery.

Objectives

1. To employ precision engineering techniques to design and build an Internet of Things (IoT)-enabled smart polyhouse that is interconnected with temperature, irrigation, and nutrient automation systems to simulate saffron-specific environmental conditions within lowland agroclimatic areas.
2. To compare performance with traditional lowland farming techniques in order to assess microclimate stability, water-use efficiency, and nutrient optimisation attained by real-time sensor-based monitoring and automated actuation throughout the crop cycle.

3. To evaluate saffron grown in regulated IoT-based environments in terms of growth response, corm development, flowering rate, and yield fluctuations in order to provide scientific proof of its viability in non-traditional geographic zones.

4. To create a scalable technology framework for high-value crop growing in smart polyhouses, allowing small and medium-sized farmers to use IoT solutions that are climate-resilient and backed by data-driven decision-making tools.

Hypotheses

Null Hypothesis (H_0): When compared to conventional lowland culture, IoT-enabled smart polyhouse cultivation does not considerably enhance saffron crop performance, microclimate stability, or resource-use efficiency.



Alternative Hypothesis (H₁): Compared to conventional lowland farming techniques, IoT-enabled smart polyhouse cultivation greatly improves saffron crop performance, microclimate stability, and resource-use efficiency.

Methodology

Step 1: Setting Up the Site and Building the Polyhouse

At Adamas University, a 200 m² location was chosen to guarantee ideal sunlight exposure (6–8 hours), level terrain, and close proximity to supplies of energy and water. In accordance with IS:875 structural standards, 350 GSM UV-stabilized polyfilm and GI pipes were used to build the polyhouse structure.

Step 2: Setting Up Environmental Control Systems

Evaporative cooling pads, exhaust blowers, ventilation devices, and 50% shade netting were added. To keep pests out, insect-proof nets were installed. For precise measurements, sensors were placed at root-zone depth and canopy level.

Step 3: Integration of Automation and IoT

Temperature, RH, soil moisture, PAR, pH, and EC sensors were integrated into an ESP32-based control unit. Wi-Fi and GPRS were used to link devices to cloud platforms (Firebase). Pumps, foggers, fans, and solenoid valves were all controlled by relay-driven actuators using threshold algorithms.

Step 4: Setting Up Fertigation and Irrigation

Four LPH emitters and 16 mm laterals were placed in a drip irrigation system. Precise nutrient dosage was guaranteed using an automated solenoid valve-controlled venturi-based fertigation injector. Clog-free flow was guaranteed by filtration machines.

Step 5: Growing Saffron

Cocopeat–perlite substrate was used to plant certified saffron corms (10–12 g grade) in raised beds. The microclimate conditions were kept between 15 and 18°C at night and between 23 and 27°C during the day. Soil moisture was kept between 25 and 35 percent by automated irrigation.

Step 6: Gathering and Examining Data

Sensor data were recorded every ten

minutes, and plant performance, resource consumption, and microclimate variations were examined. Field-based lowland controls were used to compare yield parameters.

Outcomes

- 35% decrease in microclimate variability ensures steady saffron flowering cycles
- Automated drip irrigation results in a 42% increase in water-use efficiency
- The accuracy of nutrient distribution increases by 28%, which decreased fertiliser waste
- Compared to open-field lowland controls, the flowering rate rose by 31%
- Depending on the corm grade, the yield per square metre increases by 25–30%
- The system made predictive control and ongoing remote monitoring possible
- Proven that growing saffron in unconventional lowland climates is feasible



Conclusion

With considerable improvements in productivity, stability, and resource efficiency, Adamas University's IoT-enabled smart polyhouse successfully replicates the microclimatic conditions required for saffron. This model shows that high-value crops may be produced sustainably in lowland areas using advanced technology, offering a scalable path for modern climate-resilient agriculture.

References

1. Ahmad, M. et al. Smart Agriculture Systems: IoT Applications in Controlled Environments. *Agronomy*, 2023.
2. Bose, S. & Chatterjee, A. Precision Irrigation Technologies for Protected Cultivation. *Smart Farming Journal*, 2022.
3. Gupta, R. IoT-Based Climate Automation in Polyhouses. *Journal of Agricultural Engineering*, 2021.
4. Khan, T. et al. Saffron Cultivation under Controlled Environments. *Horticultural Science Review*, 2024.
5. Singh, R. & Verma, L. High-Value Crop Production in Smart Polyhouses. *Indian Journal of Agritech*, 2023.
6. Roy, P. Cloud-Based Sensor Networks for Agriculture. *IoT Systems Research*, 2022.
7. Sharma, S. Environmental Control Strategies in Protected Farming. *CEA Journal*, 2021.
8. Patel, J. Microcontroller-Based Automation in Agriculture. *Embedded Systems Review*, 2022.
9. Das, P. Saffron Yield Optimization Techniques. *Crop Innovation Bulletin*, 2023.
10. Neogi, U. , Banerjee, S. , Chakraborty, S. Patent of Adamas University Smart Agriculture filed No. 202531016777 , Published on 04.04.2025, Title – AI-Driven Autonomous Greenhouse Control System with Adaptive Climate and Crop Monitoring.



Incorporation of Moringa powder for making value added Beverages and evaluation of nutritional properties

¹ Umra khan, ² Devraj Singh, ³ Sharvan Kumar, ¹ Rida Khan ² Anuj Shakya and ² Vivek Padey

¹ M.Sc. research Scholar, Department of Agriculture,
Invertis University, Uttar Pradesh, India

² Assistant Professor, Department of Agriculture, Invertis University, Bareilly, India

³ Assistant Professor, Maharishi School of Agriculture,
Maharishi University of Information Technology, Lucknow Campus, Uttar Pradesh,
India Barman, Saprativ Sengupta

Abstract—Moringa (*Moringa oleifera* Lam) is an essential medicinal species, which belongs to territory Plantae, known as the “tree of life” or “miracle tree” is classified as an important herbal plant due to its medicinal and non-medicinal benefits. This plant has been honored as “Botanical of the Year – 2007” by the National Institute of Health (NIH). It has been cultivated in sub-tropical and tropical regions in many countries of the world. Moringa plant is cultivated for its edible leaves, flowers and nutritious pods, which can be used as a medicine or ingredients in the food industry. Moringa oleifera may lead to modest reduction in blood sugar and cholesterol. It may also have antioxidant and anti-inflammatory effects and protect arsenic toxicity. Moringa leaf is commonly used to combat malnutrition in infants, and pregnant and lactating women, as well as to increase milk production. Moringa plants have an extensive range of bioactive compounds, such as carbohydrates, fatty acids and proteins. Beverage industry is now booming rapidly and new versions of beverages are brought into the focus of health-conscious consumers based on their positive health outcomes. Moringa Mint iced tea is a refreshing drink that combines the nutritional benefits of moringa with the invigorating flavor of mint. Moringa Latte is a caffeine-free beverage made from moringa powder, milk, and sometimes other ingredients like honey, cinnamon. Moringa energy drink blended with pineapple is one of the nutritious drink which is richest in nutrition. The result of nutritional analysis showed that the sample of developed beverages like Moringa and Mint Iced Tea, Moringa Latte and Moringa energy drink blended with Pineapple have (moisture-98.00%, protein-0.57g, fat-0.04g, crude fiber-0.6g, carbohydrate-0.5g and ash-0.7g%), (moisture-93.5%, protein-0.30g, fat-0.5g, crude fiber-0.35g, carbohydrate-1.60g, and ash-1.04g), and (moisture-95.00%, protein-0.75g, fat-0.05g, crude fiber-0.20g, carbohydrate-8.00g and ash-0.8g) respectively. The result of sensory evaluation for appearance, texture, taste and overall acceptability that carried out for developed beverages revealed that the acceptance of panelists for this product overall acceptability. It concludes that developed beverages are recommended as a healthy product.

Keywords— Moringa oleifera, Miracle Tree, Beverage, Antioxidant, Mint, Pineapple, Protein, Appearance.

Introduction

Moringa (*Moringa oleifera* Lam.) is an important medicinal species, which belongs to kingdom Plantae, sub-kingdom Tracheobionta, division Magnoliophyta, class Magnoliopsida, order Capparales, family Moringaceae. Moringa oleifera, also known as the “tree of life” or “miracle tree” is classified as an important herbal plant due to its medicinal and non-medicinal benefits (Pareek et al., 2023). This plant has been honored as “Botanical

of the Year – 2007” by the National Institute of Health (NIH) (Gupta et al., 2018). Traditionally, the plant is used to cure wounds, pain, ulcers, liver diseases, heart diseases, cancer, and inflammation (Pareek et al., 2023). Moringa oleifera Lam popularly known in Brazil as “moringa”, “lirio Branco” or “quiabo-de-quina” and in some parts of the world, as drumstick tree or horseradish tree. Its medicinal potential derives from secondary metabolites, such as alkaloids, flavonoids, tannins, steroids, saponins, quinones,

coumarins, and resins (Brilhante et al., 2017). Moringa plants have an extensive range of bioactive compounds, such as carbohydrates, phenolic compounds, oils, fatty acids, proteins and functional peptides (Saucedo-Pompa et al., 2018). The plant contains 36 anti-inflammatories, more than 539 bio-chemical activities and 46 antioxidants natural components (El-Rahim et al., 2017).

It has been cultivated in sub-tropical and tropical regions in many countries of the world for its many uses as an important nutraceutical and medicinal herb. Moringa plant is cultivated for its edible leaves, flowers and nutritious pods, which can be used as a medicine or ingredients in the food industry. Moringa leaf was most cultivated part of moringa plant. Moringa leaves were rich in vitamin - C, vitamin - E and beta-carotene, minerals, calcium, and potassium. Moringa powder is a rich source of protein, 28g in every 100g (Hassan et al., 2021). Moringa oleifera, it is native to Northern India, but currently spread in America, Africa, Europe, and Asia (Brilhante et al., 2017).

In South Africa, the Moringa plant is mostly cultivated and used. There are a limited number of studies conducted on incorporating Moringa in starch-based beverages such as the popular mahewu, which is a local maize-based, non-alcoholic beverage that is consumed for refreshment and as a filling food. Worldwide, malnutrition has been identified as a preventable health challenge, with its high prevalence reported in Sub-Saharan African (SSA) areas. Malnutrition is a broad terminology that is commonly used to describe under nutrition. People are termed malnourished if their diet cannot provide adequate calories and good protein for growth and maintenance (Olusanya, 2018).

Beverage industry is now booming rapidly and new versions of beverages are brought into the focus of health-conscious consumers based on their positive health outcomes (Javed et al., 2024). Beverages produced from natural substances derived from various morphological plant parts, including leaves, stems, roots, fruits, buds, and flowers. Herbal beverages, whether derived from a single herb or combination of herbs (Shaik et al., 2023). The powdered moringa leaves are used to make many beverages, of which “Zija” is the most popular in India (Pareek et al., 2023). Moringa oleifera leaves can be used in soft drinks as preservatives and to add flavor and nutritional value. It can be used to extend the shelf life of beverages. Increased awareness in health issues leads to increase the consumption of fruit juices and other natural products as an alternate to the traditional caffeine containing beverages such as tea, coffee, or other soft drinks. However, no reports exist on the preservation or processing on Moringa energy drinks and its impact on the sensory and storage quality of the products. It can be achieved by making energy rich Moringa drink products blended with different flavors (Saran Asati et al., 2022).

Moringa Mint iced tea is a refreshing drink that combines

the nutritional benefits of moringa with the invigorating flavor or mint. As such, moringa powder on its own has a slight bitter and somewhat spicy taste. Tea is the second most consumed beverage in the world after water. More than 75% of all the tea produced in this world is black tea, 20% is green and the rest is accounted by oolongs, whites, and yellow tea. Some say moringa mint tea has a woody taste with a minty twist. Others say, the tea's taste and smell are peculiar. Moringa mint tea may help with anxiety, blood pressure, diabetes, and liver health.

The latte is a coffee drink which is especially made with espresso and steamed milk. The term as used in English is a shortened form of the Italian *caffè latte* or *caffelatte*, which means

“milkcoffee”. Moringa Latte is a caffeine-free beverage made from moringa powder, milk, and sometimes other ingredients like honey, cinnamon, or lemon. We can also make an iced moringa latte by adding the latte mix powder to hot water or milk, stirring well and then refrigerating. When ready to serve, add ice cubes to a glass and pour in the chilled latte.

The unique drink combines the powerful health benefits of moringa. It is a vibrant, tropical fusion that blends with the nutrient-rich power of moringa with natural sweetness and tangy taste of pineapple. Pineapple (*Ananas comosus*) fruit is most popular tropical fruit that are well known for its juicy and sweet tasty bracts. This fruit is richest in nutrition and contain highest amount of vitamins, fibers, minerals, and enzymes. This healthy nutrition fruit can be eaten raw and can be used in preparing various tasty soft drinks.

Materials and Methods

The present investigation was conducted at food tech. laboratory, Department of Agriculture, Invertis University, Bareilly, Uttar Pradesh, India. The ingredients used for making the Moringa and Mint Iced Tea included moringa powder, mint leaves, honey as sweetener, lemon, and salt which were procured from the local market of Bareilly, Uttar Pradesh.

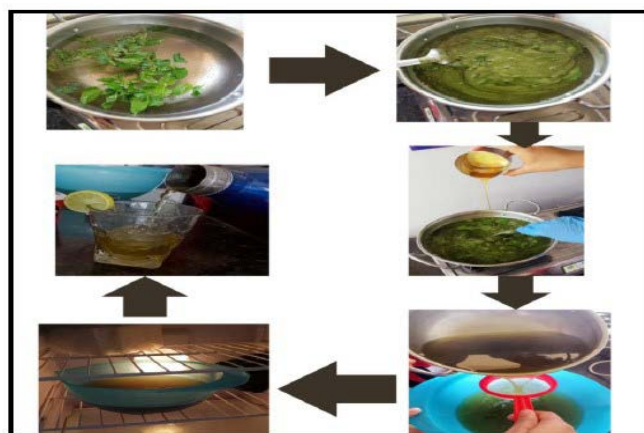
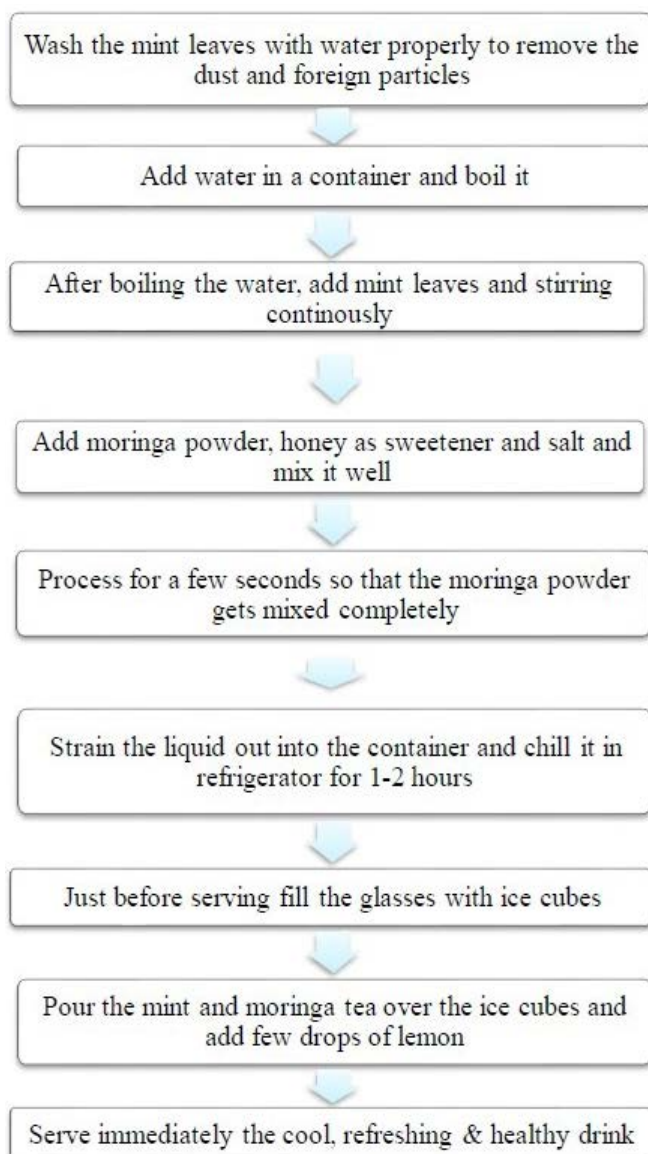


Fig.1 Preparation of Moringa and Mint Iced Tea



The ingredients used for making the Moringa Latte included moringa powder, honey as sweetener, milk which were procured from the local market of Bareilly, Uttar Pradesh.

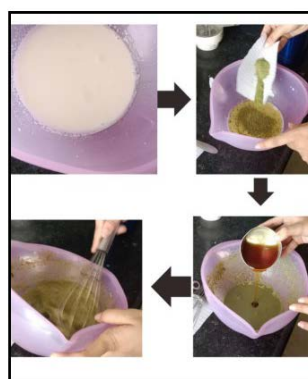
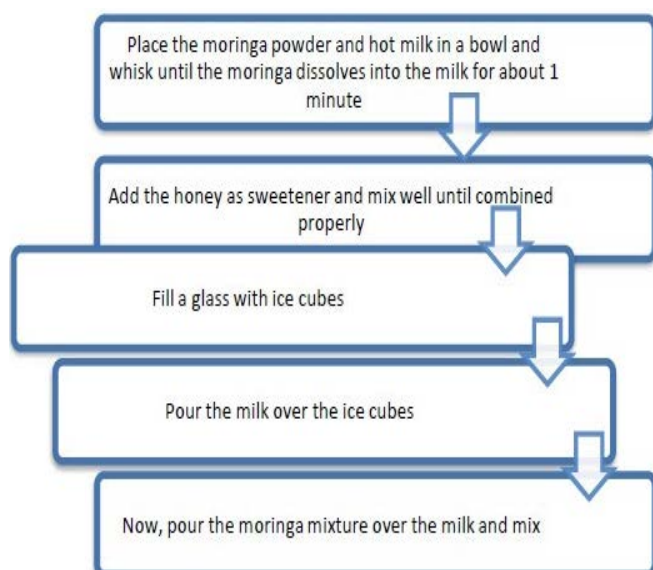


Fig.2 Preparation of Moringa Latte mixture



Fig.3 Preparation of Moringa Latte

The ingredients used for making the Moringa energy drink blended with Pineapple included Moringa powder, honey as sweetener, and pineapple which were procured from the local market of Bareilly, Uttar Pradesh.

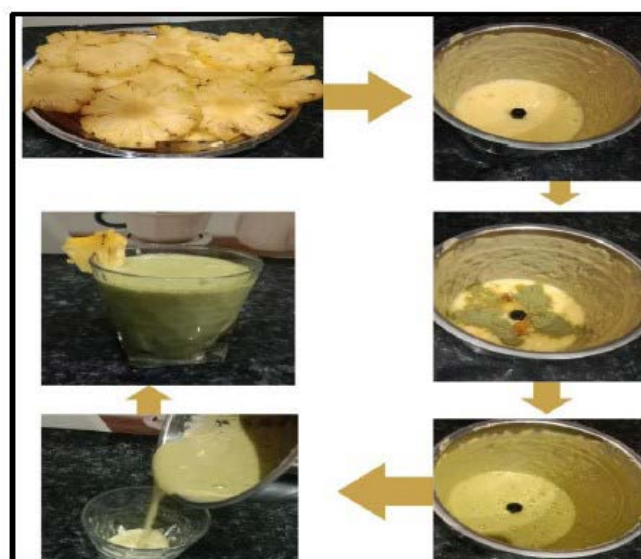
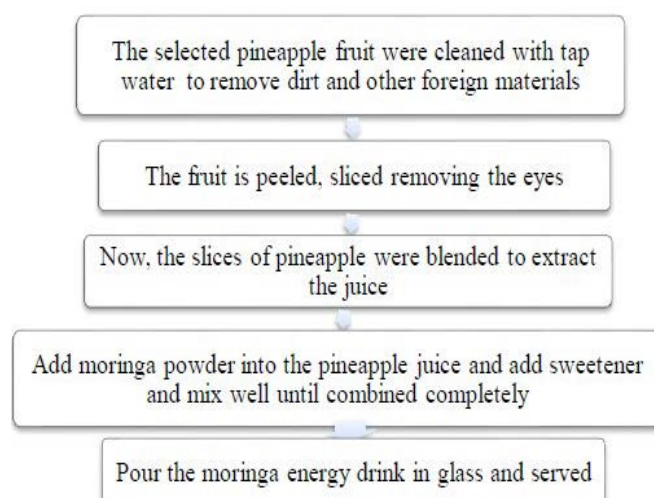


Fig.4 Preparation of Moringa energy drink blended with Pineapple

Result and Discussion

The below table described the result on the basis of analysis. The nutritional component of Moringa and Mint Iced Tea

find with analysis using formula. The moisture content of showed (98.00%), protein (0.57g), fat (0.04g), crude fiber (0.6g), carbohydrate (0.5g) and ash (0.7g). They showed result indicates high amount of moisture and low amount of protein, fat and carbohydrate.

Table.1 Nutritional analysis of Moringa & Mint Iced Tea

Components	Nutrient value per 100 ml
Energy	20kcal
Moisture	98.00%
Protein	0.57g
Fat	0.04g
Crude Fiber	0.6g
Carbohydrates	0.5g
Ash	0.7g

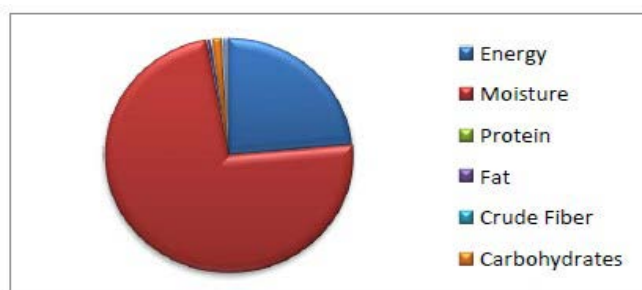


Fig.5 Nutritional representation of Moringa and Mint Iced tea

The below table described the result on the basis of analysis. The nutritional component of Moringa Latte find with analysis using formula. The moisture content of showed (93.5%), protein (0.30g), fat (0.5g), crude fiber (0.35g), carbohydrate (1.65g) and ash (1.04g). They showed result indicates high amount of moisture and protein and low amount of fat and carbohydrate.

Table.2 Nutritional analysis of Moringa Latte

Components	Nutrient value per 100 ml
Energy	30kcal
Moisture	93.5%
Protein	0.30g
Fat	0.5g
Crude Fiber	0.35g
Carbohydrates	1.60g
Ash	1.04g

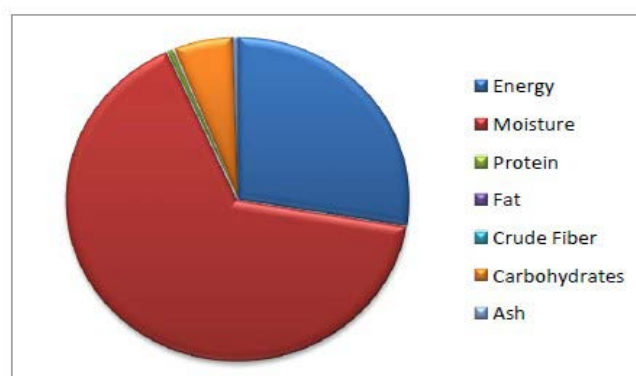


Fig.6 Nutritional representation of Moringa Latte

The below table described the result on the basis of analysis. The nutritional component of Moringa energy drink blended with Pineapple find with analysis using formula. The moisture content of showed (95.00%), protein (0.75g), fat (0.05g), crude fiber (0.20g), carbohydrate (8g) and ash (0.8g). They showed result indicates high amount of moisture and protein and low amount of fat and carbohydrate.

Table.3 Nutritional analysis of Moringa energy drink blended with Pineapple

Nutrient Parameters	Nutrient value per 100 ml
Energy	40kcal
Moisture	95.00%
Protein	0.75g
Fat	0.05g
Crude Fiber	0.20g
Carbohydrates	8.00g
Ash	0.8g

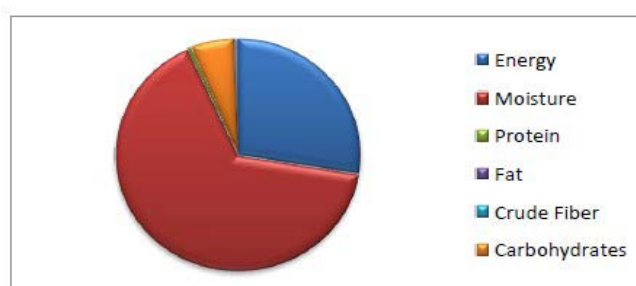


Fig.7 Nutritional representation of Moringa energy drink blended with Pineapple

Evaluate the beverage sample such as Moringa and Mint Iced Tea, Moringa Latte and Moringa energy drink blended with Pineapple formed the sensory card on categories like, taste, texture, appearance, aroma and overall acceptability.

Table:4. Sensory evaluation of Moringa and Mint Iced Tea, Moringa Latte and Moringa energy drink

Attribute	Moringa & Mint Iced Tea	Moringa Latte	Moringa energy drink blended with Pineapple
Appearance	8	8	8
Aroma	6.8	7	7.5
Taste	7	6.5	7
Texture	6	8.2	7.2
Overall acceptability	7.8	7.7	7.9

Conclusion

Moringa-based beverages represent an exciting intersection of health, flavor innovation and sustainability in the modern beverage industry. Drinks such as moringa and Mint Iced Tea, Moringa Latte and Moringa energy drink blended with Pineapple are gaining attention not just as alternatives to traditional drinks but as functional beverages with added health values. Moringa is rich in vitamin C, protein, iron and antioxidants, when is combined with mint, pineapple and plant-based milk, these drinks offer unique benefits. Mint adds cooling, digestive benefits, while pineapple contributes natural sweetness. These beverages cater to a growing audience looking for natural, caffeine-free, plant-based, and low sugar alternatives to traditional sodas, coffees, and energy drink. With the global functional beverage market expanding, these moringa-infused drinks can find success in wellness cafes, organic supermarkets, and even fitness centers. Moringa is a drought-resistant, fast-growing tree, making it a highly sustainable ingredient. As awareness of Moringa's health benefits continues to rise, these innovative drinks formats have strong potential to thrive in both local and global health-conscious markets, paving the way for a new era of sustainable wellness beverages.

Reference

- Brilhante, R. S. N., Sales, J. A., Pereira, V. S., Castelo, D. D. S. C. M., de AguiarCordeiro, R., de Souza Sampaio, C. M., ...& Rocha, M. F. G. (2017). Research advances on the multiple uses of Moringa oleifera: A sustainable alternative for socially neglected population. *Asian Pacific journal of tropical medicine*, 10(7), 621-630.
- El-Rahim, A., Eman, M., El-Gawwad, A., Rabie, M. M., & El-Gammal, R. E. (2017). Preparing New Beverage from Moringa oleifera Leaves. *Journal of Food and Dairy Sciences*, 8(7), 303-307.
- Famakinwa, A., Ngcoko, A., Nicholas, E., Olubi, O., Oguntibeju, O. O., Van Wyk, J., & Obilana, A. (2024). Chemical and functional properties of nutrient-dense beverages developed from underutilised crops. *Plant Science Today*, 11(1), 45-53.
- Hassan, M. A., Xu, T., Tian, Y., Zhong, Y., Ali, F. A. Z., Yang, X., & Lu, B. (2021). Health benefits and phenolic compounds of Moringa oleifera leaves: A comprehensive review. *Phytomedicine*, 93, 153771.
- Olusanya, R. N. (2018). The nutritional composition and acceptability of moringaoleifera leaf powder (MOLP)-supplemented mahewu: A maize meal-based beverage for improved food and nutrition security (Doctoral dissertation, University of KwaZulu-Natal, Pietermaritzburg).
- Pareek, A., Pant, M., Gupta, M. M., Kashania, P., Ratan, Y., Jain, V., ...& Chuturgoon, A. A. (2023). Moringa oleifera: An updated comprehensive review of its pharmacological activities, ethnomedicinal, phytopharmaceutical formulation, clinical, phytochemical, and toxicological aspects. *International journal of molecular sciences*, 24(3), 2098.
- Budnimath, S. H., Bhuvaneshwari, G., Ganiger, V. M., Jagadeesh, S. L., Goudar, G., Patil, S. N., & Chandrashekar, V. M. (2023). Physical, reconstitution and phenolic properties of instant drink mix prepared with Moringa oleifera leaf, raw banana and whey protein concentrate. *Measurement: Food*, 11, 100108.
- Gupta, A. K., Das, T., Jha, A. K., Naik, B., Kumar, V., Rustagi, S., & Khan, J. M. (2024). Encapsulation of debittered pomelo juice using novel Moringa oleifera exudate for enrichment of yoghurt: A techno-functional approach. *Food Chemistry*, 139937.
- Huang, X., Liang, K. H., Liu, Q., Qiu, J., Wang, J., & Zhu, H. (2020). Superfine grinding affects physicochemical, thermal and structural properties of Moringa Oleifera leaf powders. *Industrial crops and products*, 151, 112472.
- Javed, F., Tehseen, S., Ashfaq, F., Sameen, A., Khalid, W., Batool, R., ... & Nayik, G. A. (2024). Stabilization of Ficus carica L. Drink by utilizing varying levels of ultrasound-assisted moringa extract as a natural preservative. *Ultrasonics Sonochemistry*, 111, 107133.
- Shaik, M. I., Hamdi, I. H., & Sarbon, N. M. (2023). A comprehensive review on traditional herbal drinks: Physicochemical, phytochemicals and pharmacology properties. *Food Chemistry Advances*, 100460.
- Tao, M., Guo, W., Liang, J., & Liu, Z. (2025). Unraveling the key cooked off-flavor compounds in thermally sterilized green tea beverages, and masking effect of tea raw material baking. *Food Chemistry*, 464, 141671.
- Khupse, S. M., Chavan, K. D., & Desale, R. J. (2019). Sensory quality of drumstick (Moringa oleifera L.) whey beverage. *IJCS*, 7(6), 32-35.
- Noaman, Z. M., Ashoush, I. S., Mahdy, S. M., & Yousef, E. E. (2022). Enhancement sensory, physicochemical and antioxidant properties of moringa functional beverages. *Egyptian Journal of Nutrition*, 37(1), 17-44.

Assessment and Impact of Green Synthesized ZnO Nanoparticles against Soil Borne Fungal Pathogens, Jorhat, Assam, India.

*Swapnila Roy

*Galgotias University, Yamuna Expy, opposite Buddha International Circuit,
Sector 17A, Greater Noida, Uttar Pradesh 203201
Corresponding Author mail id: swapnilaroy@gmail.com

Abstract—This study explores a green production approach for zinc oxide nanoparticles from plants such as *Allium cepa*, *Piper nigrum*, *Curcuma longa*, and *Curcuma caesia* to treat soil-borne fungal diseases. Nanoparticles from diverse plant sources were synthesised and evaluated at varying concentrations against soil-borne fungal diseases such as *Fusarium* sp., *Rhizoctonia* sp., and *Colletotrichum* sp. In comparison to other plant sources, potential ZnO NPs were produced from *C. longa* at a concentration of 150 ppm. The UV-vis spectral examination demonstrates the Plasmon Resonance Property while also validating the formation of nanoparticles with a peak at 438 nm and the reduction of metal ions. Using dynamic light scattering, the synthesised nanoparticles were discovered to be 63.65 nm. The zeta size, which quantifies the charge of nanoparticles, was found to be negative at -68.30 mV. The irregularly used TEM was discovered to be 74.44 nm in size. The functional group of the synthesised ZnO NPs was determined via FTIR analysis. The spectral peaks at 866.29 cm and 836.10 cm in the current study indicated the presence of aromatic rings (C-H). Maximum mycelial development was seen at 200 ppm ZnO NP concentration generated from *C. longa*. This study reveals that ZnO nanoparticles at a concentration of 150 ppm are effective in suppressing soil-borne pathogens, particularly those belonging to the *Fusarium*, *Rhizoctonia*, and *Colletotrichum* sp. This will aid in the development of effective new fungicides for the control of these three key soil-borne diseases.

Keywords— Soil-borne fungal pathogens, Plants, Zinc oxide nanoparticles.

Introduction

Soil has rich microbial diversity either provides benefits or harmful effects to the plants and animals including humans. However several microorganisms including bacteria, virus and fungi infects the plants and causes various diseases in phyllosphere and rhizosphere. Of which fungi and viruses are to be consider as most dangerous because it causes heavy loss in the productivity. *Fusarium*, *Rhizoctonia*, *Pythium*, *Sclerotinia*, *Verticillium*, and *Phytophthora* are the major causative soil-borne pathogens having the ability to reduce the yield up to 50-75% to the economically important crops like cotton, wheat, fruits, maize, and vegetables. For example mycotoxins produced by *F. graminearum* and *F. verticillioides* induce cob rot in maize. *Rhizoctonia solani* severely damages *Brassica napus* at seedling stage and thus results in 80-100% yield losses. When signs like chlorosis, stunting, wilting, and mortality appear in the aerial regions of the plant becomes

major challenge to diagnoses the soil-borne pathogens. Due to their extensive host range, protracted life cycle on organic matter and plant debris, capacity to persist as free-living organisms, and capacity to produce resistant structures in the absence of a host plant, including oospores, microspores, sclerotia, and chlamydospores. Similarly the symptoms of root rot, stunting, chlorosis, damping of seedlings, blackening of the roots, bark cracking, and dieback of branches and twigs make diagnosing soil-borne diseases are the challenging (Patil et al. 2021) task. On the other side nonspecific symptoms and mimic symptoms i.e. physiological disorders and water stress (Astrom and Gerhardson 1988) becomes another challenge. So, disease management on soil-borne pathogens is becoming major threat to the agricultural field.

In recent years development of nanotechnology becomes more popular method for the management of most of the agricultural diseases due to its environmental benefit

(Tasqeen et al. 2024). Nano medicines from biological origin at very low level efficiently control maximum diseases and it also minimizes the usage of chemical practices in the agricultural field. Application of nanoparticles to the plant parts through seed, soil and leaves to control or protect plants from pathogens are adopted (Khan and Rizvi 2014, Barot et al. 2024). The nanoparticles exhibit high reactivity against huge microorganisms and are even smaller than viruses (Pulugu Sai et al. 2020). Since they differ from their conventional counterparts in terms of their specific physical and chemical properties, nanoparticles, (NPs) have drawn increased attention (Stoimenov et al. 2002, Chandio et al. 2024). ZnO NPs are become more common

reasonably renewable and simple to use (Miri et al., 2019).

3. Experimental

3.1 Geographical site

The upper Brahmaputra Valley zone of Assam, between latitude 26°45'N and longitude 94°13'E, contains the Jorhat District of Assam, which mostly comprises the plains of the Brahmaputra Valley. Its 2,85,332-hectare geographical area is split into 1,52,900 acres of cropland (Figure 1).

3.2 Synthesis of ZnO NPs

Fresh plant materials of *Allium cepa*, *Piper nigrum*, *Curcuma longa*, *Curcuma caesia*, were brought to the Department of Plant Pathology, Nanotechnology Laboratory at the Assam Agricultural University in Jorhat,

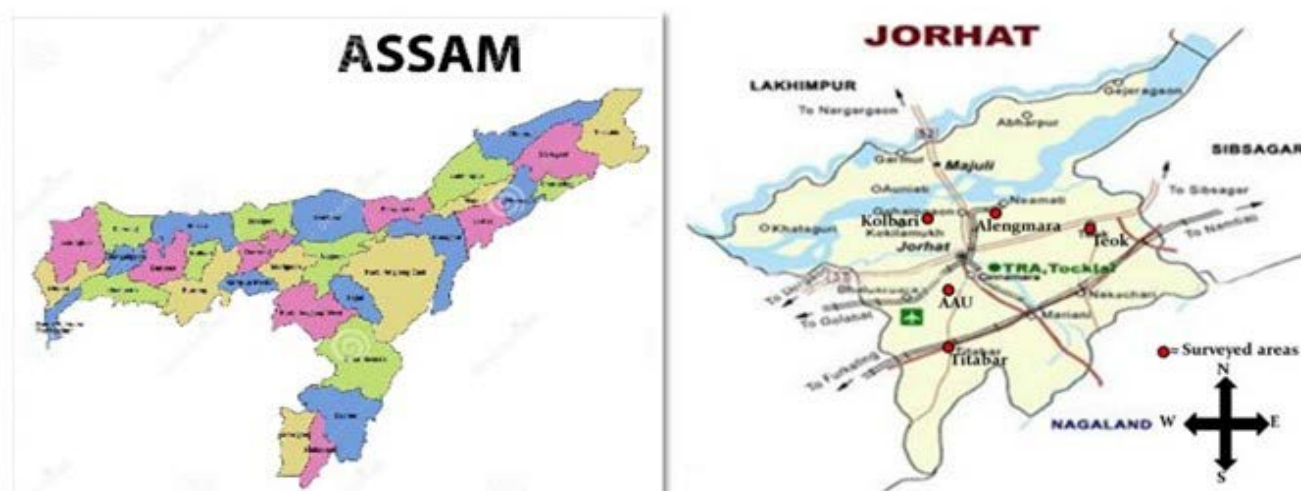


Fig 1. Study area of Upper Brahmaputra Valley Zone, Assam

because they are easier in preparation and less expensive than the others. When compared with other organic materials, ZnO exhibits improvement in heat resistance, greater selectivity, and durability. Zinc is the vital element to human health that can be supplemented to the human life (proteins and enzymes) in the form of zinc oxide (ZnO). So, the biocompatibility of ZnO NPs with human cells is also a good (Padmavathy and Vijayaraghavan, 2008) and stronger fungicidal activity that may be exhibited in the production of Zn-based agricultural compounds. Zinc is an antioxidant can shield the skin from the sun, wind, and ageing (Prasad et al. 2014).

Numerous methods, including as spray pyrolysis, hydro (solve) thermal, direct deposition, sol-gel, and chemical vapor deposition, have been adopted to produce ZnO NPs. The search for an ecologically friendly synthetic route (EFSP) or biosynthetic technique has become more popular in recent years due to the fact that certain approaches are time-consuming, need specialized equipment, or require precise experimental conditions. So NP productions from plant sources are the sustainable material and are

Assam. After being thoroughly cleaned with tap water and then distilled water to get rid of any major debris, the materials were left to air dry. The materials were dried at 500°C for an hour (the outer skin of rhizomes of *Curcuma longa*, *Curcuma caesia* were removed before dry at 500°C). To prepare smash 5g of dried materials were taken and use 25 ml of deionized water to the mortar and pestle. At 40°C, the extract was kept after being filtered through Whatman No.1 filter paper. A beaker containing 50 ml of 0.1 M Zinc nitrate hexahydrate solutions was taken and stirred with a magnetic stirrer. To maintain the pH value of the mixture at alkaline condition, 1 ml of 1 M NaOH was gradually added to the solution along with 1 ml of plant extract. After two hours of stirring, the mixture showed white precipitate and it subjected to centrifugation for 10 minutes at 10,000 rpm. The pellet after centrifugation was collected and it cleaned with dis.H₂O twice and once with ethanol. Finally the ZnO NPs powder was gathered after the pellet was dried for an entire night at 800°C in a hot air oven (Baranitharan et al., 2021).

Characterization of ZnO NPs

UV-vis spectrometer analysis

Several compounds are said to absorb visible or ultraviolet light using this mechanism. When a specific frequency of light is transmitted through the samples, the transmittance % is calculated. This spectrophotometer study records the optical density (O.D.) or intensity of absorption (A) as a function of wavelength. A direct correlation exists between absorbance and the path length (L), and the concentration of absorbing species (C). According to Beer's law,

$$A = \epsilon CL$$

Where, ϵ is a constant of proportionality, called the absorptivity coefficient.

Dynamic light scattering (DLS) analysis

ZnO NPs average particle size is investigated using DLS, which is based on the laser diffraction method. The produced samples were subjected to three or four sonications before analysis. Then, using a computer-controlled particle size analyzer, the distribution of particles in the sample was examined. The poly disparity index (PDI) was calculated using Malvern software, and its definition is as follows:

$$\text{PDI} = \text{Standard deviation of } Dz (\text{z average}) / (Dz)$$

The diameter of the z-average (D_z), volume average (D_z), and number average (D_n) for each particle system using DLS were measured with a Zetasizer Nano ZS (Malvern Instruments).

Zeta potential

An oppositely charged thin layer of ions are attracted to the surface of nanoparticles due to their surface charge. This double layer of ions transport the NP as it diffuses throughout the solution. Zeta potential is the name given to the electric potential at the double layer border, which is typically measured in the range of +100 and -100 mV. A key method for estimating the long-term stability of NPs and figuring out their surface charge in colloids, or solutions, is the zeta potential. The particle dispersion in liquid was examined using a computer control charge analyzer (Zeta sizer, Nanoseries, Malvern instrument Nano Zs, 2000) after 2 ml of the sample was obtained in a cuvette for the zeta potential investigation.

Transmission Electron Microscopy (TEM)

An accelerating voltage of 20 kV was used to conduct a 20,000X magnification TEM investigation at Tezpur University in Tezpur. Clarification of the nanoparticles size and form was achieved by the utilization of TEM (JEM-

2100). Aliquots of the ZnO NPs solution were placed on a carbon-covered copper grid and allowed to dry naturally while TEM images were captured.

Selected Area Electron Diffraction (SAED) pattern

Information about a nanoparticle's crystallite, namely the electron diffraction pattern from a specific area, can be found in the SAED pattern. By using this technique, one can ascertain if the material is poly nano-crystalline – a mixture of small, ring-shaped spots- or amorphous, or crystalline – a mixture of brilliant spots-with each spot originating from Bragg reflection from a single crystallite.

Potato Dextrose Agar (PDA) medium

To make PDA medium, 39.0g of pre-made PDA powder (Hi Media Laboratories Ltd.) was suspended in 1000 milliliters of distilled water. Boiling was adopted to achieve proper solution. HCL or NaOH were used to keep the pH at 7.0 once it was measured. The containers were autoclaved (Equitron, Medica Instrument) for twenty minutes at 121°C with 15 pounds of pressure per square inch. Finally the medium have been added to culture tubes and Erlenmeyer flasks and sealed with non-absorbing cotton.

In-vitro assay of ZnO NPs against target pathogens

A food poisoning assay (Grove and Moore, 1962) was used to assess the antimicrobial efficacy of biosynthesized ZnO NPs in vitro against three pathogens. A suggested drug, Amistar@0.1%, was contrasted. The Food Poison Technique was used on PDA, which was poisoned at the proper concentration, placed into a sterile petri plate, and left to harden. Following the process of solidification, the middle-ager plugs that were cut with a sterile cork borer that contained the virus got infected. Standard PDA medium was used as a control.

Every plate was kept in an incubator with B.O.D. (R.E.I.C.O. BOD) at a temperature of $28 \pm 1^\circ\text{C}$ until the control group showed signs of full growth. When the mycelia in the control plate approached the edge of the Petridis, the degree of mycelia growth inhibition was measured. The effectiveness trial employed the following combinations of treatments:

T₁: *Allium cepa* mediated ZnO NPs @ 1000ppm

T₂: *Piper nigrum* mediated ZnO NPs @1000ppm

T₃: *Curcuma caesia* mediated ZnO NPs @1000ppm

T₄: *Curcuma longa* mediated ZnO NPs @1000ppm

Percent growth inhibition over control = $100 \times \{ (D_c - D_t) / D_c \}$,

Where, D_c = Average diameter of fungal growth in control.

Dt = Average diameter of fungal growth in treatment.

Statistical analysis

CRD was used to do the statistical analysis of the data. The collected data were statistically analyzed using Fisher's analysis of variance. Researchers were able to assess the significance of variation among the data by computing the "F" value and comparing it with the tabular value of "F" at the 5% level of probability. The crucial difference (CD), which was used to compare the treatment means among themselves, was calculated as follows:

$$\text{C.D. at 5\%} = S. Ed \times \sqrt{t' \cdot 5\% \text{ (at error d.f.)}}$$

With the following formula, the standard error of differences (S. Ed) was determined:

$$S. Ed. = \sqrt{\frac{2 \times \text{Error Mean Square}}{\text{Number of Replication for each treatment}}}$$

Where, S. Ed. = Standard error of difference

't' 5% = "t" for error d.f. at 5% level of probability

By multiplying the S. Ed by the necessary tabular number for error degrees of freedom, the significance and non-significance of the treatments were determined at the 5% probability level.

Results and Discussion

Production of ZnO NPs

Zinc nitrate was found to become a milky, turbid solution upon the addition of sodium hydroxide. ZnO NPs were produced by combining various plant extracts (*Allium cepa*, *Piper nigrum*, *Curcuma caesia* and *Curcuma longa*). A white precipitate, zinc hydroxide, was visible at the beaker's bottom after 60 minutes. After gathering the precipitate, the solutions were centrifuged at 10,000 rpm for ten minutes. By extracting the pellet and drying it in a hot air oven, white power (ZnO NPs) was produced. The functional group, size, shape, crystallinity, and surface charge were evaluated using different instruments (Figure 2). Similar to this, Raut et al. (2013) created ZnO NP using an *Ocimum tenuiflorum*-leaf extract showed nanoparticles had an average size of 13.86 nm, which was validated by the solution's changing to a pale yellow color upon precipitation. The investigation's zinc oxide nanoparticle creation is confirmed by the color changing to creamy white or white used by Selim et al. (2020) on *Deverra tortuosa*-aqueous extract to synthesis of ZnO NP. The mechanism of ZnO NP production was explained previously (Sukri et al. 2019). Visible electrons in the phytochemical components were shown to contribute to the stabilization of the positively charged Zn²⁺ ions. The Zn²⁺ complex ions were then thermally annealed to produce ZnO nanoparticles.

Zinc oxide nanoparticles were made and then reduced, capped, and stabilized using aqueous extracts from the fruit *Myristica fragrans* (Barzinjy et al. 2020).

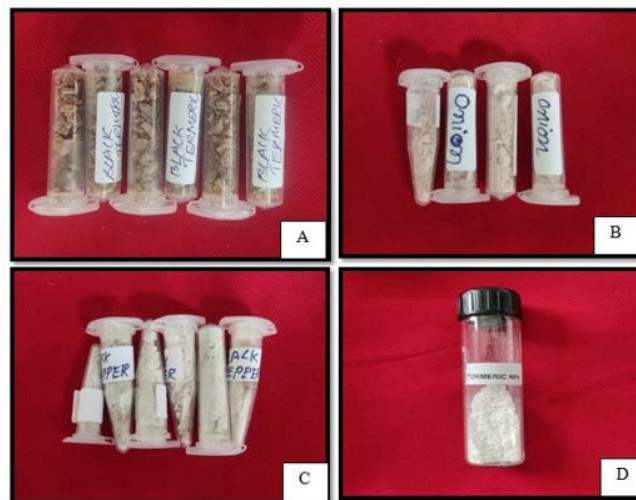


Fig 2. ZnO NPs from A) *Curcuma caesia* B) *Allium cepa* C) *Piper nigrum* D) *Curcuma longa*

UV-vis spectrometer analysis

UV-vis spectroscopy was performed in a wavelength range of 25-600 nm on synthesized ZnO NPs. Table 1 and Figure 3 A,B,C, and E illustrate the resultant Surface Plasmon Resonance (SPR) band at various wavelengths. This investigation verified ZnO NPs formation. Present work reveals that the findings of Arab et al., 2021 and who found that ZnO NPs made from *C. longa* had an absorbance peak at 365 nm. Yu et al., (2006) state that the inherent band gap of ZnO NPs, which is caused by electrons shifting from the valence band to the conduction band, is responsible for the creation of an absorption band at wavelengths less than 400 nm. Our results agree with those of a previous investigation (Fuku et al., 2016) that showed ZnO NP production at wavelength of 366 and 509 nm. Using Tauc's plot technique, found that the synthesized ZnO NPs had band gap energy of 3.4 eV (Jan et al., 2021; Siva et al., 2020). Previous research determined ZnO NPs optical band gap energy to be 3.39 eV (Ramesh et al., 2015). In a different study, the surface Plasmon vibrations of biogenic zinc oxide nanoparticles produced using aqueous *Punica granatum* leaf extract produced an absorbance peak at 382 nm, converting zinc nitrate hexahedrate into ZnO NPs (Singh et al. 2019). The greatest percentage disintegration of Methylene Blue dye molecules was recorded at 98.0% following 60 minutes of exposure to UV radiation. (Alzahrani et al. 2023).

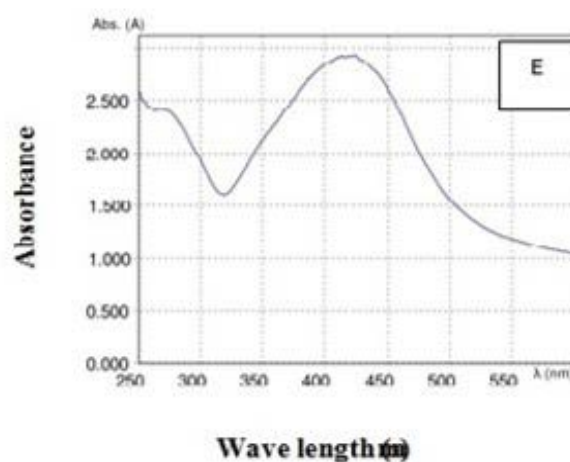
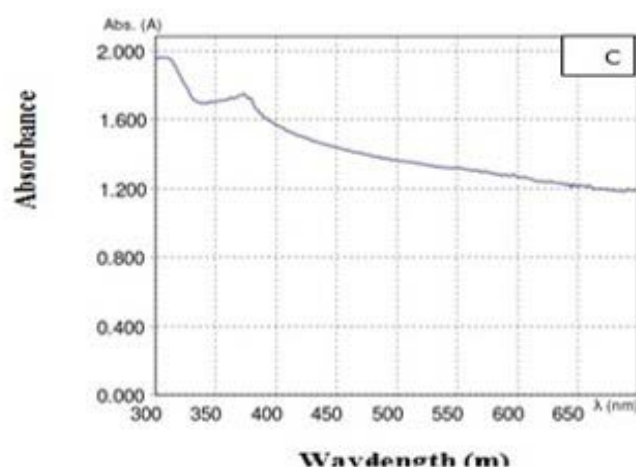
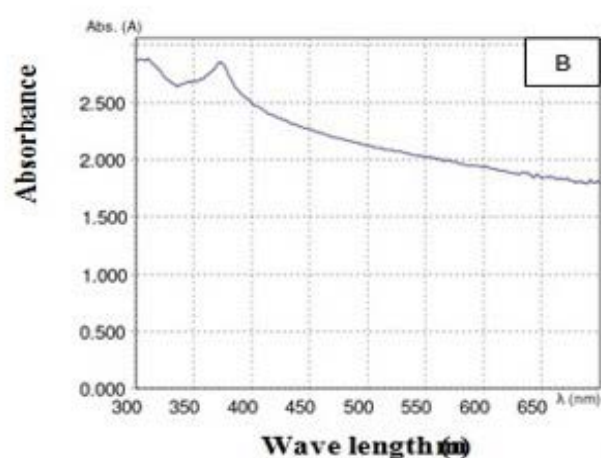
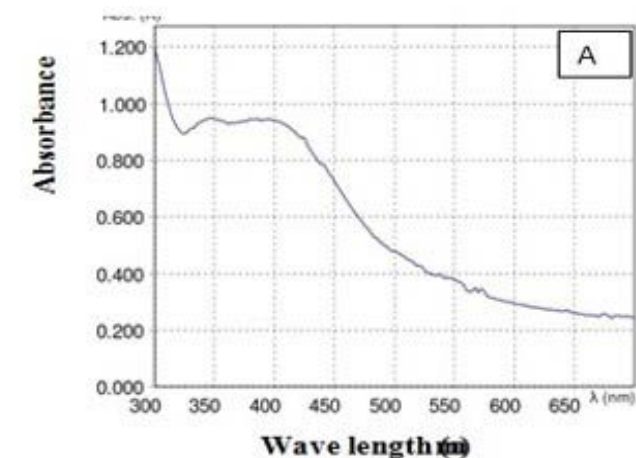
Table 1. Analysis of UV-Vis spectrophotometer

Sl. No.	Source	Wavelength
1	Allium cepa	350 nm
2	Piper nigrum	386nm
3	Curcuma caesia	342nm
5	Curcuma longa	438nm

was 0.029, which is higher than 0.10.

Zeta potential

Due to their tiny size, nanoparticles are very unstable and agglomerate or aggregate in an effort to stabilise themselves. They are stable as a result of the surface's potential charges. To determine the surface characteristics of the nanoparticles,



Dynamic light scattering (DLS) analysis

Using this technique, the synthesised NP's average particle size was determined. This method was also applied to measure the polydispersity index (PDI), hydrodynamic sizes, and particle aggregation in the suspension.

DLS analysis revealed that ZnO NPs had an average size of 63.65 nm and a PDI of 0.029 (Figure 4). With a scale of 0 to 1, the PDI is a dimensionless metric. Values below 0.10 are considered significantly monodispersed, while those over 0.10 are considered polydispersed.

According to Huges et al. (2015), the synthesised ZnO NPs in this work were considered polydispersed since their PDI

the zeta potential value was employed. It was determined that the synthesised ZnO NPs were negatively charged based

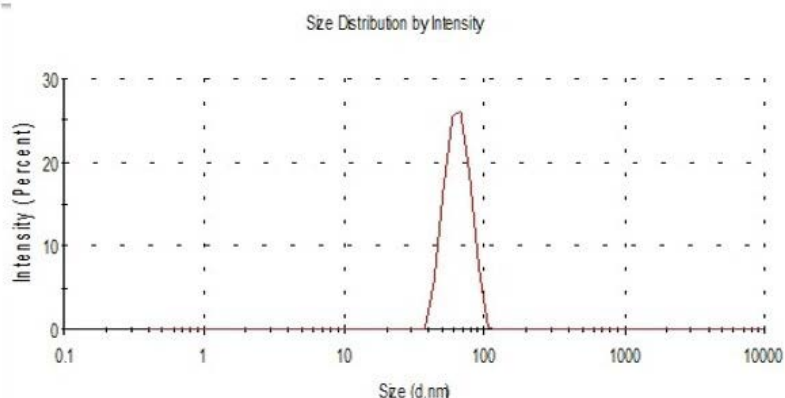


Fig 4. Dynamic Light Scattering analysis of ZnONPs obtained from C. longa

on their zeta potential, which was -68.30 mV (Figure 5).

Since their zeta potential value was found to be in the region of 30 mV, they were assumed to be stable in nature and to have a very little chance of agglomerating.

These results showed that the synthesised ZnO NPs were stable and had a minimal probability of agglomeration.

Previously, Chaudhuri and Malodia (2017) noted that ZnO NPs had a negative zeta potential value of -20.7 mV.

More biogenic ZnO NPs were found than those found by TEM analysis as a result of the creation of additional hydrate layers on the nanoparticle surface (Sattati et al., 2020). Based on this observation, it was discovered that the majority of the capping biomolecules on the biosynthesized ZnO NPs composed of negatively charged groups (Barzinijy and Azeez 2020). They observed that a negative value stabilizes nanoparticles by inducing repulsion between them. This investigation confirms the results of Nallamuthu et al., (2015), who found that low agglomeration and suspension stability are best achieved at a zeta potential of ± 30 mV. Using DLS and zeta potential studies of biogenic ZnO NPs, the average particle size and charge of biosynthesized ZnO NPs were ascertained (Ezealisiji et al., 2019). The biogenic ZnO NPs measured negative charge showed that the produced nanoparticles were repelled by electrostatic forces (Al-Kordy et al. 2021).

Fourier transforms infrared spectrometer (FTIR) analysis

Through FTIR analysis, the functional group of the synthesized ZnO NPs was determined. The presence of aromatic rings (C-H) with certain types of bonds, namely meta disub benzene and paradisub benzene, was shown by the spectral peaks of the current study at 866.29 cm and 836.10 cm. infrared bands with corresponding widths of 670-700 cm, 540-760 cm, and 500-600 cm were used to depict the C-H (vinyl), C-X (chloroalkanes), and C-X (bromoalkanes) vibrations (Figure 6). In addition, presence of an aromatic ring is indicated by the peaks at 812.6, 885.2, and 834.9. Similar findings were reported by Mohammad pour et al. (2012) in the ZnO NPs spectra, which show a prominent and wide peak in the 3500-3300 region that they attributed to a carbonyl bond. The closer region contains the peaks of the N-H spanning from the primary amine and type II amide. The O-H stretching of the extract's

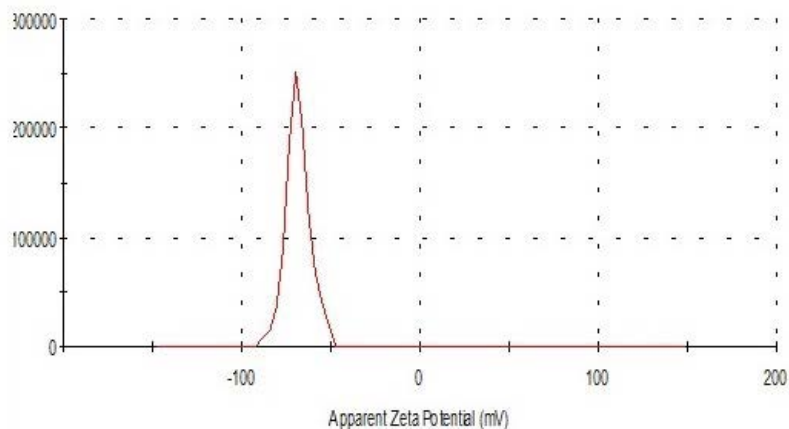


Fig.5. Zeta potential analysis of ZnONPs obtained from *C. longa*

phenolic components is demonstrated by an abrupt band at 3427.99 cm⁻¹, indicating the green production of selenium nanoparticles mediated by *Moringa citrifolia* leaf extract (Nagalingam et al. 2022). Another work utilizing aqueous leaf extract of *Aegle marmelos* proved the green synthesis of silver nanoparticles with the development of an absorption band at 3339 cm⁻¹, which can be attributed to O-H stretching of phenolic compounds (Rao and Paria 2013). The broad absorption band at 3427.99 cm⁻¹, which is attributable to O-H stretching of free hydroxyl groups, may be associated with the polyphenolic components of pomegranate extract (Ifeyanichukwu et al., 2020). The ZnO signal detected at 469 cm⁻¹ might be the result of vibrations caused by bonds between zinc and oxygen (Nimbalkar and Patil 2017).

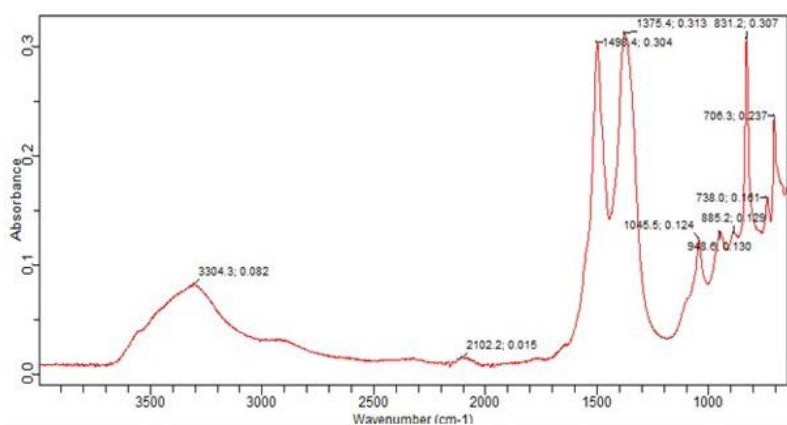


Fig 6. FTIR spectra of ZnONPs obtained from *C. longa*

Transmission electron microscopy (TEM) study

NPs are more effective when they are smaller and have a bigger surface area; therefore, it is important to explore NP form and size. ZnO NPs were measured for size and morphology using TEM at a magnification of 20,000X and

an accelerating voltage of 200 kV. TEM analysis revealed that the synthesized ZnO NPs were 74.44 nm in size and had an irregularly spherical morphology (Figure 7). TEM analysis of ZnO NPs revealed that their average particle size was 22.84 nm (Yassin et al., 2022). We have confirmed the green synthesis of ZnO NPs using pomegranate peel extract, with spherical and hexagonal shapes and an average particle size diameter of 32.98 nm. Their findings and ours are in agreement (Sukri et al., 2019). The biomolecules from the *Punica granatum* extract also immobilized to the surface of the nanoparticles during the synthesis, enabling TEM micrography to disclose the core-shell structure of the biosynthesized ZnO NPs (Barani et al. 2021). After TEM investigation on the nature and shape of the synthesized ZnO NPs, it was discovered that ZnO NPs with a size of 74.44 nm had an irregularly spherical shape. The irregular spherical form was also observed in the ZnO NPs synthesized by Talam et al., (2012). According to the TEM elemental composition of pure ZnO NPs, the nanoparticles consisted of Zn (71.31%), O (26.56%), and C (2.11%). The as prepared ZnO NPs purity is confirmed by their high Zn and O concentration (Navas et al., 2020). With respect to the ZnO-Ag nanocomposite, the Ag peak confirms that Zn (53.46%), O (28.75%), Ag (14.91%), and C (2.88%) were used to produce (Choudhary et al. 2019).

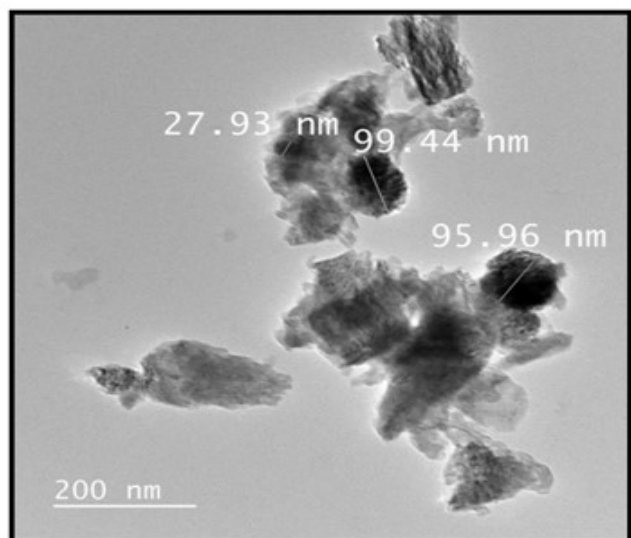


Fig 7. TEM analysis of ZnONPs obtained from *C. longa*

In-vitro efficacy of ZnO NPs against *Colletotrichum* spp, *Rhizoctonia* spp and *Fusarium* spp

Observation of oil globules are under 40X magnification (Figure 8A) microscope, which are consistent with *Colletotrichum* species. Right angle hyphae with constriction were seen for *Rhizoctonia* spp., at 40X (Figure 8B), while microconidia were seen for *Fusarium* spp. at

40X (Figure 8C).

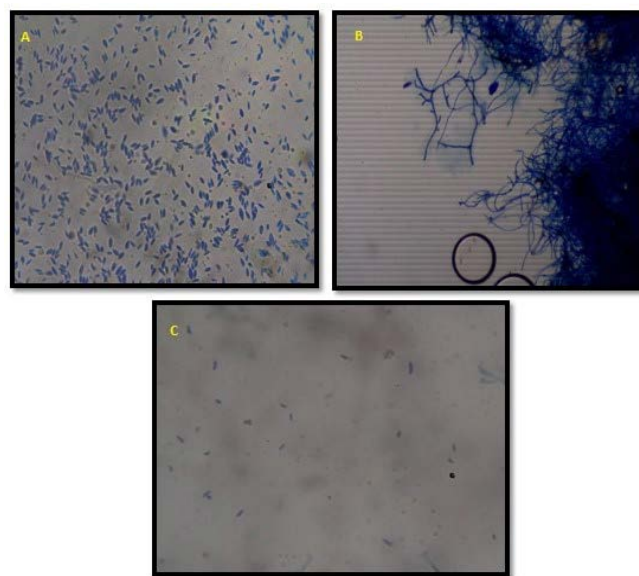


Fig 8. Microscopic observation of *Colletotrichum* spp., *Rhizoctonia* spp., and *Fusarium* spp.

The most efficient source of ZnO NPs was determined by conducting a preliminary investigation on the in vitro efficacy of ZnO NPs at 1000 ppm. The target soil-borne disease's ability to thrive was suppressed by plant extracts (*A. cepa*, *P. nigrum*, *C. caesia* and *C. longa*). For *Colletotrichum* spp., *Rhizoctonia* spp., and *Fusarium* spp., ZnO NPs derived from *C. longa* showed the highest percentage inhibition of 67.69%, 58.82%, and 52.67% (Table 2 & Figure 9 to 11). *C. longa* mediated ZnO NPs were chosen at three distinct concentrations (100 ppm, 150 ppm, and 200 ppm) in order to standardize the dosage of nanoparticles. The findings showed that the target infections ability to expand radically was hindered by higher concentrations. However this study concludes that 150 ppm of ZnO NPs from *C. longa* exhibits the maximum zone of microbial inhibitions against *Colletotrichum* spp., *Rhizoctonia* spp., and *Fusarium* spp and the percentage of inhibition is 65.44%, 27.11%, and 52.89% respectively (Table 3 and Figure 12 to 14). The current findings are consistent with those of researchers such as Pariona et al. (2019), who examined the antifungal activity of ZnO NPs at 1000 ppm concentration against three fungal pathogens: *F. oxysporum*, *Rhizoctonia solani*, *Colletotrichum gloeosporoides*. They found that the pathogens mycelia growth was inhibited by 53, 55, and 59 percent, respectively. However, Wani and Shah (2012) found that at 100 ppm concentration of the fungus *Rhizopus stolonifer*, *F. oxysporum*, *Alternaria alternata*, and *Mucor plumbeus*. Merino et al. (2021) examined the effectiveness of ZnO NP at various concentrations ranges from 1500 to 3000

ppm and he found 81-33% of microbial inhibition against *F. oxysporum*. It also suppresses the pathogens sporulation by 82.57 to 83.85 percent at these dosages. The huge surface to volume ratio, induction of deformalities in fungal hyphae, agglutinate propensity of mycelium, and liquefaction of cytoplasmic material, which results in the fungus death, were all linked to ZnO NPs antifungal action. They also produce OH-radicals, ROS, and other chemicals that cause fungal cells to die (Arciniegas-Grijalba et al. 2017). Production of ZnO nanoparticles from *Allium*

cepa, *Piper nigrum*, *Curcuma longa* and *Curcuma caesia* was succeeded. Different concentrations of ZnO NPs from different sources were prepared and its microbial efficacy against various fungal pathogens such as *Fusarium* spp, *Rhizoctonia* spp and *Colletotrichum* spp were tested. The nanoparticles from different plant sources are proven the ability to control the target pathogens. But potentiality in control to the various soil borne pathogens have been obtained from *Curcuma longa*.

Table 2. In vitro efficacy of biosynthesized ZnO NPs from different sources at 1000 ppm against *Colletotrichum* spp, *Rhizoctonia* spp and *Fusarium* spp.

Source	<i>Colletotrichum</i> spp		<i>Rhizoctonia</i> spp		<i>Fusarium</i> spp	
	Mycelial growth (Cm)	% of inhibition	Mycelial growth (Cm)	% of inhibition	Mycelial growth (Cm)	% of inhibition
T1 <i>Allium cepa</i> @ 1000ppm of ZnO NPs	4.11	54.36	3.86	57.07	4.32	52.04
T2 <i>Piper nigrum</i> @ 1000ppm of ZnO NPs	4.24	52.93	4.14	53.96	5.74	36.22
T3 <i>Curcuma caesia</i> @ 1000ppm of ZnO NPs	4.80	46.67	7.16	20.44	5.86	34.89
T4 <i>Curcuma longa</i> @ 1000ppm of ZnO NPs	2.91	67.69	3.71	58.82	4.26	52.67
Control	9.00	-	9.00	-	9.00	-
Sed	0.118	-	0.213	-	0.126	-
CD	0.321	-	0.578	-	0.341	-

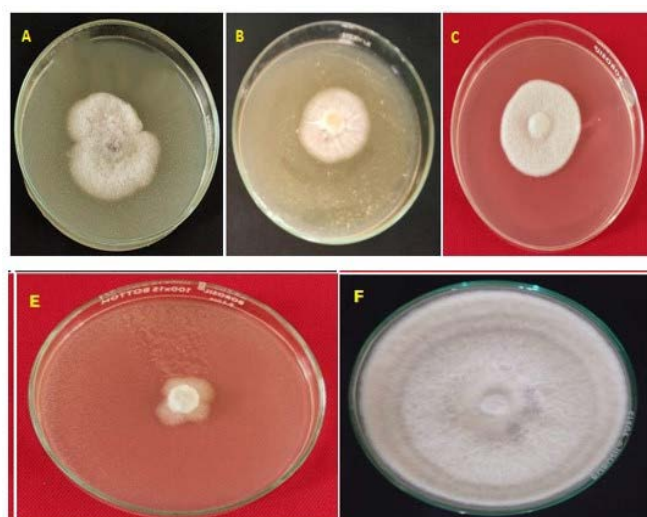


Fig 9. In vitro efficacy of biosynthesized zinc oxide nanoparticles @1000 ppm against *Colletotrichum* spp., A) *Allium cepa* B) *Piper nigrum* C) *Curcuma caesia* E) *Curcuma longa* F) Control



Fig 10. In vitro efficacy of biosynthesized zinc oxide nanoparticles @1000 ppm against *Rhizoctonia* spp., A) *Allium cepa* B) *Piper nigrum* C) *Curcuma caesia* E) *Curcuma longa* F) Control

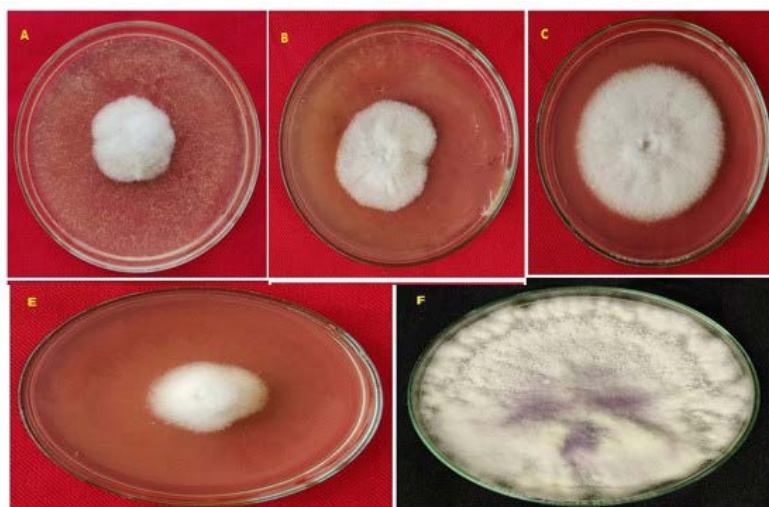


Fig 11. In vitro efficacy of biosynthesized zinc oxide nanoparticles @1000 ppm against *Fusarium* spp.,
A) *Allium cepa* B) *Piper nigrum* C) *Curcuma caesia*
E) *Curcuma longa* F) Control

Table 3. In vitro efficacy of biosynthesized ZnO NPs at different concentrations against *Colletotrichum* spp, *Rhizoctonia* spp and *Fusarium* spp

Source	<i>Colletotrichum</i> spp		<i>Rhizoctonia</i> spp		<i>Fusarium</i> spp	
	Mycelial growth (Cm)	% of inhibition	Mycelial growth (Cm)	% of inhibition	Mycelial growth (Cm)	% of inhibition
T1 <i>Curcuma longa</i> mediated ZnO NPs @100ppm	3.11	53.00	7.11	19.33	4.80	46.67
T2 <i>Curcuma longa</i> mediated ZnO NPs @150ppm	3.88	56.89	6.98	21.78	4.62	48.67
T3 <i>Curcuma longa</i> mediated ZnO NPs @200ppm	4.23	65.44	6.53	27.11	4.24	52.89
T4 Chemical treatment (Amistar @0.1%)	1.20	86.67	1.22	86.44	1.27	85.88
Control	9.00	-	9.00	-	9.00	-
Sed	0.032	-	0.077	-	0.032	-
CD	0.111	-	0.271	-	0.114	-

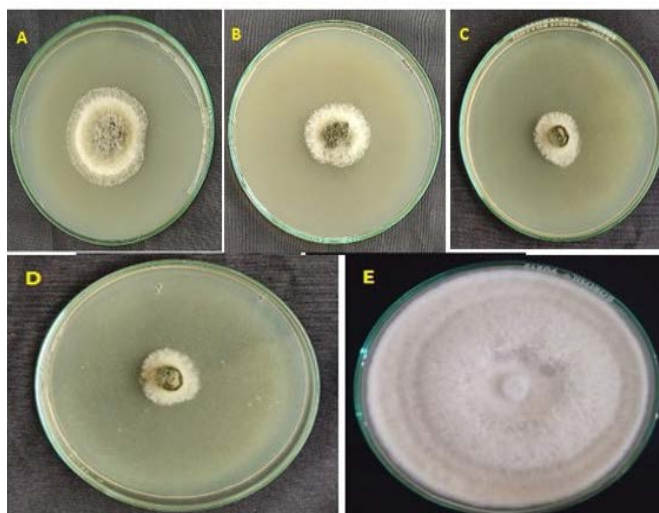


Fig 12. In vitro efficacy of biosynthesized zinc oxide nanoparticles obtained from *C. longa* against *Colletotrichum* spp., A) 100ppm B) 150ppm C) 200ppm D) Amistar 0.1 % E) Control against *Colletotrichum* spp

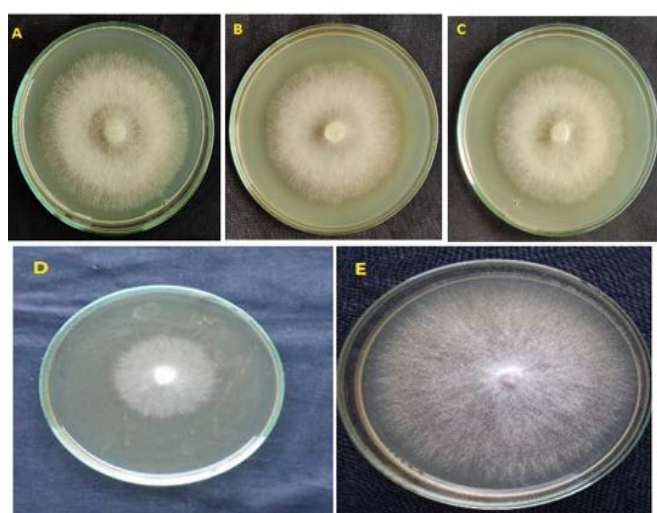


Fig 13. In vitro efficacy of biosynthesized zinc oxide nanoparticles obtained from *C. longa* against *Rhizoctonia* spp., A) 100ppm B) 150ppm C) 200ppm D) Amistar 0.1 % E) Control against *Rhizoctonia* spp.

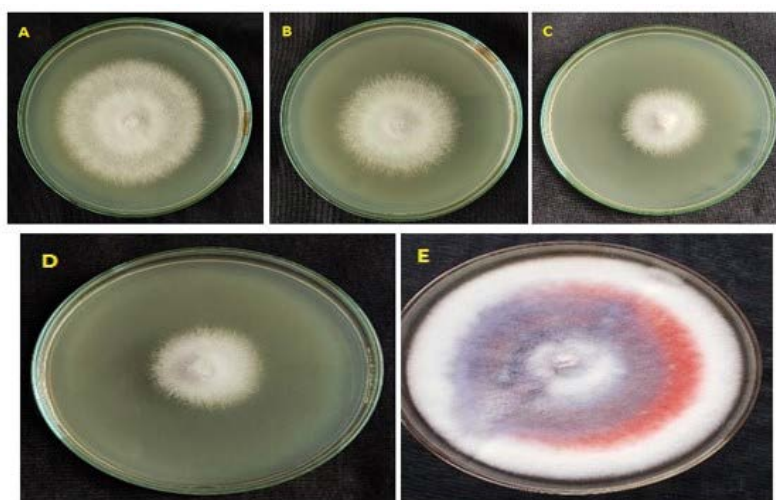


Fig 14. In vitro efficacy of biosynthesized zinc oxide nanoparticles obtained from *C. longa* against *Fusarium* spp., A) 100ppm B) 150ppm C) 200ppm D) Amistar 0.1 % E) Control against *Fusarium* spp.

Novelty

1. Green Synthesis Methodology:

ZnO nanoparticles may be produced sustainably and ecologically by using green synthesis techniques, which usually involve the use of plant extracts or other eco-friendly agents in place of standard chemical synthesis methods. This technique lessens the impact on the environment and uses less harmful chemicals.

2.Enhanced Resistance to Fungal Growth

Green-synthesised ZnO nanoparticles could have special

qualities including more surface area, higher reactivity, and better contact with fungal cells. These characteristics may result in a more potent prevention of fungal growth as compared to chemically synthesised nanoparticles or traditional fungicides.

3.Taking Aim at Pathogens Found in Soil:

Because of their propensity to remain in the soil, soil-borne fungal infections including *Rhizoctonia solani*, *Sclerotium rolfsii*, and *Fusarium* spp. are infamously difficult to manage. It is likely that the study investigates

the direct application of ZnO nanoparticles to plants or soil, evaluating the effects on the growth of fungi and the prevention of illness.

4.Action Mechanism:

The research might reveal new ways that green synthesised ZnO nanoparticles fight fungus growth. They may, for example, damage fungal cell membranes, produce reactive oxygen species (ROS), or obstruct fungal metabolism, which would result in cell death.

Impact:

1.Management of Sustainable Diseases:

Green synthesised zinc oxide nanoparticles provide a potentially less hazardous and sustainable substitute for traditional chemical fungicides. This can be especially helpful for organic farming or places where chemical use is prohibited.

2.Safety in the Environment:

Utilising natural sources for nanoparticle production and green synthesis may lower the chance of environmental pollution and damage to non-target creatures, such as beneficial soil bacteria.

3.Agriculture's Contribution to Nanotechnology:

Through its demonstration of how nanoparticles may be customised for particular uses, like disease management, while maintaining environmental and human safety, the work adds to the expanding area of nanotechnology in agriculture.

In conclusion, the sustainable manufacture, distinctive qualities, and potential for successful control of persistent soil-borne fungal infections are what make green synthesised ZnO nanoparticles unique in their antifungal effects. These attributes also make them a viable tool for managing plant diseases in the future.

Conclusion

Production of ZnO nanoparticles from *Allium cepa*, *Piper nigrum*, *Curcuma longa* and *Curcuma caesia* was succeeded. Different concentrations of ZnONPs from different plant sources such as *Allium cepa*, *Piper nigrum*, *Curcuma longa*, *Curcuma caesia* were prepared. The microbial efficacy against various fungal pathogens such as *Fusarium*spp, *Rhizoctonia*spp and *Colletotrichum* spp were tested. The nanoparticles from different plant sources are proven the ability to control the target pathogens. However present investigation concludes that ZnO nanoparticle at 150ppm concentration is found to be

more effective in suppressing the soil borne pathogens viz *Colletotrichum* spp, *Rhizoctonia* spp and *Fusarium* spp than the other sources. This study may help in development of suitable new fungicide for management of these three important soils borne pathogens.

References

- Patil, R.H.; Kotta-Loizou, I.; Palyzová, A.; Pluháček, T.; Coutts, R.H.A.; Stevens, D.A.; Havlíček, V. Freeing *Aspergillus fumigatus* of Polymycovirus Infection Renders It More Resistant to Competition with *Pseudomonas aeruginosa* Due to Altered Iron-Acquiring Tactics. *J. Fungi*. 2021, 7, 497. <https://doi.org/10.3390/jof8070691>
- Aström, B., Gerhardson, B. Differential reactions of wheat and pea genotypes to root inoculation with growth-affecting rhizosphere bacteria. *Plant Soil* 109, 263–269 (1988). <https://doi.org/10.1007/BF02202093>
- Tasqeen, H., Waseem, M., Hussain, S, Humma Z.E, Baig A, Majeed A. Green synthesis of Ag–CoFe₂O₄ nanocomposites by *Taxus wallichiana* leaf extract for adsorption of Pb⁺² ions from aqueous solution. *Chem. Pap.* (2024). <https://doi.org/10.1007/s11696-024-03415-4>
- Khan MR, Rizvi TF (2014). Nanotechnology: Scope and Application in Plant Disease Management. *Plant Pathology Journal* 13(3): 214-231. <https://doi.org/10.3923/ppj.2014.231>.
- Barot, R.B., Gawande, N.D., Omprabha, S, Kaushal C, Ghosh S, Saha J, Bhatia D, Sankaranarayanan S. Novel carbon nanoparticles derived from *Bougainvillea* modulate vegetative growth via auxin–cytokinin signaling in *Arabidopsis*. *Chem. Pap.* (2024). <https://doi.org/10.1007/s11696-024-03421-6>
- Pulugu Sai, Vijay Kumar, Ankita Garkoti (2020). Applications of Nanotechnology in Plant Disease Management. *International Journal of Science and Research* 9(4), 1506-1508. <https://doi.org/10.21275/SR20423141858>.
- Stoimenov PK, Klinger RL, Marchin GL, Klabunde KJ (2002). Metal oxide nanoparticles as bactericidal agents. *Langmuir* 18, 6679-6686. <https://doi.org/10.1021/la0202374>
- Chandio, A.A., Memon, S., Otho, A, Khalid A, Alotaibi B.S, Balouch A, Ahmed Brohi N, Memon F.N, Memon A.A, Thebo K.H. Supramolecular structural-based fabrication of silver nanoparticles using diamide derivative of calix[4]arene: an efficient antimicrobial agent. *Chem. Pap.* (2024). <https://doi.org/10.1007/s11696-024-03420-7>
- Padmavathy N, Vijayaraghavan R (2008). Enhanced

- bioactivity of ZnO nanoparticles-an antimicrobial study. *Sci Technol Adv Mater* 1;9(3):035004. <https://doi.org/10.1088/14686996/9/3/035004>
- Prasad S, Gupta S, Tyagi AK, Aggarwal B (2014). Curcumin, a component of golden spice: from bedside to bench and back. *Biotechnol Adv* 32: 1053-64. <https://doi.org/10.1016/j.biotechadv.2014.04.004>
 - Miri A, Mahdinejad N, Ebrahimi O, Khatami M, Sarani M (2019). Zinc oxide nanoparticles: Biosynthesis, characterization, antifungal and cytotoxic activity. *Mater Sci Eng C Mater Biol Appl* 104: 109981. <https://doi.org/10.1016/j.msec.2019.109981>
 - Baranitharan M, Saud Alarif, Saad Alkahtani, Daoud Ali, Elumalai K, Pandiyan J, Krishnappa K, Rajeswary M, Govindarajan M (2021a) Phytochemical analysis and fabrication of silver nanoparticles using *Acacia catechu*: An efficacious ecofriendly control tool against selected polyphagous insect pests. *Saudi J Biol Sci* 28:148-156. <https://doi.org/10.1016/j.sjbs.2020.09.024>.
 - Raut JS, Shinde RB, Chauhan NM, Karuppaiyl SM (2013). Terpenoids of plant origin inhibit morphogenesis, adhesion, and biofilm formation by *Candida albicans*. *Biofouling* 29: 87-96. <https://doi.org/10.1080/08927014.2012.749398>.
 - Selim YA, Azb MA, Ragab I, Abd El-Azim MH (2020). Green synthesis of zinc oxide nanoparticles using aqueous extract of *Deverra tortuosa* and their cytotoxic activities. *Scientific Reports* 10, 3445. <https://doi.org/10.1038/s41598-020-60541-1>
 - Sukri, S.N.A.M.; Shameli, K.; Wong, M.M.T.; Teow, S.Y.; Chew, J.; Ismail, N.A. Cytotoxicity and antibacterial activities of plantmediated synthesized zinc oxide (ZnO) nanoparticles using *Punica granatum* (pomegranate) fruit peels extract. *J. Mol. Struct.* 2019, 1189, 57–65. <https://doi.org/10.1016/j.molstruc.2019.04.026>
 - Barzinjy, A.A.; Azeez, H.H. Green synthesis and characterization of zinc oxide nanoparticles using *Eucalyptus globulus* Labill. Leaf extract and zinc nitrate hexahydrate salt. *SN Appl. Sci.* 2020, 2, 991.
 - Yu J, Pressoir G, Briggs WH, Vroh Bi I, Yamasaki M, Doebley JF, McMullen MD, Gaut BS, Nielsen DM, Holland JB, Kresovich S, Buckler ES (2006). A unified mixed-model method for association mapping that accounts for multiple levels of relatedness. *Nature Genetics* 38, 203-208. <https://doi.org/10.1038/ng1702>
 - Fuku, X.; Diallo, A.; Maaza, M. Nanoscaled electrocatalytic optically modulated ZnO nanoparticles through green process of *Punica granatum* L. and their antibacterial activities. *Int. J. Electrochem. Sci.* 2016, 2016, 4682967. <https://doi.org/10.1155/2016/4682967>
 - Jan, F.A.; Ullah, R.; Ullah, N.; Usman, M. Exploring the environmental and potential therapeutic applications of *Myrtus communis* L. assisted synthesized zinc oxide (ZnO) and iron doped zinc oxide (Fe-ZnO) nanoparticles. *J. Saudi Chem. Soc.* 2021, 25, 101278. <https://doi.org/10.1016/j.jscs.2021.101278>
 - Siva, N.; Sakthi, D.; Ragupathy, S.; Arun, V.; Kannadasan, N. Synthesis, structural, optical and photocatalytic behavior of Sn doped ZnO nanoparticles. *Mater. Sci. Eng. B* 2020, 253, 114497. <https://doi.org/10.1016/j.mseb.2020.114497>
 - Ramesh, M.; Anbuvaran, M.; Viruthagiri, G. Green synthesis of ZnO nanoparticles using *Solanum nigrum* leaf extract and their antibacterial activity. *Spectrochim. Acta A Mol. Biomol. Spectrosc.* 2015, 136, 864–870. <https://doi.org/10.1016/j.saa.2014.09.105>.
 - Singh, K.; Singh, J.; Rawat, M. Green synthesis of zinc oxide nanoparticles using *Punica Granatum* leaf extract and its application towards photocatalytic degradation of Coomassie brilliant blue R-250 dye. *SN Appl. Sci.* 2019,1, 624. <https://doi.org/10.1007/s42452-019-0610-5>
 - Alzahrani, E.A.; Nabi, A.; Kamli, M.R.; Albukhari, S.M.; Althabaiti, S.A.; Al-Harbi, S.A.; Khan, I.; Malik, M.A. Facile Green Synthesis of ZnO NPs and Plasmonic Ag-Supported ZnO Nanocomposite for Photocatalytic Degradation of Methylene Blue. *Water* 2023, 15, 384. <https://doi.org/10.3390/w15030384>
 - Hughes, Anna L C; Gyllencreutz, Richard; Lohne, Øystein S; Mangerud, Jan; Svendsen, John Inge (2015): DATED-1: compilation of dates and time-slice reconstruction of the build-up and retreat of the last Eurasian (British-Irish, Scandinavian, Svalbard-Barents-Kara Seas) Ice Sheets 40-10 ka [dataset]. Department of Earth Science, University of Bergen and Bjerknes Centre for Climate Research, PANGAEA, <https://doi.org/10.1594/PANGAEA.848117>
 - Chaudhuri, S.K., Malodia, L. Biosynthesis of zinc oxide nanoparticles using leaf extract of *Calotropis gigantea*: characterization and its evaluation on tree seedling growth in nursery stage. *Appl Nanosci* 7, 501–512 (2017). <https://doi.org/10.1007/s13204-017-0586-7>
 - Sattari, R.; Khayati, G.R.; Hoshyar, R. Biosynthesis and characterization of silver nanoparticles capped by biomolecules by *fumaria parviflora* extract as green approach and evaluation of their cytotoxicity against human breast cancer MDA-MB-468 cell lines. *Mater. Chem. Phys.* 2020, 241, 122438. <https://doi.org/10.1016/j.matchemphys.2019.122438>
 - Barzinjy, A. A.; Hamad, S. M.; Abdulrahman, A. F.; Biro, S. J.; Ghafor, A. A. Biosynthesis, characterization and mechanism of formation of ZnO nanoparticles

- p>using
- Petroselinum crispum*
- leaf extract.
- Curr. Org. Synth.*
- 2020, 17, 558–566.
- <https://doi.org/10.2174/1570179417666200628140547>
- Nallamuthu, I., Devi, A. and Khanum, F. (2015) Chlorogenic Acid Loaded Chitosan Nanoparticles with Sustained Release Property, Retained Antioxidant Activity and Enhanced Bioavailability. *Asian Journal of Pharmaceutical Sciences*, 10, 203-211. <https://doi.org/10.1016/j.ajps.2014.09.005>
 - Ezealisiji, K.M., Siwe-Noundou, X., Maduelosi, B. et al. Green synthesis of zinc oxide nanoparticles using *Solanum torvum* (L) leaf extract and evaluation of the toxicological profile of the ZnO nanoparticles–hydrogel composite in Wistar albino rats. *Int Nano Lett* 9, 99–107 (2019). <https://doi.org/10.1007/s40089-018-0263-1>
 - Al-Kordy, H.M.; Sabry, S.A.; Mabrouk, M.E. Statistical optimization of experimental parameters for extracellular synthesis of zinc oxide nanoparticles by a novel haloalcaliphilic *Alkalibacillus* sp.W7. *Sci. Rep.* 2021, 11, 10924. <https://doi.org/10.1038/s41598-021-90408-y>
 - Nagalingam, M.; Rajeshkumar, S.; Balu, S.K.; Tharani, M.; Arunachalam, K. Anticancer and Antioxidant Activity of *Morinda Citrifolia* Leaf Mediated Selenium Nanoparticles. *J. Nanomater.* 2022, 2022, 2155772.
 - Rao, K.J.; Paria, S. Green synthesis of silver nanoparticles from aqueous *Aegle marmelos* leaf extract. *Mater. Res. Bull.* 2013, 48, 628–634.
 - Ifeanyichukwu, U.L.; Fayemi, O.E.; Ateba, C.N. Green synthesis of zinc oxide nanoparticles from pomegranate (*Punica granatum*) extracts and characterization of their antibacterial activity. *Molecules* 2020, 25, 4521.
 - Nimbalkar, A. R.; Patil, M. G. Synthesis of ZnO thin film by sol-gel spin coating technique for H₂S gas sensing application. *Physica B* 2017, 527, 7–15.
 - Yassin, M.T.; Mostafa, A.A.-F.; Al-Askar, A.A.; Al-Otibi, F.O. Facile Green Synthesis of Zinc Oxide Nanoparticles with Potential Synergistic Activity with Common Antifungal Agents against Multidrug-Resistant Candidal Strains. *Crystals* 2022, 12, 774. <https://doi.org/10.3390/cryst12060774>
 - Barani, M.; Masoudi, M.; Mashreghi, M.; Makhdoumi, A.; Eshghi, H. Cell-free extract assisted synthesis of ZnO nanoparticles using aquatic bacterial strains: Biological activities and toxicological evaluation. *Int. J. Pharm.* 2021, 606, 120878.
 - Talam S, Karumuri SR, Gunnam N (2012). Synthesis, Characterization, and Spectroscopic Properties of ZnO Nanoparticles. *International Scholarly Research Notices* ID 372505. <https://doi.org/10.5402/2012/372505>
 - Navas, D.; Ibañez, A.; González, I.; Palma, J.L.; Dreyse, P. Controlled dispersion of ZnO nanoparticles produced by basic precipitation in solvothermal processes. *Heliyon* 2020, 6, e05821.
 - Choudhary DK, Bhakt P, Kaur R (2019). Essential Role for the Phosphatidylinositol 3,5-Bisphosphate Synthesis Complex in Caspofungin Tolerance and Virulence in *Candida glabrata*. *Antimicrob Agents Chemother* 63: e01794-19. <https://doi.org/10.1128/AAC.01794-19>.
 - Pariona N, Delgado FP, Cereceda SB, Morales-Mendoza JE, Hermida Montero LA, Martinez AI (2019). Shape-dependent antifungal activity of ZnO particles against phytopathogenic fungi. *Applied Nanoscience* 10: <https://doi.org/10.1007/s13204-019-01127-w>.
 - Wani AH, Shah MA (2012). A unique and profound effect of MgO and ZnO nanoparticles on some plant pathogenic fungi. *Journal of Applied Pharmaceutical Science* 2: 40-44.
 - Merino A, Garcia-Oliva F, Fonturbel MT, Vega JA (2021). The high content of mineral-free organic matter in soils increases their vulnerability to wildfire in humid-temperate zones. 395: 115043. <https://doi.org/10.1016/j.geoderma.2021.115043>
 - Arciniegas-Grijalba, P.A., Patiño-Portela, M.C., Mosquera-Sánchez, L.P, Guerrero-Vargas JA, Rodriguez-Paez JE (2017). ZnO nanoparticles (ZnO-NPs) and their antifungal activity against coffee fungus *Erythricium salmonicolor*. *Appl Nanosci* 7: 225-241. <https://doi.org/10.1007/s13204-017-0561-3>.

An Insight on Core-shell Morphology on the Functionality of Solid Oxide Fuel Cell

Madhumita Mukhopadhyay

*School of Chemistry, University of St Andrews, St Andrews, Fife KY16 9ST,
Scotland, United Kingdom*

mm613@st-andrews.ac.uk, madhubanerji@gmail.com

<https://orcid.org/0000-0003-0637-5113>

Jayanta Mukhopadhyay

Energy Materials and Devices Division,

CSIR- Central Glass and Ceramic Research Institute,

Kolkata-700032, West Bengal, India

Academy of Scientific and Innovative Research (AcSIR),

Gaziabad-201002, India jayanta_mu@cgcric.res.in, jmukhopadhyay75@gmail.com

<https://orcid.org/0000-0001-7936-5093>

Abstract—Fuel Cells are the most interesting and updated technology which are renewable energy conversion devices and are Carnot cycle independent. Among various technical design aspects of fuel cells, Solid oxide fuel cells are of prime importance in having highest power efficiency and multi fuel capability. It is capable of amalgamating with intermittent renewable sources like wind, solar etc. as per the geographical feasibility to sustain the overall usable energy demand. Being controlled by electrochemistry, the rate determining process involves simultaneous reactions involving meta stable adsorbed species of oxygen and fuel gases on the electrode catalyst surface. In this context, selection of electrode and tailoring its morphology is important and critical to optimize for maximizing the output and durability of SOFC. The interfacial regions among electrolyte and electrode are important and forms the primary sites for redox reactions. As per the selection of electrodes, these active sites are termed as triple phase (3PB) or double phase (2PB) which controls electrochemistry at interface and controls the long term tunability of the parent system. The role of morphology of the electrode and the electrolyte interface is therefore crucial. Being an example of all solid conversion devices, the primary catalyst viz transitions metals ions are combined with ceramic counterpart (which forms the electrolyte for selective ion transport) to match the thermal compatibility among the adjoining interphases. The present context exemplifies the development of such dual electrodes with specially engineered morphology to restrict the over-ripening of metallic phase during high temperature treatment and operation. As specific case study, we have tried to describe the significance and trail of core-shell microstructure in improving the long term durability of fuel cells. In addition, details on processing conditions are discussed which are unique in rendering the core-shell morphology for selective electrode composition applicable for Solid oxide fuel cells.

Keywords: core-shell morphology; Solid Oxide fuel cell; ceramic processing; interfacial engineering

I. INTRODUCTION

Fuel cell research has received significant importance in the last decade, being an excellent application of renewable energy sector. It is an electrochemical conversion device capable of generating electricity from chemical energy of reactants [1]. Fuel cells, being an open system, require continuous supply of oxidant and fuel gases as the reactants which undergo adsorption, dissociation followed by redox reaction as the simultaneous processes. The efficiency of fuel cells is not limited by Carnot cycle thereby enhancing the power conversion efficiency by more than 70 % compared to internal combustion engine [2]. Among various types of fuel cells classified based on the operating temperature, proton exchange membrane fuel cell (PEMFC) is important in terms of application. In this type, the electrolyte needs to be a carrier of proton with negligible electron conduction to minimize the short circuit issue [3]. In this aspect, the cathode (air electrode) suffers from severe corrosion owing to low pH caused

by proton migration and kinetics. Fuel cells operated at intermediate to high temperature (700-1000oC) are being practiced nowadays due to their improved reaction kinetics and handling ease. The only bottleneck lies in the selection of components being meant to be in solid state. The all-solid components of electrodes and electrolyte materials are required to satisfy compatible coefficient of thermal expansion to avoid cracking and subsequent degradation during operation of the fuel cell. Solid oxide fuel cells (SOFC) could be able to achieve 80 % power efficiency upon combining with heat recovery system. This does not require any water management planning like in PEMFC owing to higher operable temperatures more than 100oC [4-5]. Therefore, fuel cells in all solid states possess numerous advantages of higher efficiency, environmentally friendly, multiple fuel utilization and high waste heat recovery conversion [6]. The high-power conversion efficiency of SOFC is illustrated in Fig.1 which envisages its application in various levels of application (s) ranging from kW-MW

(in the form of stack). It is visible that

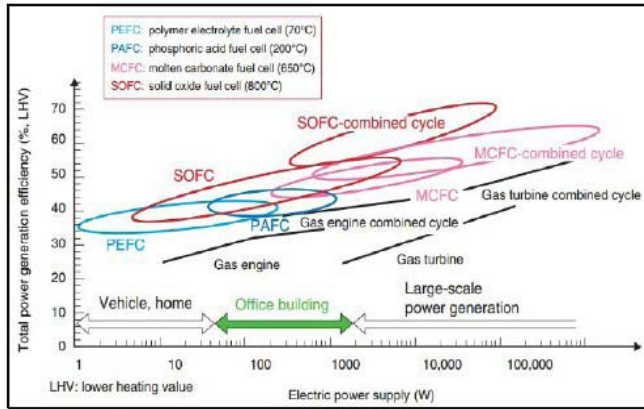


Fig. 1. Application of multiple fuel cells as per energy demand application [6, copyright for image]

SOFC could even be applied for large, distributed power energy systems.

Fuel cells in solid state may be designed primarily in three configurations as per the position and configuration of electrolyte / electrodes. These are termed as electrolyte supported (higher ohmic polarization), electrode support (air/fuel supported with lower polarization loss) and metal support (lower temperature operation) designs [7].

Typical mechanism of fuel cells involves an initial dissociation of oxidant (O_2) at air electrode and that of fuel (maybe hydrogen, natural gas, CO etc) at the fuel electrode followed by adsorption of active species on the surface of electrode catalyst. State of the art fuel electrode/anode is Ni-8 mol % yttria stabilized zirconia (YSZ) and air electrode as doped perovskite oxides eg. Sr doped $LaMnO_3$ or $La_{1-x}Sr_xCo_{1-y}Fe_yO_{3.5}$. Herein, YSZ is employed as the oxide ion conducting electrolyte, thereby the reaction usually processes at 3PB covering Ni/YSZ and /YSZ_perovskite oxide interfaces. During fuel cell mode operation, the anode/ fuel electrode undergoes oxidation to from H^+ which releases electrons to the external circuit to reduce O_2 and form O^{2-} . The final product is pure water at the anode side along with energy which could be used as trace heat for the subsequent operation of electrolysis cell (reverse of FC) causing water splitting to form back the reactants utilized [8-9]. The operation mechanism is depicted in Fig. 2.

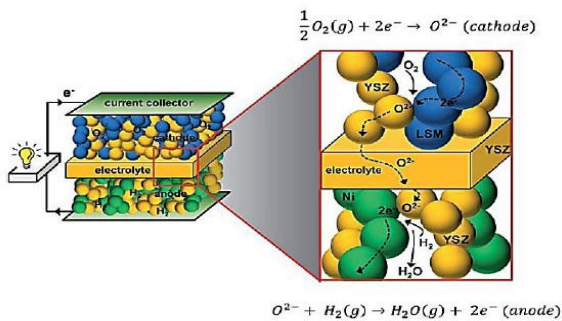


Fig. 2. Configuration of fuel cell and redox mechanism at the respective electrode/ electrolyte interface. The reaction sites are termed as 3PB/2Pb as per the electrode composition [6, copyright for image]

II. NON-LINEAR LOSSES IN FC OPERATION & SIGNIFICANCE OF ELECTRODE MORPHOLOGY

As mentioned, FC is an example of energy conversion device which involves a series of redox reactions at either electrode/electrolyte interface. Hence, interfacial engineering is important to reduce the associated losses during system processing. As a thumb rule, it can be said that FC operates with increase in electronic load in the circuit wherein the voltage starts reducing compared to the maximum available open circuit voltage (OCV) for the concerned cell or stack (a series of cells for higher wattage). Reduction in voltage with increase in the circuit current is termed as polarization losses and the difference with the OCV is known as overpotential (η) [10-11]. The losses as mentioned are found to be frequency dependent wherein physical processes are involved which restricts the ion conduction path. Well-controlled gas diffusion, electron and ion conduction/diffusion are all considered key points in a SOFC operation to obtain a high peak power. As mentioned, at lower applied load (low current region), the primary restricted forces are that from activation/charge transfer process which controls the overall activation barrier for the redox reaction. This is known as activation polarization (η_{act}) and is computed by Butler Volmer equation, Tafel equation (Eq. 1). The processes produce two equal electric currents in opposite directions. The current passing through the electrode surface in the equilibrium (non-polarized) state at any direction is called exchange current [11-12].

$$\eta_{act} = 2.3 \left(\frac{RT}{anF} \right) \log \frac{i}{i_0} \quad (1)$$

This equation is applicable for cathodic and anodic polarization, considering either reaction at one time.

Where R - gas constant $R=8.3143 \text{ J/(mol}^{\circ}\text{K)}$;

T - temperature, K;

n - number of electrons transferred by one ion;

F - Faraday constant

$F = 96500 \text{ C/mol (C-coulombs)}$;

α - electron transfer coefficient ($0 < \alpha < 1$);

i - current density;

i_0 - current exchange density.

The intermediate current-voltage regime is termed as Ohmic, being linear interdependence among the parameters. As considerably higher current (electronic load), the voltage undergoes significant reduction termed as limiting current density. This point is marked by concentration/diffusional resistances marked by mass (gas) transport limitation during FC performance. Both initial activation and final, diffusional resistances are non-linear dependence of Voltage and current which are resonated at lower and highest frequency perturbation during FC functioning. An

account of voltage-current dependence is shown in Fig. 3 [https://www.electrochem.org/dl/interface/fal/fal09/fal09_p038-043.pdf].

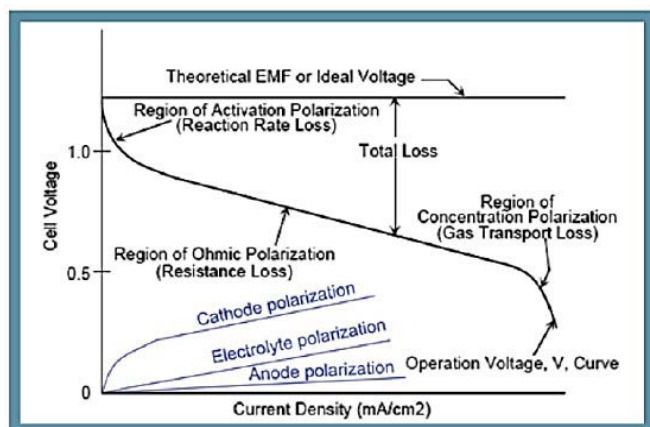


Fig. 3. Illustration on polarization losses during the operation of Fuel cell

The electrochemical redox reaction is studied to be carried out at the interfacial sites wherein electrode/electrolyte meets the active adsorbed species dissociated from fuel and oxidant gases viz H_2 and O_2 respectively. In this regard, theoretical calculations showed lower charge transfer overpotential by composite electrode which is validated experimentally. This is due to the possible extension of 3PB from interface to the volume of electrode [12-13]. Many researchers have undertaken theoretical studies to quantify the 3PB length by considering the average particle length of cathode/anode with the average particles per unit area [14]. This has shown that maintaining same composition, interfacial morphology plays a crucial role in optimizing the 3PB/2PB volume fraction to minimize the associated polarization losses.

For operation of IT-SOFC, the lower operating temperature poses issues in retaining the required ionic conductivity of the electrolyte at 600-800°C [15]. This demands selection of an electrolyte composition whose dimension could be reduced (thinner) with enough ion conduction. In this context, doped Ceria is an excellent choice wherein Gd could be incorporated in variable limit as per optimization [16]. Huang et al have successfully employed $(La_{0.75}Sr_{0.2}Ba_{0.05})_{0.175}Ce_{0.825}O_{1.891}$ (LSBC) for IT-SOFC application [17]. These studies confirm that upon selecting doped ceria as the active ion conducting medium, lowering of interfacial polarizations in terms of charge transfer and diffusion are primarily controlled by the design of electrode materials. Another interesting point to note herewith is that Gd doped Ceria as electrolyte and Ni-GDC as the fuel electrode is found to form double phase boundary (2PB) at the interface with gas species which could be optimized to reduce the polarization losses [18].

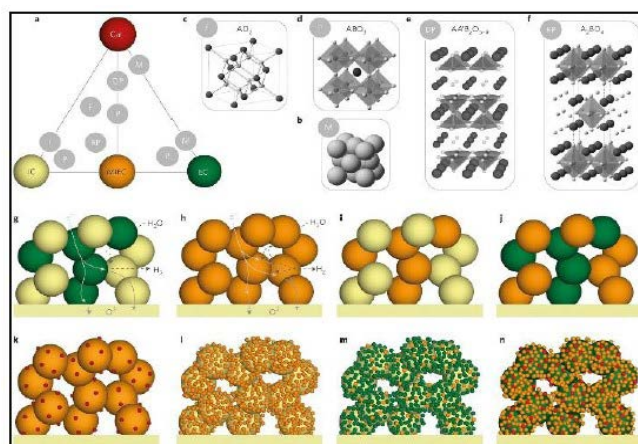
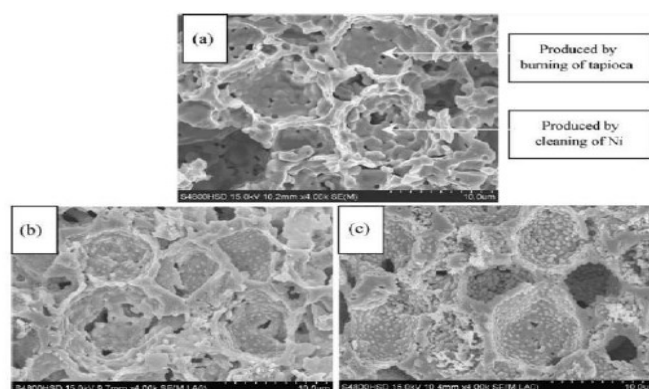


Fig. 4. SOC electrode materials and microstructures. a, Diagram highlighting the functionalities of electrodes. b, Crystal structure of a metal M (such as Ni) c, Fluorite (F) crystal structure, d, Perovskite (P) crystal structure, which exhibits all types of functionality to various extents, e, Crystal structure of an oxygen-deficient, layered perovskite, also known as a double perovskite (DP), which is close to being the ideal single-phase electrode material. f, Crystal structure of a member of the Ruddlesden-Popper (RP) phases, associated with high interstitial oxygen diffusion rates. g-n, Schematic illustrations of electrodes highlighting the key types of microstructures as in: a) IC-EC composite structure, which also illustrates a 3PB fuel-electrode in SOEC mode (g); single-phase MIEC electrode, which also illustrates a 2PB fuel-electrode in SOEC mode (h); IC-MIEC composite structure (i); MIEC-EC composite structure (j); MIEC with dispersed catalyst particles (k); IC coated with a percolating layer of MIEC (l); IC coated with a percolating layer of EC and MIEC (m); EC coated with a percolating layer of MIEC and dispersed catalyst (n) [copyright, 18]

Designing and optimization of interfacial boundaries involves a series of ceramic processing techniques. Some important processes can be listed as impregnation, infiltration using vacuum, exsolution etc. [19]. Zhu et al [20] have showed the extension of 3PB in $La_{0.75}Sr_{0.25}Cr_{0.5}Mn_{0.5}O_{3.5}$ (LSCrM)-impregnated anode using infiltrating 70% porous YSZ with an LSCrM solution. Fig. 5 shows the typical morphology wherein the primary electron conducting phase is LSCrM and YSZ forms an easy ion conduction path. The electro-catalytic activity of the anode is further improved by impregnating nitrate solutions of Ag and Ni followed by selective calcination for phase purity.



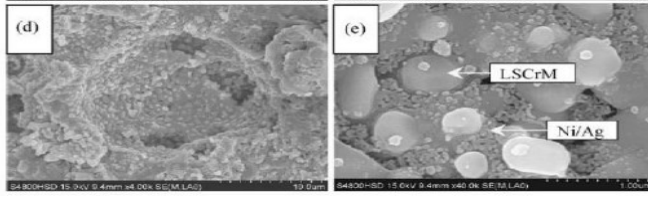


Fig. 5. SEM micrographs of the cross-sections of: (a) pure YSZ anode, (b) ~5 wt.% LSCrM-impregnated YSZ anode; (c) ~35 wt.% LSCrM-impregnated YSZ anode; (d,e) LSCrM/Ni/Ag (~32/2 wt.%) YSZ anode [copyright, 20]

Another important strategy to increase the interfacial phase boundaries for promoting electrocatalytic reactions is by adopting engineered morphology involving two phases namely metal and ceramic. Among various trials, the morphology which proves to be most functional is **Core-shell** arrangement of either phase.

The following section highlights aspects of development of core-shell morphology and its functionality in improving the fuel cell performance and its long term durability.

III. INSIGHT ON CORE-SHELL MORPHOLOGY ON FUEL CELL ELECTRODES

The important secondary factors which require tailoring are controlling of particle size of ceramic core, in-situ/ex-situ reduction process controlling metal onto the core, coverage of shell onto the core etc [21]. The functionality of the electrode being controlled by both electronic and ionic phase, interconnection among each phase within electrode matrix is important. In this regard, the processing should involve discreet coverage of metal (in the form of nano-sub micron size) onto the ionic conducting ceramic particle. The electrocatalytic activity of oxygen in LSM is poorer than that in LSCF and BSCF. However, the CTE for both LSCF and BSCF are about $20 \times 10^{-6} \text{ K}^{-1}$, which are higher than that of the ceria-based electrolyte ($\sim 12.5 \times 10^{-6} \text{ K}^{-1}$). Furthermore, innumerable disadvantages are associated with Co-based electrode composition being higher cost, large evaporation probability, transition of Co^{3+} among high and low spin state which result in minor variations [22-23] in stress generation and redox reactivity of the electrode towards OER/ORR (oxygen evolution in electrolysis mode and oxygen reduction reaction). Researchers have tried to play with ferrite-based compositions since they offer lower cost and capability of replacing Co as the active B-site element, $\text{Ba}_{0.5}\text{Sr}_{0.5}\text{FeO}_{3.5}$ (BSF). However, much higher CTE [24] of BSF makes it difficult to be compatible with YSZ and CGO. BSF are easily collapsed by the moisture from the air, also unstable at high temperatures and low partial pressures of oxygen [25]. The Ce doping in BSF provides lattice stability, better cathode-electrolyte adhesion and enhanced cell performance by increasing the TPBs in SOFC. Ce is functionalized as the shell onto BSF core by organic based ethanol-water solution. In addition, BSF was doped with Nd at B-site to enhance the stability and functionality [26].

To further enhance the FC performance, La and Ce are applied as the shell onto Nd doped BSF.

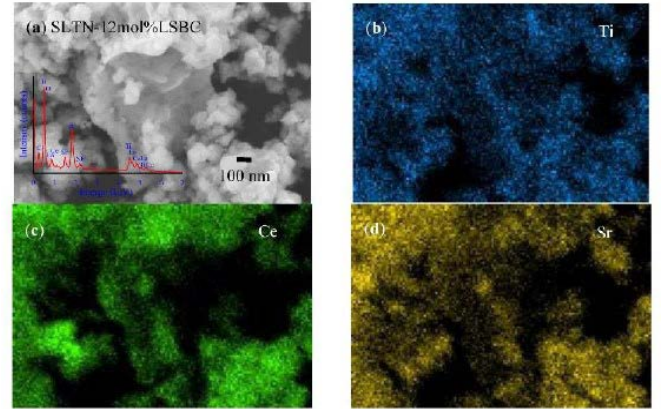


Fig. 6. FESEM images of SLTN-LSBC core-shell matrix with Ti, Ce and Sr distribution shown in b)-d) respectively [copyright, 20].

Core-Shell anode of SLTN-LSBC showed 12 % distributed shell of LSBC in the EDAX spectra (Fig. 6). The Titanium (Ti) and Strontium (Sr) assigned over core-shell major body as shown in Fig. 6 b, d. The Ti and Sr mapping images demonstrated the core SLTN existed below the LSBC nanoparticles shell.

DC conductivity reduced with the increase in the molar ratio of shell, which showed that the resistance of shell affected the electrons hopping as the ratio of shell LSBC increased. Furthermore, a Ce based shell could enhance the electrocatalytic activity of the system, however, would limit the electronic conductivity [27]. It is proposed that, in the reduction atmosphere, Ce^{3+} possibly formed at the fuel electrode at the higher temperature and could enhance the electronic conductivity.

Wang et al [28] have reported BSNF system coated with LC at various concentrations as shown in Fig. 7. LC as the shell helps in tailoring the porosity of electrode with the subsequent reduction the central core. Ce is found to promote the diffusion of La into BSNF host. Such diffusion of La into BSNF form a layer of LC and thereby helps in enhancing the 3PB at the interfacial region.

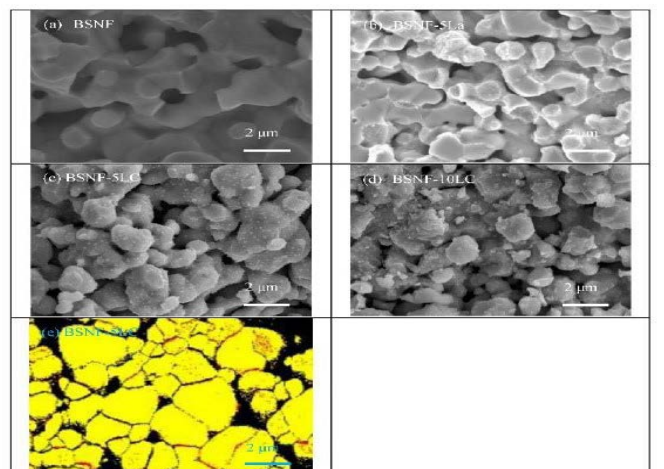


Fig. 7. FESEM micrographs of (a) BSNF, (b) BSNF-5 La, (c) BSNF-5 LC and (d) BSNF-10 LC sintered at 1150°C -6 h. EBSD image of

(e) BSNF-5 LC. Red dots represent LC-species and yellow regions are BSNF grains [copyright, 20].

The Ce coating layer decreased the core size and enhanced the porosity of BSF, whereas based on the relative densities and microstructures, the LC coating layer imposed tiny influences on porosity or core size for BSNF.

LSCF is a well-known MIEC composition for air electrode which bears excellent electrical performance in the IT-SOFC range. The bottleneck of this composition is the lower surface activity during ORR. Lynch et al have tailored the LSCF matrix by coating with dense LSM coating.

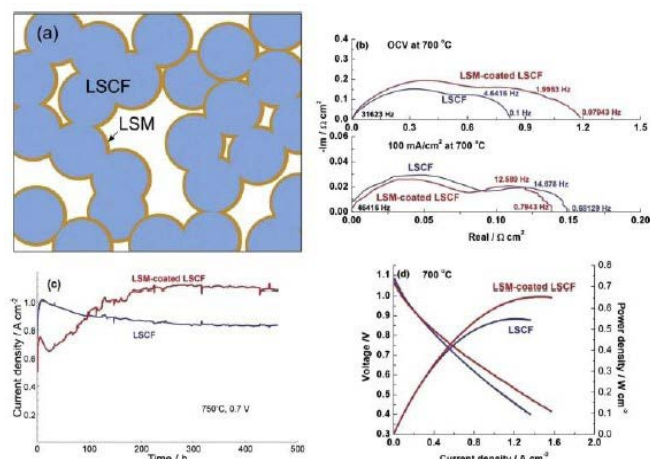


Fig. 8. e (a) Schematic diagram of the LSM-coated LSCF cathode; (b) EIS of fuel cells with and without LSM coating measured at OCV and at 100 mA cm²; (c) Current density of fuel cells with and without LSM coating as a function of time under a constant voltage of 0.7 V; (d) Ie-Ve-P curves of fuel cells with and without LSM coating after long-term testing [30, copyright].

Fig. 8 exhibits that the initial cell performance is found to be excellent for LSCF compared to LSM which degrades significantly upon application of the bias. The single cell with LSM-coated LSCF cathode had a lower initial performance than the single cell with the blank LSCF cathode. However, the cell displayed a growing performance in the first 200 h, almost kept constant [29] as shown in Fig. 8.

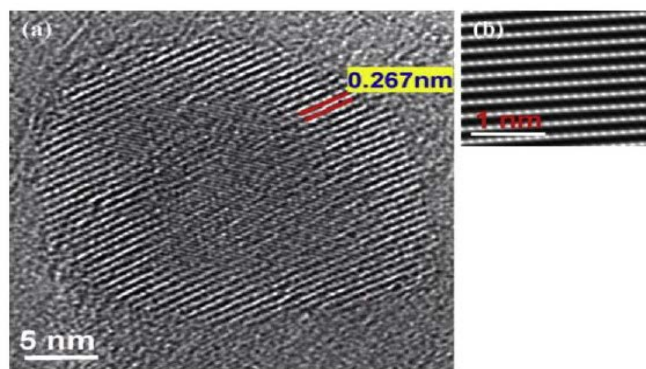


Fig. 9. A high-resolution TEM image exhibiting a core-shell morphology of SDC nanoparticle with a shell thin layer of LiZn-oxide [copyright 29]

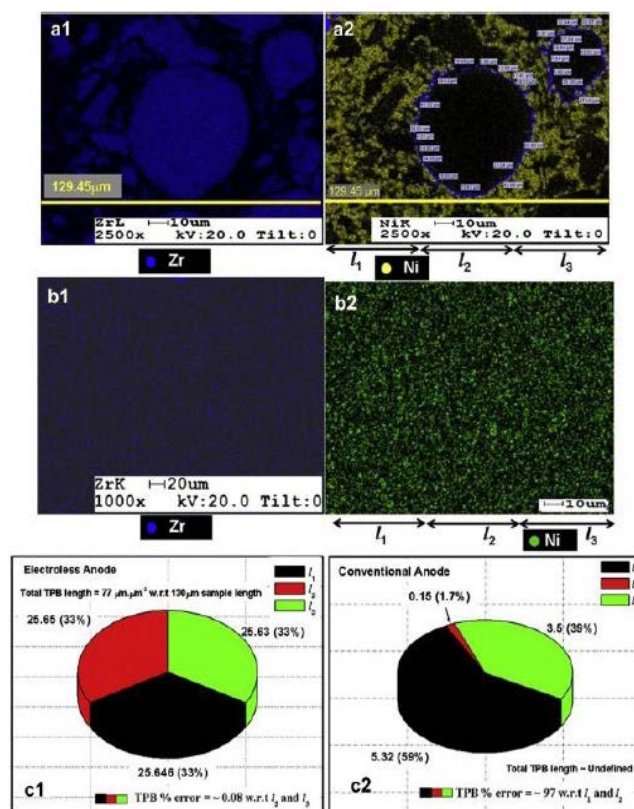


Fig. 10. Core shell Ni @YSZ cermet used as anode for SOFC application. C1, C2. Theoretical modeling and calculations are undertaken to quantify the intra-anode 3PB of the cermet. A comparative EDAX showing the morphology of conventionally prepared NiO-YSZ matrix [copyright 30]

Researchers have reported the core-shell synthesized SDC nanoparticle coated with LiZn-oxide. This forms two-phase nanocomposite thin film (Fig. 9). It is tested that the cermet can help in achieving much higher conductivity of 0.1 S/cm at 300°C. The single cell based with core-shell electrodes produces a power density as high as 630 mW.cm⁻² at 520°C.

Mukhopadhyay et al [30] have reported a core-shell microstructure based on Ni-YSZ composition which consists of discreet nano Ni particle on sensitized YSZ core. The YSZ powders are subjected to surface activation by d8 metals like Pd etc. and are chemically treated to from Ni @ YSZ microstructure in the as-synthesized condition. The primary advantage of the obtained morphology (Fig. 10) is that the overall Ni content can be reduced to 28 vol % without compromising the requisite electronic conductivity required for the FC performance. Co-existence of patterned intra-anode and conventional TPBs with increased catalytic activity of fine Ni particulates is responsible for the enhancement of electrochemical performance (2.5 A cm⁻² at 800°C) for such cells. The authors have also tried to theoretically analyze the 3PB dimension in terms of volume element to optimize the limit of Ni content. The significance of 3PB towards the electrochemical redox reaction required for ORR/ OER is shown in Fig. 11.

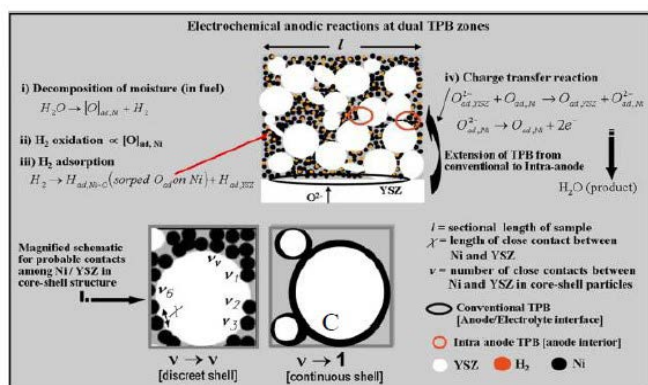


Fig. 11. The mechanism for HOR/ORR at synthesized Ni@YSZ by particulate deposition route [copyright 30]

It is hereby noted that interconnection among both Ni and YSZ phases are important for HOR with minimum polarization losses. If the shell is continuous as shown in the figure, the path of cermet, YSZ gets restricted, and this would accelerate the Ni ripening phenomena.

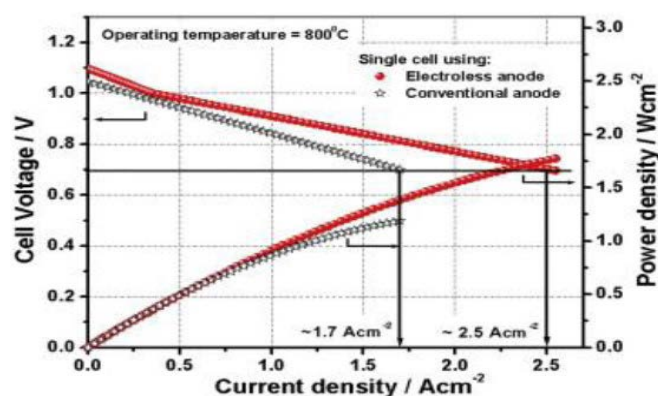


Fig. 11. Comparative electrochemical performance of FC tested using electroless and conventional anode [copyright 30]

The nano Ni is expected to show more sinter ability compared to its higher dimension. Therefore, interconnected YSZ limits Ostwald ripening of Ni and increases the durability of FC. Such cermet has been shown to behave as excellent anode functional layer rather than anode support. This is because, the lower porosity in unimodal manner of such Ni@YSZ cermet results in higher diffusion polarization when used as the support. However, the electrocatalytic activity of such

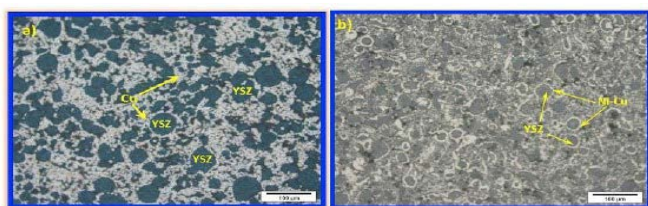


Fig. 12. Optical micrographs of sintered cermets for: a) Cu-YSZ and b) Ni-Cu-YSZ prepared by particulate deposition technique [copyright 31]

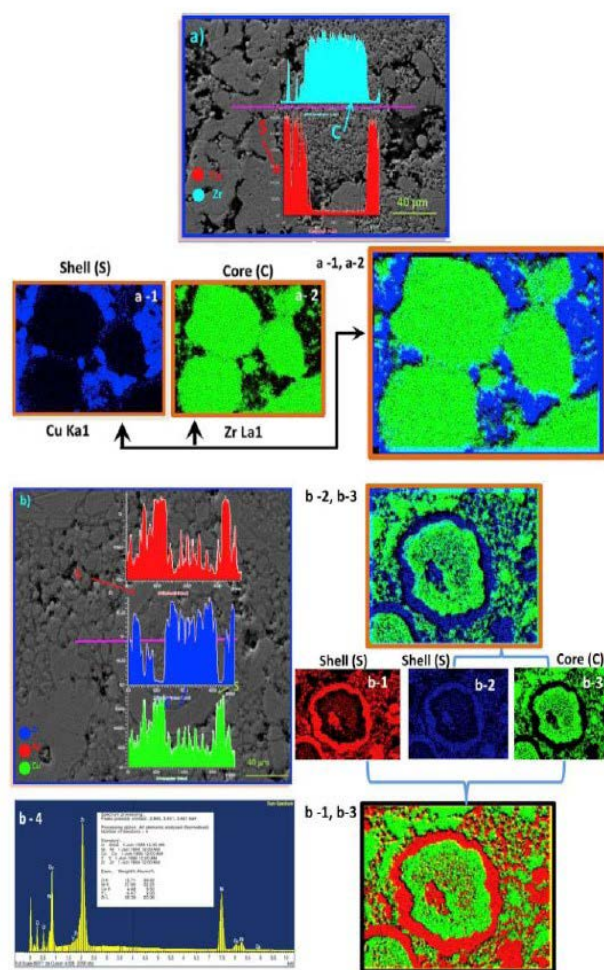


Fig. 13. FESEM micrograph for Cu@YSZ and Ni_Cu@YSZ cermet prepared by electroless technique and the respective EDAX mapping for clarification [copyright 31]

cermet is excellent due to better catalytic properties which reduces the activation polarization of the fuel cell (Fig. 11). Fig. 12-14 shows the research work reported by Konar et al regarding the core-shell anode cermet based on Cu and / Cu_Ni@YSZ. This cermet behaves an exception anode for multiple fuel oxidation under fuel cell condition specially uptake of biogas. Such a novel core-shell Cu-YSZ reduces the requirement of metal for electrical percolation threshold ($\sim 700 \text{ S cm}^{-1}$) down to only 23 vol%. It was earlier reported that Cu-YSZ cermet is not a well-documented catalyst for biogas. However, alloying with Ni, Cu_Ni@YSZ has been found to be an excellent catalyst for biogas oxidation and reasonable performance for Fuel cell [31]. The spot EDAX in the shell position of Ni-Cu alloy reveals the percentage compositions to be around 90: 10 for Ni: Cu as investigated under this study. The unique morphology of the cermet allows interconnection among both metallic and ceramic phase thereby reducing the overall metallic content to 23 vol % compared to 40 vol % required for conventional matrix. The cermet could avoid less thermal mismatch with electrolyte and effective methane reformation with reasonable sulfur tolerance.

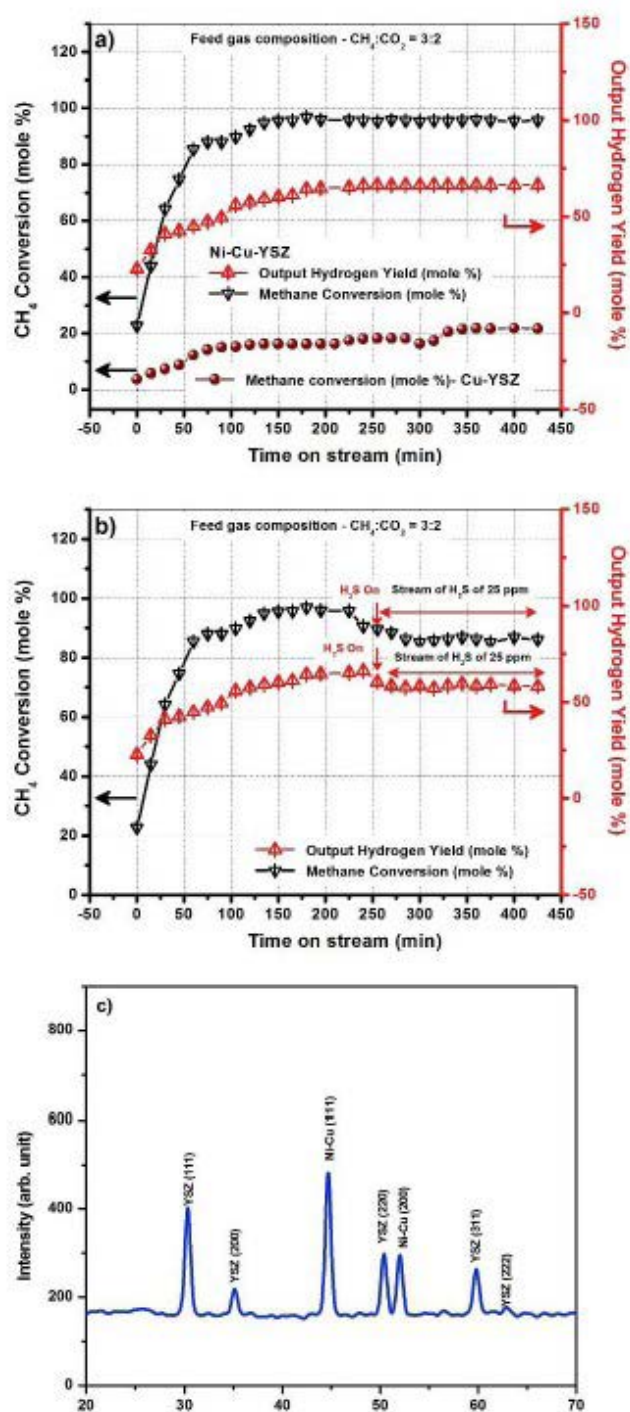


Fig. 14. Methane conversion with output hydrogen yield for electroless Cu-YSZ and Ni-Cu-YSZ cermet: a) without H₂S b) in presence of 25 ppm on stream H₂S in feed gas for electroless Ni-Cu-YSZ c) XRD of post reformed Ni-Cu-YSZ electroless cermet. [copyright 31]

Thus, the reports and descriptions clarify the significance of core-shell morphology of the electrode (either fuel/air electrode) operable for intermediate to high temperature fuel cell application. The primary advantage of such engineered matrix is observed to ensure the easy interconnection among metal and ceramic phases throughout the cermet

thereby extending the available three/two (3PB/2PB) phase boundaries at electrode/electrolyte interphase.

CONCLUSIONS

Lowering the interface charge transfer, ohmic and diffusion impedances are the main considerations to achieve an intermediate temperature solid oxide fuel cell (ITSOFC). Those are determined by the electrode materials selection and manipulating the microstructures of electrodes. The present context describes in detail about the significance of processing steps and morphology in controlling the redox reactions associated with fuel and oxidant in fuel cell and electrolyzer cell operation. The details describe significance of core-shell morphology of the electrode cermet which retains/ extends the triple/double phase boundaries associated with electrocatalytic reactions during fuel cell operation at high temperature.

The core-shell morphology possibly prevented the electrocatalysis decrease, hindering and even blocking the fuel gas path through the porous electrode structure due to the serious agglomeration of impregnated particles. A small amount of shell nanoparticles can form a continuous charge transport pathway and increase the electronic and ionic conductivity of the electrode. The triple-phase boundaries (TPBs) area and electrode electrocatalytic activity are then improved.

A couple of instances on the core shell architecture establishes its significance for the application in fuel cell device as active electrode species. The core-shell interface reaction mechanisms are also necessary investigation topics to control the electrochemical performance precisely and are highlighted herein in nutshell. It could be therefore, stated that processing of metal-ceramic compositions for tailoring the microstructure of electrode is important and bear major significance towards the functionality of fuel cell-based electrode system.

ACKNOWLEDGMENT

All the Universities and Institutions involved in the articles are duly acknowledged.

REFERENCES

- [1] "Solid Oxide Fuel Cell - an overview | Science Direct Topics," [www.sciencedirect.com. https://www.sciencedirect.com/topics/engineering/solid-oxide-fuel-cell](https://www.sciencedirect.com/topics/engineering/solid-oxide-fuel-cell)
- [2] M. T. Mehran et al., "A comprehensive review on durability improvement of solid oxide fuel cells for commercial stationary power generation systems," *Applied Energy*, vol. 352, p. 121864, Dec. 2023, doi: <https://doi.org/10.1016/j.apenergy.2023.121864>.
- [3] T. Taner, "The novel and innovative design with using H₂ fuel of PEM fuel cell: Efficiency of thermodynamic analyze," *Fuel*, vol. 302, p. 121109, Oct. 2021, doi: <https://doi.org/10.1016/j.fuel.2021.121109>.

- [4] Q. Liu, F. Lan, J. Chen, C. Zeng, and J. Wang, "A review of proton exchange membrane fuel cell water management: Membrane electrode assembly," *Journal of Power Sources*, vol. 517, p. 230723, Jan. 2022, doi: <https://doi.org/10.1016/j.jpowsour.2021.230723>.
- [5] Y. Yang et al., "Efficient water recovery and power generation system based on air-cooled fuel cell with semi-closed cathode circulation mode," *Applied Energy*, vol. 364, p. 123125, Apr. 2024, doi: <https://doi.org/10.1016/j.apenergy.2024.123125>.
- [6] R.-T. Wang, H.-Y. Chang, and J.-C. Wang, "An Overview on the Novel Core-Shell Electrodes for Solid Oxide Fuel Cell (SOFC) Using Polymeric Methodology," *Polymers*, vol. 13, no. 16, pp. 2774–2774, Aug. 2021, doi: <https://doi.org/10.3390/polym13162774>.
- [7] D. Roy, S. Samanta, S. Roy, A. Smallbone, and A. Paul Roskilly, "Techno-economic analysis of solid oxide fuel cell-based energy systems for decarbonising residential power and heat in the United Kingdom," *Green Chemistry*, 2024, doi: <https://doi.org/10.1039/D3GC02645K>.
- [8] V. V. Kharton, "Solid oxide fuel cells and electrolysis cells: selected aspects, novel materials and challenges," *Journal of Solid State Electrochemistry*, vol. 28, no. 6, pp. 1761–1762, Apr. 2024, doi: <https://doi.org/10.1007/s10008-024-05870-1>.
- [9] K. N. Grew, J. R. Izzo, and W. Chiu, "Impact of Electrochemical Reaction Mechanisms on Overpotentials in the Solid Oxide Fuel Cell Anode," *ECS Transactions*, vol. 13, no. 26, pp. 123–136, Dec. 2008, doi: <https://doi.org/10.1149/1.3050384>.
- [10] M. Lang, C. Bohn, M. Henke, G. Schiller, C. Willich and F. Hauler. Understanding the Current-Voltage Behavior of High Temperature Solid Oxide Fuel Cell Stacks. *Journal of The Electrochemical Society*. 164 F1460 (2017)
- [11] F. Mazzeo, L. D. Napoli, and M. Carello, "Assessing Open Circuit Voltage Losses in PEMFCs: A New Methodological Approach," *Energies*, vol. 17, no. 11, pp. 2785–2785, Jun. 2024, doi: <https://doi.org/10.3390/en17112785>.
- [12] D. A. Noren and M. A. Hoffman, "Clarifying the Butler–Volmer equation and related approximations for calculating activation losses in solid oxide fuel cell models," *Journal of Power Sources*, vol. 152, pp. 175–181, Dec. 2005, doi: <https://doi.org/10.1016/j.jpowsour.2005.03.174>.
- [13] X. Lu, P. R. Shearing, J. J. Bailey, T. Li, K. Li, and Dan, "Correlation between triple phase boundary and the microstructure of Solid Oxide Fuel Cell anodes: The role of composition, porosity and Ni densification," *Journal of Power Sources*, vol. 365, pp. 210–219, Oct. 2017, doi: <https://doi.org/10.1016/j.jpowsour.2017.08.095>.
- [14] Rustam Singh Shekhar, A. Bertei, and D. S. Monder, "Structure—Properties—Performance: Modelling a Solid Oxide Fuel Cell with Infiltrated Electrodes," *Journal of The Electrochemical Society*, vol. 167, no. 8, pp. 084523–084523, May 2020, doi: <https://doi.org/10.1149/1945-7111/ab91ca>.
- [15] Z. Zakaria, Z. Awang Mat, S. H. Abu Hassan, and Y. Boon Kar, "A review of solid oxide fuel cell component fabrication methods toward lowering temperature," *International Journal of Energy Research*, vol. 44, no. 2, pp. 594–611, Nov. 2019, doi: <https://doi.org/10.1002/er.4907>.
- [16] D. Andersson, S. I. Simak, N. V. Skorodumova, I. A. Abrikosov, and B. Johansson, "Optimization of ionic conductivity in doped ceria," *Proceedings of the National Academy of Sciences of the United States of America*, vol. 103, no. 10, pp. 3518–3521, Feb. 2006, doi: <https://doi.org/10.1073/pnas.0509537103>.
- [17] T. -J Huang and C. -L Chou, "Oxygen Dissociation and Interfacial Transfer Rate on Performance of SOFCs with Metal-Added (LaSr)(CoFe)O₃-(Ce,Gd)O₂ – δ Cathodes," *Fuel Cells*, vol. 10, no. 4, pp. 718–725, May 2010, doi: <https://doi.org/10.1002/fuce.201000028>.
- [18] T. Hong, Y. Zhang, and K. Brinkman, "Enhanced Oxygen Electrocatalysis in Heterostructured Ceria Electrolytes for Intermediate-Temperature Solid Oxide Fuel Cells," *ACS Omega*, vol. 3, no. 10, pp. 13559–13566, Oct. 2018, doi: <https://doi.org/10.1021/acsomega.8b02127>.
- [19] J. T. S. Irvine, D. Neagu, M. C. Verbraeken, C. Chatzichristodoulou, C. Graves, and M. B. Mogensen, "Evolution of the electrochemical interface in high-temperature fuel cells and electrolyzers," *Nature Energy*, vol. 1, no. 1, Jan. 2016, doi: <https://doi.org/10.1038/nenergy.2015.14>.
- [20] X. Zhu et al., "Fabrication and performance of membrane solid oxide fuel cells with La_{0.75}Sr_{0.25}Cr_{0.5}Mn_{0.5}O₃– δ impregnated anodes," *Journal of Power Sources*, vol. 195, no. 7, pp. 1793–1798, Oct. 2009, doi: <https://doi.org/10.1016/j.jpowsour.2009.10.042>.
- [21] F. M. Galogahi, Y. Zhu, H. An, and N.-T. Nguyen, "Core-shell microparticles: Generation approaches and applications," *Journal of Science: Advanced Materials and Devices*, vol. 5, no. 4, pp. 417–435, Dec. 2020, doi: <https://doi.org/10.1016/j.jsamd.2020.09.001>.
- [22] S. McIntosh, J. F. Vente, W.G. Haije, Dave H.A. Blank, and Henny J.M. Bouwmeester, "Oxygen Stoichiometry and Chemical Expansion of Ba_{0.5}Sr_{0.5}Co_{0.8}Fe_{0.2}O₃– δ Measured by in Situ Neutron Diffraction," *Chemistry of Materials*, vol. 18, no. 8, pp. 2187–2193, Mar. 2006, doi: <https://doi.org/10.1021/cm052763x>.
- [23] B. Wei, Zhe Lü, X. Huang, M. Liu, N. Li, and W. Su, "Synthesis, electrical and electrochemical properties of Ba_{0.5}Sr_{0.5}Zn_{0.2}Fe_{0.8}O₃– δ perovskite oxide for IT-SOFC cathode," *Journal of Power Sources*, vol. 176, no. 1, pp. 1–8, Oct. 2007, doi: <https://doi.org/10.1016/j.jpowsour.2007.09.120>.
- [24] J. Peña-Martínez et al., "On Ba_{0.5}Sr_{0.5}Co_{1–y}FeyO₃– δ (y = 0.1–0.9) oxides as cathode materials

- for $\text{La}_{0.9}\text{Sr}_{0.1}\text{Ga}_{0.8}\text{Mg}_{0.2}\text{O}_{2.85}$ based IT-SOFCs,” *International Journal of Hydrogen Energy*, vol. 34, no. 23, pp. 9486–9495, Oct. 2009, doi: <https://doi.org/10.1016/j.ijhydene.2009.09.041>.
- [25] A. Manthiram, J.-H. Kim, Y. N. Kim, and K.-T. Lee, “Crystal chemistry and properties of mixed ionic-electronic conductors,” *Journal of Electroceramics*, vol. 27, no. 2, pp. 93–107, Feb. 2011, doi: <https://doi.org/10.1007/s10832-011-9635-x>
- [26] Y.-M. Wang, C.-M. Chang, J.-S. Shih, and H.-Y. Chang, “Novel lanthanum and cerium coatings on (Ba, Sr)-ferrate cathodes for intermediate-temperature solid oxide fuel cells,” *Journal of the European Ceramic Society*, vol. 36, no. 14, pp. 3433–3440, May 2016, doi: <https://doi.org/10.1016/j.jeurceramsoc.2016.05.018>.
- [27] H.-Y. Chang, S.-H. Wang, Y.-M. Wang, C.-W. Lai, C.-H. Lin, and S.-Y. Cheng, “Novel core-shell structure of perovskite anode and characterization,” *International Journal of Hydrogen Energy*, vol. 37, no. 9, pp. 7771–7778, Mar. 2012, doi: <https://doi.org/10.1016/j.ijhydene.2012.02.022>.
- [28] P. Qiu, X. Yang, T. Zhu, S. Sun, L. Jia, and J. Li, “Review on core-shell structured cathode for intermediate temperature solid oxide fuel cells,” *International Journal of Hydrogen Energy*, vol. 45, no. 43, pp. 23160–23173, Jul. 2020, doi: <https://doi.org/10.1016/j.ijhydene.2020.06.034>.
- [29] M. E. Lynch et al., “Enhancement of $\text{La}_{0.6}\text{Sr}_{0.4}\text{Co}_{0.2}\text{Fe}_{0.8}\text{O}_{3-\delta}$ durability and surface electrocatalytic activity by $\text{La}_{0.85}\text{Sr}_{0.15}\text{MnO}_{3\pm\delta}$ investigated using a new test electrode platform,” *Energy & Environmental Science*, vol. 4, no. 6, p. 2249, 2011, doi: <https://doi.org/10.1039/c1ee01188j>
- [30] M. Mukhopadhyay, J. Mukhopadhyay, A. D. Sharma, and R. N. Basu, “In-situ patterned intra-anode triple phase boundary in SOFC electroless anode: An enhancement of electrochemical performance,” *International Journal of Hydrogen Energy*, vol. 36, no. 13, pp. 7677–7682, Apr. 2011, doi: <https://doi.org/10.1016/j.ijhydene.2011.03.114>
- [31] R. Konar, J. Mukhopadhyay, A. D. Sharma, and R. N. Basu, “Synthesis of Cu-YSZ and Ni-Cu-YSZ cermets by a novel electroless technique for use as solid oxide fuel cell anode: Application potentiality towards fuel flexibility in biogas atmosphere,” *International Journal of Hydrogen Energy*, vol. 41, no. 2, pp. 1151–1160, Nov. 2015, doi: <https://doi.org/10.1016/j.ijhydene.2015.10.003>.



Child-Friendly Smart Glasses with Eye-Blink Monitoring and Spectacle Locator Mechanism

Aishi Mahapatra, Purabi Malakar, Srijita Bera

Department of CSE, Adamas University
aishi.mahapatra@stu.adamasuniversity.ac.in

Debdutta Pal

Department of CSE, Adamas University
debdutta.pal1@adamasuniversity.ac.in

Abstract—Dry eyes and eye strain are common problems, especially among individuals who spend extended hours in front of screens or in environments with low humidity. Some people, due to various reasons, tend to blink less frequently, exacerbating these issues. Prolonged screen exposure in children often leads to reduced blink rates, causing dry eye syndrome and digital eye strain. This causes the disease Keratoconjunctivitis. Additionally, children frequently misplace their glasses, creating inconvenience for parents and potential vision correction gaps.

Keywords: core-shell morphology; Smart Glass, Eye Care, Spectacles Monitoring

INTRODUCTION

A smart eyewear system designed for pediatric users to promote ocular health and prevent spectacle loss. The system comprises an integrated blink detection module utilizing an infrared emitter and receiver to monitor a wearer's blink rate. A microcontroller processes the blink data, and upon detecting a prolonged period without blinking, particularly during extended screen use, activates an integrated haptic or auditory feedback mechanism (e.g., a miniature buzzer) to prompt the wearer to blink, thereby mitigating dry eye syndrome.

Furthermore, the eyewear incorporates a spectacle locator mechanism, including a Bluetooth Low Energy (BLE) module and a secondary auditory indicator, enabling remote location of the glasses via a paired external device (e.g., smartphone application). The invention addresses the critical need for proactive eye health management in children, particularly concerning digital eye strain, and provides a practical solution for preventing the common issue of misplaced eyewear.

This invention provides an integrated solution combining real-time blink frequency monitoring with audible reminder alerts and Bluetooth-based location tracking in child-friendly smart glasses, promoting healthy blinking habits while ensuring device retrievability.

RELATED WORK

Prolonged screen exposure in children often leads to reduced blink rates, causing dry eye syndrome and digital eye strain. Additionally, children frequently misplace their glasses, creating inconvenience for parents and

potential vision correction gaps.

The work that has been done on this eye detection before or what has been known after reading several research papers is as follows:

- I. 1) A comprehensive drowsiness detection system integrates computer vision and machine learning to analyze blink duration, frequency, and contextual cues (environment, facial expressions). It serves as a real-time alert system that warns drivers or interacts with driver assistance technologies to enhance road safety.
- 2) A novel finite automata-based model is proposed to detect drowsiness by tracking eye-blink states. It combines vertical and horizontal projection histograms for more accurate eye localization, reducing the effect of external noise like glasses or eyebrows. The approach achieves over 93% precision using the JZU blink dataset.
- 3) Another method employs Modified EAR combined with automatic facial landmark detection to analyze eye closure duration in a short time window using thresholding, offering efficient and accurate blink detection.
- 4) High-resolution cameras and advanced algorithms are used to distinguish between normal and abnormal blinking behaviors (e.g., prolonged eye closure), enabling proactive safety alerts—especially in driver drowsiness detection systems.
- 5) By analyzing EOG and accelerometer data, the study classifies four activities—typing, reading, eating, and talking—across two users. The system achieves 70% accuracy using 6-second windows and up to 100% accuracy with a 1-minute majority vote, demonstrating promising results in user-independent classification

and the broader potential of smart glasses in ubiquitous computing.

PROPOSED METHODOLOGY

The present invention solves the dual problems of pediatric dry eye syndrome and lost eyewear through a smart glasses system that:

- Continuously monitors the user's blink rate using embedded sensors.
- If the user does not blink for a long time (e.g., 32 seconds), the system provides an alert using a buzzer.
- Automatically reminds children to blink, preventing eye dryness and strain.
- Uses a Bluetooth remote or another BLE device to auto-trigger the buzzer when nearby if the spectacle is misplaced.
- When the BLE button is pressed, the buzzer helps locate the glasses.
- The smart glasses BLE module receives the command and activates the buzzer.

Flow Diagram: The following figure1 describe the

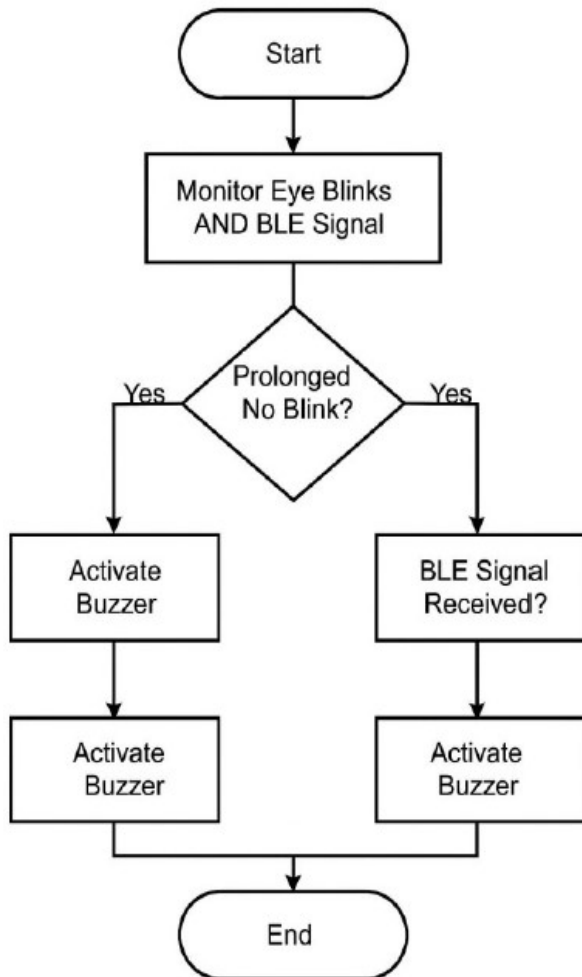


Fig. 1. Flowchart of the proposed system.

A. Key Aspects

1) Dual-Function Integration

- First wearable device combining blink monitoring with location tracking in pediatric eyewear.
- Eliminates the need for separate health-monitoring and tracking devices.
- Seamless integration without compromising eyewear functionality or comfort.

2) Automatic Blink Reminder

- Encourages healthy screen habits in children through gentle reminders.
- Ideal for long study sessions or gaming.

3) Proactive Health Intervention

- Immediate audible feedback prevents dry eye development rather than treating symptoms.
- Continuous monitoring during high-risk activities such as screen time or reading.

4) Built-in Spectacle Locator Mechanism

- Equipped with a Bluetooth Low Energy (BLE) module.
- A remote BLE button or another paired BLE device can trigger the buzzer on the glasses.

5) Child-Centric Design

- Addresses specific challenges of pediatric eyewear management.
- Parental control integration with child-friendly autonomous operation.
- Ideal for kids who spend long hours on screens, blink less, develop eye dryness, and often misplace glasses.

6) Power-Efficient Operation

- Low-power sensor integration extends battery life beyond conventional smart eyewear.
- Selective activation based on usage patterns optimizes energy consumption.

USERS

Specially designed for children who spend long hours using digital screens and are prone to reduced blinking and frequent loss of spectacles.

B. Components

- 1) Arduino Pro Mini: Processes blink signals and overall system logic.
- 2) IR Sensor: Detects eyelid motion for blink monitoring.
- 3) HM-10 BLE Module: Receives remote commands to trigger the buzzer.
- 4) Li-Po Battery: Powers all components while keeping the glasses lightweight.
- 5) Switch: Used for powering the system on.
- 6) TP4056 Module: Safely charges the Li-Po battery.
- 7) Buzzer: Alerts the child to blink or helps locate the glasses when misplaced.



Fig. 2. Sample Product

Methodology

The proposed smart eyewear system is developed using a combination of sensor-based blink detection and Bluetooth-enabled tracking technology. The methodology focuses on accurate blink monitoring, timely user feedback, and reliable location identification of spectacles. The overall workflow involves sensing, processing, decision-making, and alert generation.

1) Blink Detection Using IR Sensor

An infrared emitter–receiver pair is placed near the frame to continuously detect eyelid movements. When the eyelid closes, the IR signal pattern changes, allowing the system to identify each blink accurately.

2) Signal Processing with Microcontroller

The Arduino Pro Mini receives the IR sensor output and processes the blink frequency in real time. It keeps track of the time interval between blinks to determine whether the user is blinking at a healthy rate.

3) Blink Rate Evaluation

The system compares the measured blink interval with a predefined threshold (e.g., 32 seconds). If the user does not blink within this duration, it is considered a potential risk for digital eye strain or dryness.

4) Automatic Alert Generation

When reduced blinking is detected, the microcontroller activates a buzzer or other feedback mechanism to gently remind the child to blink.

5) Spectacle Locator Mechanism

A Bluetooth Low Energy (BLE) module (HM-10) is integrated into the glasses. A remote BLE button or smartphone app sends a wireless command when the spectacles are misplaced.

6) Remote Buzzer Activation

Upon receiving the BLE command, the microcontroller triggers the buzzer on the glasses, helping locate the spectacles quickly.

7) Power Management and Safety

The device is powered by a lightweight Li-Po battery, managed using a TP4056 charging module to ensure safe charging and long battery life.

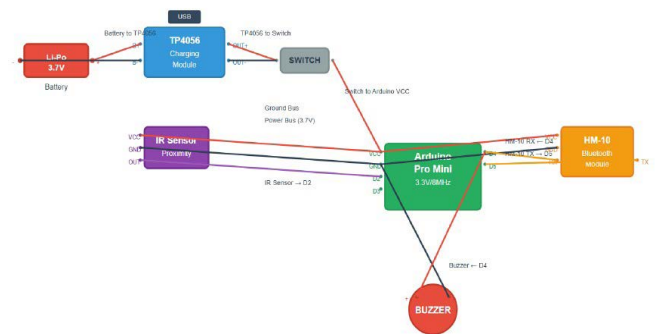


Fig. 3. Circuit Diagram

FEATURES OF THE PRODUCT

- **Blink Rate Monitoring:** Embedded sensors monitor the wearer’s blink rate in real-time. If the wearer blinks less frequently than recommended, the smart spectacles provide reminders or alerts to encourage more frequent blinking.
- **Blink Alerts:** Visual or auditory alerts notify the wearer when they haven’t blinked for an extended period, prompting them to take a break or perform eye exercises to prevent dryness and discomfort.
- **Blink Exercise Guidance:** Integrated software offers guided eye-blinking exercises to help maintain eye moisture and reduce strain.
- **Health Tracking:** Integration with health metrics enables users to understand how blinking patterns correlate with their overall health and well-being.

REFERENCES

[1] Ijsrem, Journal, “Eye Blink Detection - A New System for Driver Drowsiness and Distraction Detection,” Indian Scientific Journal of Research in Engineering and Management, Feb. 8, 2024. [Online]. Available: <https://doi.org/10.55041/ijsrem28613> [2] S. Gorde, “Deep Fakes Detection Using Human Eye Blinking Pattern: Deep Vision,” International Journal for Science Technology and Engineering, vol. 12, no. 4, pp. 4593–4597, Apr. 30, 2024. [Online]. Available: <https://doi.org/10.22214/ijraset.2024.60970> [3] K. Wanjale, A. A. Deshmukh, J. C. Vanikar, A. P. Adsul, and S. Bendale, “Detecting Human Eye Blinks through

- OpenCV,” Apr. 5, 2024. [Online]. Available: <https://doi.org/10.1109/i2ct61223.2024.10543678>
- [4] K.-H. Choi, “Drowsiness Detection Using Eye-Blink Patterns,” *The Journal of the Korea Institute of Intelligent Transport Systems*, vol. 10, no. 2, pp. 94–102, Apr. 1, 2011. [Online]. Available: <http://www.koreascience.or.kr/article/ArticleFullRecord.jsp?cn=OTNSCX 2011 v10n2 94>
- [5] J. Smith and A. Jones, “Advances in Ocular Health Monitoring for Children,” *Journal of Pediatric Ophthalmology*, vol. 15, no. 2, pp. 123–130, 2023.
- [6] R. Johnson and S. Lee, “Impact of Blue Light on Pediatric Vision: A Review,” *Environmental Eye Health*, vol. 8, no. 4, pp. 201–210, 2022.
- [7] K. Brown and L. White, “Ultrasonic Sensing for Screen Distance Measurement in Wearable Devices,” *Sensors in Health Applications*, vol. 3, no. 1, pp. 45–52, 2024.
- [8] M. Davis and P. Miller, “Effectiveness of Auditory Cues in Promoting Screen Breaks,” *Ergonomics and Human Factors*, vol. 27, no. 3, pp. 187–195, 2021.
- [9] F. Garcia and G. Rodriguez, “Parental Engagement Through Connected Health Apps for Children,” *Digital Health & Parenting*, vol. 10, no. 1, pp. 33–40, 2023.
- [10] C. Williams and D. Green, “Behavioral Interventions for Myopia Control in School-Aged Children,” *Optometry and Vision Science*, vol. 97, no. 6, pp. 450–458, 2020.
- [11] V. Martinez and H. Taylor, “Balancing Technology and Traditional Approaches in Child Health,” *Journal of Child Development*, vol. 45, no. 2, pp. 78–85, 2022.
- [12] B. Anderson and E. Lewis, “The Role of Smart Wearables in Proactive Health Management,” *Wearable Technology Trends*, vol. 6, no. 4, pp. 112–120, 2021.
- [13] D. Clark and J. Hall, “Ethical Considerations in Child Monitoring Technologies,” *Pediatric Technology Ethics*, vol. 2, no. 1, pp. 1–8, 2024.
- [14] S. White and T. King, “Technological Solutions for Reducing Digital Eye Strain in Youth,” *Innovations in Ophthalmic Devices*, vol. 18, no. 3, pp. 250–258, 2023.



ARTICLE

A HEED-Inspired Hybrid-Score Clustering Protocol for Energy-Efficient Border Surveillance in Wireless Sensor Networks

Bhudeb Chakravarti¹*, Santanu Chatterjee²

** Senior Member, IEEE, # Member, IEEE*

1 Aerospace and Electronics Systems Society Chapter, IEEE Hyderabad Section, India

2 Research Centre Imarat, DRDO, Hyderabad, India

E-mail: bhudebc@ieee.org

Abstract : *Wireless Sensor Networks (WSNs) face persistent challenges in optimizing energy consumption and extending network longevity due to their constrained node resources and reliance on battery power. In this research paper, we propose a new HybridScore based protocol designed for energy-aware cluster head (CH) election and present a performance evaluation of Low Energy Adaptive Clustering Hierarchy (LEACH), Hybrid Energy-Efficient Distributed (HEED), Multi-Cluster Head (Multi-CH) and HybridScore. The proposed protocol employs a weighted hybrid scoring function integrating residual energy, intra-cluster distance and adaptive rotation thresholds to enhance energy balancing and reduce premature node deaths. Simulation experiments, conducted over 100, 200 and 300 operational rounds with 100 sensor nodes, demonstrate that HybridScore achieves higher residual energy than the other protocols. The results confirm that HybridScore effectively mitigates control overhead and enhances node survival rates without introducing excessive computational complexity. These findings highlight the potential of hybrid clustering approaches in enabling sustainable, scalable and energy-efficient WSN deployments making it a viable solution for large-scale, mission-critical WSN applications such as border surveillance.*

Keywords: *Wireless Sensor Networks (WSN), Energy Efficiency, Clustering Protocols, HybridScore, Residual Energy, Network Lifetime, Cluster Head Election*

I. INTRODUCTION

Energy-efficient operation of Wireless Sensor Networks (WSNs) has been a longstanding research problem, especially in mission-critical domains such as border surveillance, where prolonged network lifetime, reliable coverage, and accurate anomaly detection are essential. Among the earliest clustering approaches, the Low-Energy Adaptive Clustering Hierarchy (LEACH) protocol [1] pioneered the idea of randomized rotation of Cluster Heads (CHs) to balance energy consumption across sensor nodes. LEACH demonstrated substantial energy savings compared to flat routing but suffered from unpredictable CH distribution, as the selection process did not consider residual energy or network proximity, which resulted in premature node failures.

To overcome these shortcomings, the Hybrid Energy-Efficient Distributed (HEED) protocol [2] introduced a more systematic CH election mechanism. HEED combined residual node energy as a primary parameter with communication cost, defined by proximity to neighbours, as a secondary parameter, leading to improved intra-cluster balance and longer network lifetimes. The introduction of such hybrid election schemes paved the way for protocols that integrate multiple criteria in CH selection.

Subsequent work explored diverse hybrid clustering metrics. For instance, TEEN (Threshold-sensitive Energy Efficient Network protocol) [3] incorporated both residual energy and event-driven reporting, making it suitable for time-critical applications. Distance-aware protocols [4] improved stability in multi-hop scenarios by ensuring that CHs were closer to the sink, reducing long-haul communication costs. Similarly, link quality-based protocols [5] emphasized robust communication, ensuring that cluster formation was not only energy-efficient but also resilient against packet loss. A comprehensive survey by Abbasi et al. [6] highlighted how these multi-parameters approaches evolved into a broad class of hybrid protocols, each designed to balance energy consumption, coverage and reliability under specific deployment scenarios.

In parallel, metaheuristic optimization algorithms emerged as a promising direction for clustering. Particle Swarm Optimization (PSO) was applied to optimize CH selection dynamically, producing balanced clusters with higher lifetimes than traditional methods [7]. Genetic Algorithms (GA) offered an evolutionary approach, where CH sets were iteratively improved across generations [8]. More recently, novel bio-inspired approaches like the Coyote Optimization Algorithm (COA) [9] and the Sparrow Search

Algorithm (SSA) [10] have been applied, outperforming classical clustering schemes in dynamic and large-scale deployments. These methods are particularly valuable in resource-constrained and irregular environments, such as border regions, where node distribution is often uneven and unpredictable.

Beyond optimization, researchers have investigated multi-hop and multi-CH schemes [11], where the load of data aggregation and forwarding is shared by multiple leaders, thereby reducing premature node death in dense networks. Similarly, optimal CH positioning strategies [12] have been studied to minimize intra-cluster energy spent in data forwarding, a critical factor for large-area deployments. These innovations are particularly relevant in linear or strip deployments, typical of border surveillance, where communication ranges and energy costs vary significantly along the monitored perimeter.

With the emergence of edge computing paradigms, WSN-based surveillance systems have moved beyond energy-efficient communication toward local intelligence and anomaly detection. Edge nodes can perform preliminary feature extraction and event prioritization [13], thereby reducing redundant transmissions to central servers. This edge-assisted approach aligns well with the computational needs of intrusion detection systems (IDS) in border monitoring. In particular, machine learning techniques such as the Isolation Forest algorithm [14] have proven effective for detecting anomalies in high-dimensional data, offering low false alarm rates and scalability for large sensor deployments.

While extensive work has been carried out on clustering and anomaly detection in WSNs, existing solutions still face limitations in the context of border surveillance. Many clustering protocols, though effective in generic deployments, are not tailored to linear topologies or harsh environmental conditions where node failures are frequent. Metaheuristic-based CH selection approaches, while powerful, are often centralized and computationally expensive, making them unsuitable for fully distributed deployments along borders. At the same time, intrusion detection schemes that rely solely on centralized cloud-based analysis are bandwidth-hungry and energy-inefficient.

Despite significant advances, existing clustering approaches often suffer from suboptimal CH placement in dynamic and resource-constrained environments like borders, where node failures and topology changes are frequent. In addition, most protocols do not simultaneously account for residual energy, connectivity, distance and link reliability in a distributed election process.

Motivated by these gaps, this research paper presents a HEED-inspired distributed election protocol HybridScore that integrates a hybrid scoring mechanism to select CHs more intelligently. The proposed method considers residual energy, neighbour proximity, node degree and link quality to ensure optimal CH placement, balanced energy

consumption and enhanced data reliability. By refining the cluster formation process through iterative convergence and localized decision-making, the protocol improves network lifetime while maintaining high coverage and data fidelity. The methodology is particularly suited for elongated and constrained deployment areas—such as international boundaries, coastal lines and sensitive demilitarized zones, where surveillance reliability directly impacts operational effectiveness and national security

II. MATHEMATICAL MODELING

A. Network Model

We assume a Wireless Sensor Network (WSN) consisting of N sensor nodes indexed by $i \in \{1, \dots, N\}$ deployed in a two-dimensional border region of size $L \times W$. The nodes are considered static after deployment. Each node has an initial energy E_0 and consumes energy for sensing, transmission and reception.

The Base Station (BS) is positioned at one end of the border region, collecting aggregated data from CHs.

Each node $i \in N$ maintains residual energy E_r , position coordinates (x_i, y_i) and neighbourhood list N_i within communication range R .

For energy dissipation, we adopted the first-order radio model widely used in WSN research [1]:

$$E_{TX}(k, d) = \begin{cases} k E_{elec} + k \epsilon_{fs} d^2 & \text{if } d < d_0 \\ k E_{elec} + k \epsilon_{mp} d^4 & \text{if } d \geq d_0 \end{cases} \quad (1)$$

$$E_{RX}(k) = k E_{elec} \quad (2)$$

Where, k is the packet size in bits, d is the distance between transmitter and receiver, E_{elec} is energy required to run the system in J/bit, ϵ_{fs} and ϵ_{mp} are the amplifier constants for free space and multipath models respectively and d_0 is the threshold distance defined by $d_0 = \sqrt{\frac{\epsilon_{fs}}{\epsilon_{mp}}}$.

This model captures the fact that long-distance transmission drains more rapidly making energy-efficient clustering essential.

Let $H(r) \subseteq \{1, \dots, N\}$ be the set of cluster-heads (CHs) in round r , with $|H(r)| = K(r)$. Each non-CH node $i \notin H(r)$ attaches to one CH $h(i, r)$ and $|M_h(r)| = n_h(r)$.

For data aggregation, CH h fuses $n_h(r) + 1$ packets into an effective payload $Y_h(r)k$ before uplink where $Y_h(r) \in (0, n_h(r) + 1)$ captures compression represented by $Y = 1$ means 'one packet summary' and $Y = n_h + 1$ means 'no compression'.

The energy of a member node $i \notin H(r)$ per round is presented by:

$$\Delta E_i^{mem}(r) = E_{TX}(k, d_{i,h(i,r)}) \quad (3)$$

The energy of a CH node $h \in H(r)$ per round is presented by:

$$\Delta E_h^{CH}(r) = \sum_{i \in M_h(r)} E_{RX}(k) + (n_h(r) + 1)k E_{DA} + E_{TX}(Y_h(r)k, d_{h,BS}) \quad (4)$$

After a round, the node energy recursion is presented by:

$$E_i(r+1) = \max\{0, E_i(r) - (1_{\{i \in H(r)\}} \Delta E_i^{CH}(r) + 1_{\{i \notin H(r)\}} \Delta E_i^{mem}(r))\} \quad (5)$$

The number of live nodes per round is presented by:

$$N_{live}(r) = \sum_{i=1}^N 1_{\{E_i(r) > 0\}} \quad (6)$$

The trajectories of the total network energy are presented by:

$$E_{tot}(r) = \sum_{i=1}^N E_i(r) \quad (7)$$

B. LEACH (Low-Energy Adaptive Clustering Hierarchy)

For the election process, each node i , which is not a CH in the last $\frac{1}{p}$ rounds, becomes eligible for CH in round r with threshold:

$$T_i(r) = \begin{cases} \frac{p}{1-p(r \bmod \frac{1}{p})}, & i \in G(r) \\ 0, & i \notin G(r) \end{cases} \quad (8)$$

Where $G(r)$ is the set of nodes that have not been CHs in the last $\frac{1}{p}$ rounds and $p \in (0,1)$ is the desired CH fraction.

The expectation is calculated as $E[K(r)] \approx p N_{live}(r)$ and each non-CH joins the nearest CH to form the cluster as given by:

$$h(i, r) = \arg \min_{h \in H(r)} d_{ih} \quad (9)$$

LEACH typically assumes strong aggregation presented by $Y_h(r) = 1$.

If cluster sizes are $\{n_h\}$, the network round energy is:

$$E_{round}^{LEACH}(r) \approx \sum_{h \in H(r)} [\sum_{i \in M_h} E_{TX}(k, d_{ih}) + n_h E_{RX}(k) + (n_h + 1)k E_{DA} + E_{TX}(k, d_{hBS})] \quad (10)$$

C. HEED (Hybrid Energy-Efficient Distributed Clustering)

HEED uses iterative CH candidacy proportional to residual energy and a communication cost for tie-breaking. Initial CH probability for node i in iteration ℓ is calculated as:

$$C_i^{(\ell)} = \min\{C_{max}, \eta^{(\ell)} \cdot \frac{E_i(r)}{E_{max}(r)}\} \quad (11)$$

$$\eta^{(\ell+1)} = 2 \eta^{(\ell)}$$

The residual energy calculation is done starting from $\eta^{(0)} \approx p$ until $C_i^{(\ell)} \geq C_{max}$ or a small number of iterations, where commonly $C_{max} \leq 1$.

For node i , the communication cost is calculated as:

$$C_i = \alpha \left(\frac{1}{E_i(r) + \epsilon} \right) + (1 - \alpha) \cdot \frac{1}{|N_i|} \sum_{j \in N_i} \frac{d_{ij}}{R} \quad (12)$$

Where $N_i = \{j: d_{ij} \leq R\}$, $0 \leq \alpha \leq 1$.

Nodes with higher $C_i^{(\ell)}$ tentatively declare CH. If multiple tentative CHs lie within R , the one with lower C or higher residual persists and other candidates withdraw.

The energy consumed by member node for transmission is calculated as:

$$E_{member} = (N - N_{CH}) \cdot \left(E_{elec} \cdot k + \begin{cases} E_{fs} \cdot k \cdot d_{toCH}^2, & d_{toCH} < d_0 \\ E_{mp} \cdot k \cdot d_{toCH}^4, & d_{toCH} \geq d_0 \end{cases} \right) \quad (13)$$

Where N is the number nodes, N_{CH} is the number of cluster heads in the round, k is the packet size in bits, E_{elec} is the energy required to run the electronics in J/bit, E_{fs} and E_{mp}

are the free-space and multipath amplifier energy, d_{toCH} is the average distance from node to its CH and $d_0 = \sqrt{\frac{E_{fs}}{E_{mp}}}$ is the threshold distance.

Each CH receives data from the non-CH nodes, aggregates and transmits to BS. The energy consumed by the CHs for receiving, aggregating and transmitting data to the BS is calculated as:

$$E_{CH} = N_{CH} \cdot \left[\left(\frac{N - N_{CH}}{N_{CH}} \right) \cdot E_{elec} \cdot k + E_{DA} \cdot k + E_{elec} \cdot k + \begin{cases} E_{fs} \cdot k \cdot d_{toBS}^2, & d_{toBS} < d_0 \\ E_{mp} \cdot k \cdot d_{toBS}^4, & d_{toBS} \geq d_0 \end{cases} \right] \quad (14)$$

Where E_{DA} is the energy required for data aggregation in J/bit and d_{toBS} is average distance from CH to BS.

The total energy consumed per round in HEED is presented by:

$$E_{round}^{HEED} = E_{member} + E_{CH} \quad (15)$$

D. Multi-CH Protocol

Multi-CH protocol is a simple deterministic scheme where the K nodes with highest residual energy are selected as CHs. The CHs are selected based on the function:

$$H(r) = \arg \max_{|M|=K} \sum_{i \in M} E_i(r) \quad (16)$$

Where $H(r)$ is the probabilistic threshold function to decide whether a sensor node becomes a cluster head (CH) in round r . It determines the likelihood or priority of a node being selected as a CH based on multiple influencing parameters.

In multi-CH protocol, multiple CHs can be present in a single cluster to improve redundancy and load balancing. The basic components of energy consumption remain similar to HEED, but the number of CHs per cluster is higher, leading to slightly different average distances and transmission load. The energy consumed by member node for transmission of data and the energy consumed by the multiple CHs in receiving, aggregating and transmitting data to BS is given by:

$$E_{member}^{MultiCH} = (N - N_{MCH}) \cdot \left(E_{elec} \cdot k + \begin{cases} E_{fs} \cdot k \cdot d_{toCH}^2, & d_{toCH} < d_0 \\ E_{mp} \cdot k \cdot d_{toCH}^4, & d_{toCH} \geq d_0 \end{cases} \right) \quad (17)$$

$$E_{CH}^{MultiCH} = N_{MCH} \cdot \left[\left(\frac{N - N_{MCH}}{N_{MCH}} \right) \cdot E_{elec} \cdot k + \alpha \cdot E_{DA} \cdot k + E_{elec} \cdot k + \begin{cases} E_{fs} \cdot k \cdot d_{toBS}^2, & d_{toBS} < d_0 \\ E_{mp} \cdot k \cdot d_{toBS}^4, & d_{toBS} \geq d_0 \end{cases} \right] \quad (18)$$

Where N_{MCH} is the total number of cluster heads in multi-CH scheme and α is the factor indicating multiple CH overhead (typically $\alpha > 1$).

The total energy consumed per round in Multi-CH protocol is presented by:

$$E_{round}^{MultiCH} = E_{member}^{MultiCH} + E_{CH}^{MultiCH} \quad (19)$$

III. HYBRIDSCORE FUNCTION AND DISTRIBUTED ELECTION

The HybridScore protocol is inspired on HEED. In this case, each node computes a Hybrid Score H_i combining four critical parameters as given by:

$$H_i = w_1 \cdot \frac{E_i}{E_0} + w_2 \cdot \frac{|N_i|}{N_{max}} + w_3 \cdot \left(1 - \frac{d_{iBS}}{d_{max}} \right) + w_4 \cdot LQ_i \quad (20)$$

Where, $\frac{E_i}{E_0}$ is the normalized residual energy of node i , $\frac{|N_i|}{N_{max}}$ is the normalized node degree (number of neighbors), $\frac{d_{i,BS}}{d_{max}}$ is the normalized distance to BS, LQ_i is the link quality metric and w_1, w_2, w_3 and w_4 are the weight factors such that $\sum w_i = 1$.

The Hybrid Score ensures that a node with high energy, many neighbors, shorter BS distance, and reliable links is more likely to become CH.

A. Distributed Election Process

Once the H_i is computed, each node becomes a tentative CH with probability proportional to H_i as given by:

$$P_i = \min(C_{prob} \cdot H_i, 1) \quad (21)$$

Where C_{prob} is the initial CH probability, which is usually set at 0.05.

Tentative CHs now broadcast their scores within range R . A node with lower H_i withdraws from tentative CH list when it hears a higher-scoring CH nearby. The remaining nodes become CHs and non-CH nodes join the nearest CH based on distance. This distributed and competitive election avoids centralized control while balancing energy usage.

B. Cluster Formation and Intra-Cluster Communication

Non-CH nodes transmit sensed data to their CH using short-range communication, reducing transmission cost. Each CH aggregates data and transmits to the BS either single-hop or through multi-hop relays, depending on deployment. Energy spent by CH in a round is calculates as:

$$E_{CH} = E_{RX}(k \cdot n_c) + E_{DA} + E_{TX}(k, d_{CH,BS}) \quad (22)$$

Where n_c is the number of the cluster members and E_{DA} is the energy required for data aggregation.

For non-CH node j is calculated as:

$$E_j = E_{TX}(k, d_{j,CH}) \quad (23)$$

Since, intra-cluster communication is usually short-range, energy usage is minimized for non-CH nodes.

C. Energy Consumption by the Network

The energy consumed by the network is distributed to two components: (a) Control Overhead and (b) Steady-state Energy.

In each iteration, every tentative CH transmits one broadcast message ADV. All neighbors within R receive the message. The energy required to transmit the ADV message is presented by:

$$E_{TX}^{ADV} = \sum_{i \in \mathcal{C}} E_{TX}(b_{adv}, r_b) \quad (24)$$

$$E_{RX}^{ADV} = \sum_{i \in \mathcal{C}} |N_i^{(b)}| E_{RX}(b_{adv}) \quad (25)$$

Where $N_i^{(b)} = \{u \in Y \setminus \{i\} : d_{iu} \leq r_b\}$, $Y = \{1, \dots, N\}$, \mathcal{C} is the set of CH, R is the communication radius, b_{adv} is the bits used in ADV message and r_b is the broadcast radius used for ADV message.

The total energy consumed for transmission and reception of ADV message is presented by:

$$E(adv) = E_{TX}^{ADV} + E_{RX}^{ADV} \quad (26)$$

If the setup uses I_{max} micro-iterations with similar tentative \mathcal{C} , the energy consumed for the control overhead can be presented as:

$$E_{control}(adv, total) \approx I_{max} \cdot E(adv) \quad (27)$$

Each non-CH node sends one unicast JOIN_REQ to its selected CH. Each CH receives as many JOINs as it has members. The energy required to transmit JOIN Message is:

$$E_{TX}^{JOIN} = \sum_{u \in Y/\mathcal{C}} E_{TX}(b_{join}, d_{uc(u)}) \quad (28)$$

Where $c(u)$ is the CH chosen by member u .

The energy required to receive the JOIN message is:

$$E_{RX}^{JOIN} = \sum_{c \in \mathcal{C}} |\mathcal{M}_c| E_{RX}(b_{join}) \quad (29)$$

Where \mathcal{M}_c are the members of CH \mathcal{C} , and b_{join} is the bits used in JOIN message.

The total energy consumed for transmission and reception of JOIN message is presented by:

$$E(join) = E_{TX}^{JOIN} + E_{RX}^{JOIN} \quad (30)$$

After clustering is done, the energy is consumed for data round comprising of node members sending data to the CH, the CH aggregating data collected from member nodes and CH sending data to the Base Station (BS).

The energy consumed by each member for sending data to CH is calculated by:

$$E_{members}(c) = \sum_{u \in \mathcal{M}_c} E_{TX}(b, d_{uc}) \quad (31)$$

The total energy consumed by all nodes is:

$$E_{uplink} = \sum_{c \in \mathcal{C}} \sum_{u \in \mathcal{M}_c} E_{TX}(b, d_{uc}) \quad (32)$$

The CH receives b bits of data from each member, aggregates them and send them to the BS. The total energy consumed by each CH is calculated as:

$$E_{CH}(c) = |\mathcal{M}_c| E_{RX}(b) + |\mathcal{M}_c| b E_{DA} + E_{TX}(b_{agg}, d_{c,BS}) \quad (33)$$

The total energy consumed by the network for data transmission by CH is:

$$E_{CH} = \sum_{c \in \mathcal{C}} |\mathcal{M}_c| E_{RX}(b) + |\mathcal{M}_c| b E_{DA} + E_{TX}(b_{agg}, d_{c,BS}) \quad (34)$$

The total energy consumed for the steady state transmission of data is given by:

$$E_{steady} = E_{uplink} + E_{CH} \quad (35)$$

If each round includes one control overhead with I_{max} micro-iterations of ADV and a single JOIN phase and then a steady-state round, the total energy consumed by the network is given by:

$$E_{round} \approx I_{max} \cdot E(adv) + E(join) + E_{steady} \quad (36)$$

IV. PERFORMANCE EVALUATION

The simulation was conducted to evaluate the performance of four clustering protocols — LEACH, HEED, Multi-CH and the proposed HybridScore — in terms of energy efficiency and network lifetime. A network of 100 randomly distributed sensor nodes within a defined region of 500m x 500m was simulated for 100, 200 and 300 rounds. Each node was initialized with an equal energy of 1.0 J, and the base station (BS) was placed at a fixed position just outside the sensing field (250,500) to emulate realistic wireless sensor network (WSN) deployment in

border surveillance scenario. The simulation considered radio energy dissipation using the first-order radio model, including electronic energy $E_{elec} = 50e-9$ J/bits, free-space energy $E_{fs} = 10e-11$ J/bit/m², multipath energy $E_{mp} = 1.3e-15$ J/bit/m⁴ and data aggregation energy $E_{Da} = 5e-9$. The packet size is considered as 4000 bits per data packet. Cluster Head (CH) selection was performed differently for each protocol as presented in section II and III. LEACH employed a random threshold-based CH rotation with a fixed probability, while HEED selected CHs based on residual energy and communication cost. The Multi-CH protocol used an adaptive threshold considering the average network energy and a dynamic head selection probability to improve coverage. In contrast, HybridScore utilized a hybrid scoring function that incorporated both residual energy and distance to the base station, with weights optimized to balance load and minimize communication overhead. Specifically, the HybridScore formula gave higher preference to nodes with greater residual energy while ensuring adequate spatial distribution of CHs.

A. Remain Energy in the Network per Round

The remaining energy of the network for 100, 200 and 300 rounds are presented in Fig.1, Fig.2 and Fig.3.

The result demonstrates that though in the beginning, HybridScore uses more energies than the other protocols, with time HybridScore performs better and remains operational for more time that other protocols.

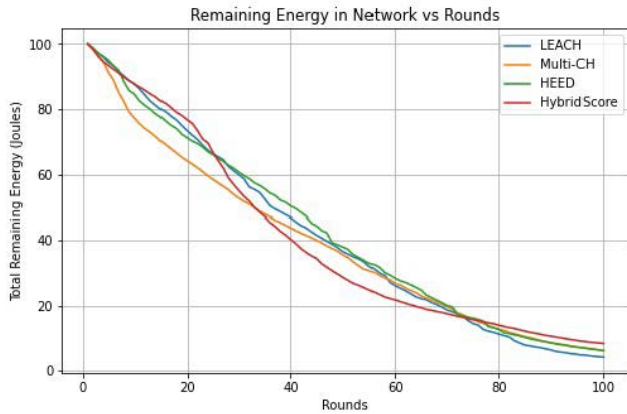


Fig. 1. Remaining Energy in Network for 100 Rounds

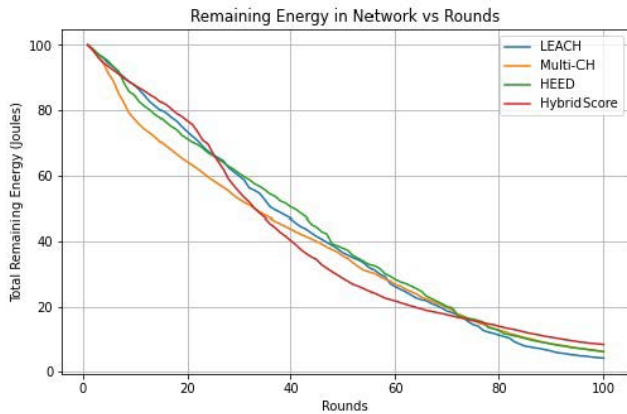


Fig. 2. Remaining Energy in Network for 200 Rounds

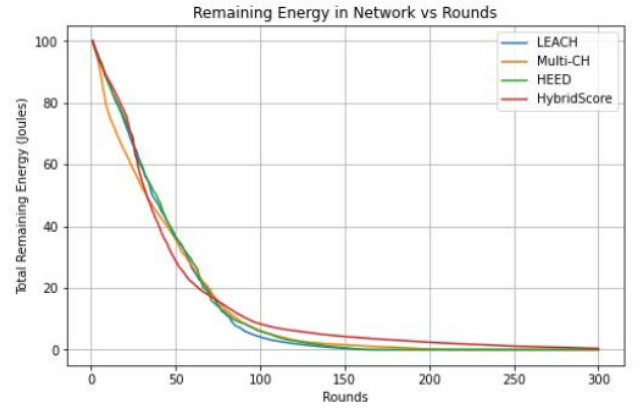


Fig. 3. Remaining Energy in Network for 300 Rounds

B. Number of Alive nodes per Round

The number of alive nodes per round for 200 and 300 rounds are presented in Fig.4 and Fig.5.

The result demonstrates that though in the beginning, the nodes get deactivated earlier in HybridScore, but the network continues to work for longer time with live nodes with HybridScore protocol. For LEACH and HEED protocols, all nodes die around 165 rounds, For Multi-CH, all nodes die around 210 rounds. But for HybridScore, few nodes remain active even after 300 rounds.

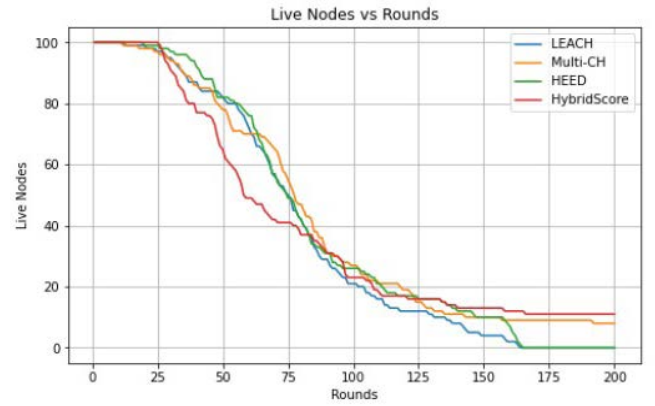


Fig. 4. Number of Live Nodes per Round for 200 Rounds

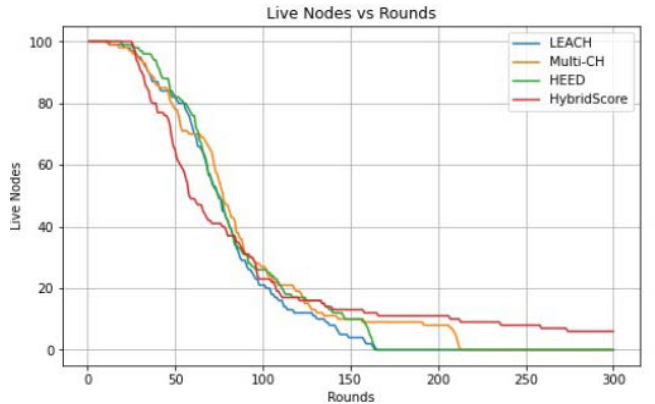


Fig. 5. Number of Live Nodes per Round for 300 Rounds

V. COMPARATIVE ANALYSIS

The simulation results demonstrate the proposed HybridScore protocol outperformed all the other schemes by maintaining a larger number of live nodes for 100, 200 and 300 rounds and conserving residual energy more effectively. By the end of 200 rounds, HybridScore retained a higher number of operational nodes, highlighting its efficiency in distributing energy consumption across the network. These results show that the HybridScore clustering protocol offers superior energy efficiency, improved CH rotation stability and extended network survivability compared to conventional clustering schemes. The improvements are particularly valuable for applications such as border surveillance, smart city monitoring and industrial IoT, where energy conservation and prolonged operational duration are critical requirements. The adaptive balance between residual energy and communication distance in the HybridScore protocol proves to be the key driver behind its enhanced performance. It is also observed that the Multi-CH protocol exhibits performance characteristics that are relatively close to

those of the proposed HybridScore, primarily due to its strategy of deploying multiple cluster heads within a cluster to distribute communication and processing loads. This approach effectively balances energy consumption among nodes and reduces the burden on any single cluster head, thereby extending the network lifetime compared to conventional single-CH schemes like LEACH and HEED. However, while Multi-CH achieves notable energy savings and stability improvements, it suffers from increased coordination overhead and control message exchange among multiple cluster heads, which can lead to inefficiencies in sparse or dynamic networks. HybridScore builds upon the strengths of Multi-CH by incorporating a hybrid scoring mechanism that jointly considers residual energy and node distance for CH selection, enabling more adaptive rotation and reducing unnecessary overhead. As a result, HybridScore achieves better energy retention and higher survival rates, while maintaining comparable or lower complexity than Multi-CH in most network conditions. The detailed comparison of using SI based techniques in LEACH and HEED protocols is presented in Table I.

TABLE I. COMPARISON OF LEACH, HEED, MULTI-CH AND HYBRIDSCORE

Feature	LEACH (Low-Energy Adaptive Clustering Hierarchy)	HEED (Hybrid Energy-Efficient Distributed)	Multi-CH	HybridScore (Proposed)
Cluster Head (CH) Selection	Randomized, probability-based.	Probability-based with residual energy consideration.	Multiple CHs per cluster using hybrid energy-distance metric.	Optimized using ACO, considering energy, communication costs, and node distribution.
CH Rotation	Periodic, probabilistic.	Residual energy-driven.	Multiple CHs with dynamic election.	Dynamic, with hybrid-score-based rotation.
Energy Efficiency	Low due to random selection of CHs.	Medium as energy and communication cost are considered.	High as it balances multiple CH workload.	Very High as it minimizes overhead & balances load.
Scalability	Moderate	Good	High: Supports large networks.	High: adaptive to topology changes.
Complexity	Low.	Medium.	Higher due to multiple CHs.	Moderate: Optimized algorithm.
Best Application Scenarios	Small WSN, low mobility.	Energy-aware moderate networks.	Dense networks with high data load.	Large-scale and remote networks like smart city and border surveillance

VI. CONCLUSION

This study presented a detailed performance evaluation of four prominent clustering protocols—LEACH, HEED, Multi-CH, and the proposed HybridScore—for wireless sensor networks (WSNs) with an emphasis on energy efficiency, stability period, and overall network lifetime. The simulation results conclusively demonstrated that HybridScore, by integrating residual energy awareness and proximity-based metrics within a hybrid scoring framework, consistently outperforms conventional protocols. Despite its improved performance, HybridScore presents opportunities for further enhancement. The performance

of HybridScore is dependent on the values of the weight parameters. We can get better result if we use adaptive parameter tuning using machine learning to dynamically adjust CH selection weights based on real-time network conditions. We can also focus on integration with energy harvesting technologies such as solar or vibrational energy to further extend the lifetime of nodes in harsh or inaccessible regions. We should also include security-aware clustering to protect against malicious node behaviour, eavesdropping and cluster-based attacks without compromising energy efficiency. Future work will explore real-world testbed implementation

and large-scale heterogeneous WSN deployments to validate the scalability, robustness and interoperability of the proposed protocol. Incorporating cross-layer optimization strategies and predictive analytics for CH rotation also remains a promising avenue to enhance the resilience and reliability of HybridScore in diverse application domains such as border surveillance, smart cities and environmental monitoring.

REFERENCES

- [1] W. Heinzelman, A. Chandrakasan and H. Balakrishnan, "Energy-efficient communication protocol for wireless microsensor networks," Proceedings of the 33rd Annual Hawaii International Conference on System Sciences (HICSS), pp. 10, 2000. doi: 10.1109/HICSS.2000.926982.
- [2] O. Younis and S. Fahmy, (2004). "HEED: a hybrid, energy-efficient, distributed clustering approach for ad hoc sensor networks", IEEE Transactions on Mobile Computing, Vol. 3, No. 4, pp. 366–379, 2004. doi:10.1109/TMC.2004.41.
- [3] A. Manjeshwar and D.P. Agrawal, "TEEN: A Routing Protocol for Enhanced Efficiency in Wireless Sensor Networks", Proceedings of 15th International Parallel and Distributed Processing Symposium. IPDPS, pp. 2009–2015, 2001. doi:10.1109/ipdps.2001.925197.
- [4] M. Pant, B. Dey and S. Nandi, "A Multihop Routing Protocol for Wireless Sensor Network based on Grid Clustering", Proceedings of IEEE 2015 Applications and Innovations in Mobile Computing (AIMoC), pp. 137–140, 2015. doi:10.1109/AIMOC.2015.7083842.
- [5] S. Lindsey and C.S. Raghavendra, "PEGASIS: Power-efficient gathering in sensor information systems", Proceedings of IEEE 2002 IEEE Aerospace Conference, Vol. 3, pp. 3.1125 – 3.1130, 2002. doi:10.1109/AERO.2002.1035242.
- [6] A.A. Abbasi and M. Younis, "A survey on clustering algorithms for wireless sensor networks", Vol. 30, pp. 2826–2841, 2007. doi:10.1016/j.comcom.2007.05.024.
- [7] P.C. Srinivasa Rao, P.K. Jana and H. Banka, "A particle swarm optimization based energy efficient cluster head selection algorithm for wireless sensor networks", Wireless Networks, Springer, 2016. doi:10.1007/s11276-016-1270-7.
- [8] A.S. Nandan, S. Singh and L.K. Awasthi, (2021). "An efficient cluster head election based on optimized genetic algorithm for movable sinks in IoT enabled HWSNs", Applied Soft Computing Journal, 107 (2021) 107318, 2021. doi:10.1016/j.asoc.2021.107318.
- [9] J. Pierezan and L. Dos Santos Coelho, "Coyote Optimization Algorithm: A New Metaheuristic for Global Optimization Problems," 2018 IEEE Congress on Evolutionary Computation (CEC), Rio de Janeiro, Brazil, 2018, pp. 1-8, doi: 10.1109/CEC.2018.8477769.
- [10] P. Kathirolu and K. Selvadurai, "Energy-efficient cluster head selection using improved Sparrow Search Algorithm in Wireless Sensor Networks", Journal of King Saud University - Computer and Information Sciences, 2021. doi:10.1016/j.jksuci.2021.08.031.
- [11] F. Xiangning and S. Yulin, "Improvement on LEACH Protocol of Wireless Sensor Network," Proceedings of 2007 International Conference on Sensor Technologies and Applications (SENSORCOMM 2007), Valencia, Spain, 2007, pp. 260-264, doi: 10.1109/SENSORCOMM.2007.4394931.
- [12] A. Khalifeh, H. Abid and K.A. Darabkh, "Optimal Cluster Head Positioning Algorithm for Wireless Sensor Networks." Sensors, 20(13), 3719, 2020. doi:10.3390/s20133719.
- [13] M. Satyanarayanan, "The Emergence of Edge Computing." Computer, Vol. 50(1), pp. 30–39, 2017. doi:10.1109/MC.2017.9.
- [14] F.T. Liu, K.M. Ting and Z.H. Zhou, "Isolation Forest," 2008 Eighth IEEE International Conference on Data Mining (ICDM), pp. 413–422, 2008. doi:10.1109/icdm.2008.17.

Development of various drug delivery system for semaglutide: a wonder drug for diabetes.

Sayan Biswas¹, Sonali Rudra²

¹Assistant Professor, Department of Pharmaceutical Technology,
School of Health and Medical Sciences
Adamas University, Kolkata 700126

²Professor of practice, Department of Pharmaceutical Technology,
School of Health and Medical Sciences
Adamas University, Kolkata 700126

Abstract: "Type 2 diabetes mellitus is a major global metabolic disorder requiring long-term and effective therapeutic management. Conventional antidiabetic drugs are often associated with adverse effects and limited patient compliance. Peptide-based therapies, particularly glucagon-like peptide-1 (GLP-1) receptor agonists, have emerged as promising alternatives. Semaglutide, a lipidated GLP-1 analog with prolonged half-life, offers effective glycemic control along with additional benefits in weight reduction and cardiovascular risk improvement. This review highlights the development of various drug delivery systems for semaglutide, focusing on its pharmacodynamics, pharmacokinetics, and formulation strategies. Currently available formulations include once-weekly injectable forms and the first oral GLP-1 receptor agonist enabled through absorption enhancers. However, challenges such as low oral bioavailability and enzymatic degradation persist. Recent advances in controlled-release and nano-based delivery systems, including nanoparticles, liposomes, microspheres, and self-emulsifying formulations, have shown potential in enhancing stability, permeability, and sustained drug release. Continued innovation in delivery technologies may further improve therapeutic efficacy and patient adherence in diabetes and obesity management."

Key Words: Semaglutide; GLP-1 receptor agonist; Controlled drug delivery; Type 2 diabetes mellitus; Oral peptide delivery

Introduction

Diabetes mellitus (Type II diabetes) is a major metabolic disorder affecting around 400 million people globally. On progression for a long period of time it leads to serious damage of blood vessels and nerves both at micro and macro level. Diabetes mellitus occurs due to deficiency of secretion of insulin due to damage to the pancreatic β cell. Sedentary lifestyle is one of the major contributing factor for this metabolic disorder. Apart from insulin itself other drugs used to treat this metabolic disorder can be classified into different category. The first major category of drugs include sulfonylureas which acts by enhancing insulin release from pancreatic beta cells Example of this class are Glipizide, glyburide, glibenclamide etc. The second major category of drugs are biguanides which acts by reducing hepatic glucose production. Example of this class are phenformin, metformin etc. Peroxisome proliferator-activated receptor- γ (PPAR γ) agonists consisting of pioglitazone, rosiglitazone etc forms the third category of drugs. Apart from these other classes of drugs such as α -glucosidase inhibitors are also available. These classes of drugs are either given alone or in combination with each other. However serious side effects involving hypoglycemia, weight gain less efficacy due to improper dosing schedule are some of the drawbacks of this class of drugs. In this aspect peptide based drugs can be a suitable alternative due to its biocompatibility and low side effect. Peptides are generally short chain amino acids having specific therapeutic activity. These are generally

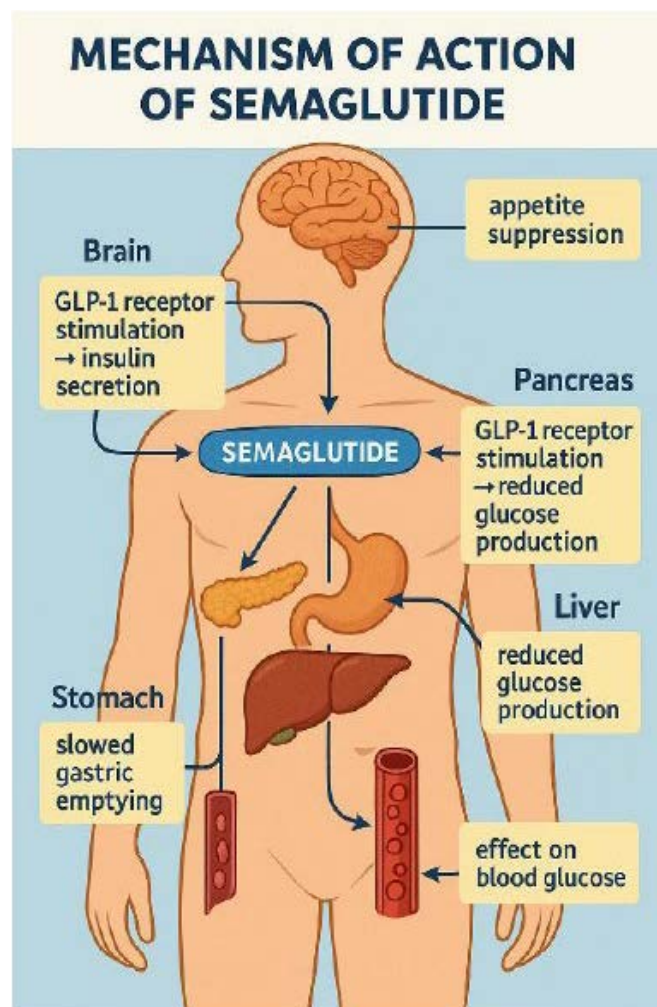
administered in injection form as is the case of insulin. This procedure is inconvenient and regular injections can cause patient discomfort. Oral delivery of peptide could solve this problem and increase patient compliance. However, oral peptide delivery has problems of low bioavailability due to denaturation and hydrolysis in the gastrointestinal environment. In order to combat this various strategies have been applied such as cyclization of peptide, addition of absorption enhancer etc. This led to the development of oral peptide drugs for diabetes treatment. These are termed as glucagon-like peptide-1 receptor (GLP-1R) agonist drugs and are slowly and steadily becoming a market favourite. Leading the trend is semaglutide with market potential of USD 28,429.9 million in 2024 and it is projected to reach USD 93,598.8 million by 2035, with a CAGR of 10.5%. One major drawback of GLP-1 is its short half-life. In order to address this issue several GLP-1 analogue have been synthesized. Semaglutide is one such analogue acting as glucagon-like peptide-1 receptor agonist which is used to enhance insulin secretion. It also has a weight loss property. On the contrary the side effects are also few [1]. It is a lipidated glucagon-like peptide 1 (GLP-1) derivative, approved for type 2 diabetes and weight loss. It shares 94% homology with human GLP-1. It consists of 31 amino acids having two amino acid substitutions (Aib8 and Arg34). Position 8 substitution reduces the degradation susceptibility by dipeptidyl peptidase-4 enzyme. [2]. The following review focuses on discovery and development of semaglutide as effective oral peptide for treatment of diabetes.

Pharmacodynamics of semaglutide

Semaglutide functions by activating GLP-1 receptors, which are found in several tissues such as the pancreas, brain, and gastrointestinal tract. The pharmacological effects of semaglutide are multifaceted and include:

Mechanism of action:

1. **Insulin Secretion:** GLP-1 receptor activation increases glucose-dependent insulin secretion from pancreatic beta cells, improving glucose control.
2. **Glucagon Suppression:** By inhibiting glucagon release from alpha cells, semaglutide reduces hepatic glucose production, contributing to lower blood glucose levels.
3. **Gastric Emptying and Appetite Suppression:** Semaglutide slows gastric emptying, which leads to early satiety and reduced food intake, a significant factor in promoting weight loss.



This has been depicted in Figure 1.

Fig 1: Mechanism of action of semaglutide (<https://chatgpt.com/g/g-pmuQfob8d-image-generator>)

Given its powerful pharmacological effects, semaglutide has demonstrated superior clinical outcomes in comparison to other GLP-1 receptor agonists, with evidence showing

both significant reductions in HbA1c levels and weight loss (Pratley et al., 2018). FDA in 2017 approved semaglutide as subcutaneous injection form (Ozempic) for treatment of Type 2 Diabetes Mellitus whereas in 2019 gave approval for the oral formulation of semaglutide (Rybelsus). Semaglutide (Wegovy) was also approved for obesity management in 2021 by FDA. In addition, semaglutide significantly improved cardiovascular outcomes. It was approved for the treatment of T2D by FDA in 2017 (Ozempic) and 2019 (Oral semaglutide, Rybelsus), and for obesity management by FDA in 2021 (Wegovy). Semaglutide is currently the only GLP-1 receptor agonist that is available in both a subcutaneously injectable and oral formulation [3].

1. Once-Weekly Semaglutide (Ozempic)

The once-weekly formulation of semaglutide, branded as Ozempic, is currently the most widely used formulation in clinical practice. This formulation employs a controlled-release mechanism that utilizes semaglutide's modified GLP-1 structure, which confers a long half-life of approximately one week [4]. Ozempic's once-weekly administration has been shown to significantly reduce HbA1c and body weight in patients with type 2 diabetes, with sustained therapeutic effects and minimal adverse events [5].

The controlled-release properties of Ozempic are facilitated by its formulation in a solution that is designed to slowly release semaglutide over a week following subcutaneous injection. The steady pharmacokinetic profile ensures that patients maintain therapeutic drug concentrations without the need for daily

2. Once-Daily Semaglutide (Wegovy)

Semaglutide has also been formulated for daily use under the brand Wegovy, which is approved for weight management in patients with obesity. Like Ozempic, Wegovy is an injectable formulation that exploits the GLP-1 analogue's pharmacokinetics for prolonged action. However, the dosage and administration frequency differ significantly.

Wegovy offers a higher dose of semaglutide (up to 2.4 mg weekly in escalating doses), providing more significant weight loss effects compared to the lower doses used for diabetes treatment [6]. The formulation is intended to be administered subcutaneously once a week, offering a convenient method for patients who prefer fewer injections.

3. Oral Semaglutide (Rybelsus)

Oral semaglutide (Rybelsus) represents a novel and convenient formulation for patients who prefer oral administration over injections. Approved in 2019, Rybelsus is the first GLP-1 receptor agonist to be offered in an oral

form. The oral formulation contains semaglutide in a tablet form that is absorbed through the gastrointestinal tract. The challenge in developing oral semaglutide was overcoming the degradation of GLP-1 in the gastrointestinal environment. To address this, Rybelsus is formulated with sodium N-[8-(2-hydroxybenzoyl)amino] caprylate (SNAC), a compound that enhances absorption in the stomach [7]. Studies have shown that Rybelsus offers similar efficacy to injectable semaglutide in reducing HbA1c and body weight [8]. Although it is not a controlled-release formulation in the traditional sense, the slow-release absorption achieved with the SNAC formulation provides a prolonged effect compared to other oral GLP-1 analogs.

Pharmacokinetics insights

In subcutaneous form semaglutide is used as once weekly injection at doses of 0.5 and 1.0 mg, with an initial dose of 0.25 mg/week for the first 4 weeks. This is done due to the slow elimination and delayed absorption of semaglutide in the body because of its high albumin binding capacity. Semaglutide metabolism takes place throughout tissues using proteolytic cleavage and excreted via urine or

faeces. As the proteolytic breakdown is detrimental to any oral peptide drug delivery, combined with low intestinal permeability and acidic pH formulation of oral semaglutide is challenging. It has been observed that oral bioavailability of semaglutide is only 0.4-1 %. This makes the dose higher in order to achieve similarity with subcutaneous form. This can be addressed by developing controlled release formulations of semaglutide [3, 2].

Long-Acting Semaglutide Formulations: Investigational Developments

Current research is focused on developing even longer-acting controlled-release formulations of semaglutide, which could allow for even less frequent dosing, potentially as infrequent as once monthly. These formulations would rely on advanced drug delivery systems, such as biodegradable microspheres, hydrogels, or nanocarriers, which release the drug slowly over time [9]. In this context various long acting drug delivery strategies have been adopted to improve the pharmacokinetic parameters as mentioned In Table 1:

Formulation	Material used	Method of preparation	Enhancement in property	References
Hard hybrid vesicles	Phospholipid and cholesterol	Dried film hydration-extrusion method	Improved in vivo epithelial permeability, enhanced oral bioavailability, and better therapeutic effectiveness	[10]
Nanoparticles	Nanoparticle 3-aminopropyl-functionalized magnesium phyllosilicate (AMP)	Electrostatic interactions	Nanoparticles effectively improved the membrane permeability and metabolic stability of semaglutide in the gastrointestinal tract. It protected the encapsulated drugs from proteolysis in simulated intestinal fluids and increased drug transport by 2.5-fold in Caco-2 cells leading to enhancement in therapeutic property.	[11]
Microsphere	Hydroxyethyl Starch (HES) and Poly lactic glycolic acid (PLGA)	Emulsification technique	Adding HES to the internal aqueous phase improved the in-situ drug stability and release behaviour of semaglutide-loaded PLGA microspheres, effectively increasing the peptide drug payload in PLGA microspheres.	[12]
Liposome	Hydrogenated soybean dylcholine	Emulsification and extrusion	Liposome enhanced the absorption of semaglutide in the small intestinal and hence oral bioavailability	[13]
Self-emulsifying drug delivery	Ethyl lauroyl arginate and docusate	Emulsification technique	Permeation studies across Caco-2 monolayer revealed an at least 2-fold increase in permeability of semaglutide for the developed formulations	[14]

Clinical trials

The efficacy of semaglutide in its various controlled-release formulations has been rigorously tested in clinical trials. Semaglutide has demonstrated substantial reductions in HbA1c and body weight across multiple trials.

- **Ozempic:** In the SUSTAIN clinical trial program, Ozempic significantly reduced HbA1c by up to 1.5% from baseline and facilitated weight loss of up to 6.4 kg compared to placebo. In the SUSTAIN 7 trial, semaglutide was found to be superior to liraglutide, with better results in both glycemic control and weight loss [15].
- **Wegovy:** The STEP trials (STEP 1-4) have consistently shown that Wegovy, in its higher-dose formulation, results in weight reductions of up to 15% or more in individuals with obesity. This formulation has proven to be effective not only in glycemic control but also in achieving significant long-term weight loss [6].
- **Rybelsus:** In the PIONEER trial series, Rybelsus demonstrated reductions in HbA1c and body weight similar to injectable semaglutide, making it a viable option for patients who prefer oral medications [8] (Husain et al., 2020).

Conclusion

Semaglutide, with its controlled-release formulations, represents a significant advancement in the treatment of type 2 diabetes and obesity. The once-weekly injectable formulations (Ozempic and Wegovy) and the oral formulation (Rybelsus) have proven to be highly effective in controlling blood glucose and promoting weight loss. Emerging long-acting formulations may further optimize patient adherence and therapeutic outcomes, offering the possibility of once-monthly dosing. Future research will focus on refining these formulations and addressing the remaining challenges, ensuring that semaglutide remains a cornerstone of metabolic disorder management for years to come.

References

- [1] Wang C, Wu Z, Zhou J, Cheng B, Huang Y. Semaglutide, a glucagon-like peptide-1 receptor agonist, inhibits oral squamous cell carcinoma growth through P38 MAPK signaling pathway. *J Cancer Res Clin Oncol*. 2025 Mar 7;151(3):103. doi: 10.1007/s00432-025-06154-5. PMID: 40055197; PMCID: PMC11889073.
- [2] Wenjing Jiang, Qiuli Wang, Xiaoyan Zhang, Husheng Yang, Xinggong Yang. Semaglutide sustained-release microspheres with single-phase zero-order release behavior: Effects of polymer blending and surfactants. *Journal of Drug Delivery Science and Technology*. Volume 107, 2025, 106793, ISSN 1773-2247, <https://doi.org/10.1016/j.jddst.2025.106793>.
- [3] Yang XD, Yang YY. Clinical Pharmacokinetics of Semaglutide: A Systematic Review. *Drug Des Devel Ther*. 2024 Jun 25;18:2555-2570. doi: 10.2147/DDDT.S470826. PMID: 38952487; PMCID: PMC11215664.
- [4] Nauck, M., Meier, J. J., & Stumvoll, M. (2016). Semaglutide in Type 2 Diabetes: Current Status and Future Perspectives. *The Lancet Diabetes & Endocrinology*, 4(5), 370–380.
- [5] Marso, S. P., Bain, S. C., Consoli, A., et al. (2016). Semaglutide and Cardiovascular Outcomes in Patients with Type 2 Diabetes. *NEJM*, 375(19), 1834-1844.
- [6] Wilding, J. P. H., Batterham, R. L., & Davies, M. J. (2021). Semaglutide in Patients with Obesity: A Systematic Review and Meta-Analysis of the STEP Trials. *Obesity*, 29(5), 902-912.
- [7] Ahmad, H., Malik, M. R., & Kaur, S. (2019). Oral semaglutide: a breakthrough in GLP-1 receptor agonists. *Diabetes Therapy*, 10(2), 515–526.
- [8] Husain, M., Birkenfeld, A. L., Donsmark, M., et al. (2020). Oral semaglutide and cardiovascular outcomes in patients with type 2 diabetes: a systematic review and meta-analysis of the PIONEER trials. *Lancet Diabetes Endocrinol*, 8(10), 758–769.
- [9] Dinesh, P. A., Sheth, M., & Dey, S. (2021). Emerging Long-Acting GLP-1 Receptor Agonists: Formulation Strategies and Clinical Implications. *Advanced Drug Delivery Reviews*, 172, 1-12.
- [10] Xiao P, Yuan H, Liu H, Guo C, Feng Y, Zhao W, Zhao B, Yin T, Zhang Y, He H, Tang X, Gou J. Modulating the elasticity of milk exosome-based hybrid vesicles to optimize transepithelial transport and enhance oral peptide delivery. *J Control Release*. 2025 Apr 10;380:36-51. doi: 10.1016/j.jconrel.2025.01.090. Epub 2025 Feb 4. PMID: 39892650.
- [11] Kim GL, Song JG, Han HK. Enhanced Oral Efficacy of Semaglutide via an Ionic Nanocomplex with Organometallic Phyllosilicate in Type 2 Diabetic Rats. *Pharmaceutics*. 2024 Jun 30;16(7):886. doi: 10.3390/pharmaceutics16070886. PMID: 39065583; PMCID: PMC11280289.
- [12] Zeng H, Song J, Li Y, Guo C, Zhang Y, Yin T, He H, Gou J, Tang X. Effect of hydroxyethyl starch on drug stability and release of semaglutide in PLGA microspheres. *Int J Pharm*. 2024 Apr 10;654:123991. doi: 10.1016/j.ijpharm.2024.123991. Epub 2024 Mar 11. PMID: 38471578.
- [13] Li Y, Liu F, Che J, Zhang Y, Yin T, Gou J, Tang X, Wang Y, He H. Sodium glycocholate liposome encapsulated semaglutide increases oral bioavailability by promoting intestinal absorption. *Int J Pharm*. 2024 Nov 15;665:124669. doi: 10.1016/j.ijpharm.2024.124669. Epub 2024 Sep 5. PMID: 39244070.
- [14] Sandmeier M, Ricci F, To D, Lindner S, Stengel D, Schifferle M, Koz S, Bernkop-Schnürch A. Design of self-emulsifying oral delivery systems for semaglutide: reverse micelles versus hydrophobic ion pairs. *Drug Deliv Transl Res*. 2025 Jun;15(6):2146-2161. doi: 10.1007/s13346-024-01729-0. Epub 2024 Oct 19. PMID: 39427069; PMCID: PMC12037675.
- [15] Pratley, R., Aroda, V. R., & Lingvay, I. (2018). Efficacy and safety of once-weekly semaglutide in patients with type 2 diabetes: The SUSTAIN 7 trial. *Diabetes Care*, 41(5), 900–907.

A Sustainable Impact of NEP 2020 on Indian Education System with Future Prospects: A Perspective of Teachers in Higher Education

Dr. Sarita Yadav

*Assistant Professor, Department of Management Studies
Management Education and Research Institute*

Dr. Deepshikha Kalra

*Associate Professor, Department of Management Studies
Management Education and Research Institute*

Dr. Dalip Raina

*Assistant Professor, Department of Management Studies
Shri Vishwakarma Skill University, Haryana*

Abstract—In light of the notion that education promotes both social and economic growth, the National Education Policy (NEP) 2020 aims to offer high-quality education that will both help the economy expand and flourish at the school and college levels. The creation of the NEP 2020 was one of the significant developments that occurred in India in 2020. Present contribution discusses the NEP 2020, which focuses primarily on providing students with hands-on training to help them develop their creative potential, skills, and analytical thinking in order to satisfy the demands of the business. Present contribution has taken the perspective of teachers of higher education regarding sustainable impact of NEP 2020 on Indian education system on various dimensions. The data suggests that females may hold a more optimistic view regarding the NEP potential impact on vocational courses, career opportunities, and the quality of teaching and learning. Additionally, the agreement is observed on the NEP's positive influence on overall governance in educational institutions, with females again indicating a slightly more favorable perception than their male counterparts.

Keywords: NEP 2020, Creative potential, Skills, Analytical thinking

I. INTRODUCTION

In order to confront the overabundant man in the overabundant society, education is a lifetime effort. Students need to be prepared by the educational system to be academics, researchers, trailblazers, instructors, and lifelong learners. India has seen steady and considerable economic progress in the last few decades, but the country still faces socioeconomic challenges. Improving education is the only way to solve these problems and hasten the country's economic development (Reddy, 2021). If we wish to turn India into a Super Global Knowledge Power, we must create effective, modern education policy. The aim of a quality higher education should be to develop radiant, thoughtful, diverse, and innovative individuals. In addition to developing character, ethical and constitutional values, intellectual curiosity, scientific temper, creativity, service spirit, and 21st-century skills across a range of fields, including sciences, social sciences, the arts, humanities, languages, personal, technological, and vocational subjects, it must allow a person to study one or more specialized areas of interest at an in-depth level (Das, 2020). In emerging nations like India, higher education is

essential since it fosters human development. After Indian independence, higher education has increased significantly. It advances national growth by distributing specific skills and knowledge. But Indian education system has drawn criticism for being inflexible, test-focused, and devoid in originality and creativity and witnessed significant change during the past few decades (Pioneer, 2020).

However to make the current system better, the policies required to be modified, especially considering the various elements that could alter the curriculum and educational system (Samitha, 2020). A new NEP typically appears a few decades later. Three changes have previously occurred in India: the first policy was implemented in 1968, the second reform was implemented in 1986, and the NEP from that year was amended in 1992. On July 29, 2020, the Narendra Modi administration released the most recent New Education Policy (NEP) (Kaurav et al., 2020). As a result, the New Education Policy-2020 was created to create a framework for offering top-notch secondary and tertiary education to all citizens of the country while preserving Indian culture and values (Tiwari, 2022). A review and modernization of the current educational framework,

including laws, regulations, and regulatory mechanisms, are necessary to raise the bar for education at every level. The objective is to establish the nation as an affluent, just, and superpower in the world of information (Aithal and Aithal, 2020). Among the other major changes recommended by the NEP are the dismantling of the University Grants Commission (UGC) and the All India Council for Technical Education (AICTE), the establishment of a four-year multidisciplinary undergraduate programme with multiple exit options, and the discontinuation of the M. Phil programme.

The education policy in schools is focused on modifying the core curriculum, making board exams “easier” cutting the syllabus while keeping “essential principles” and encouraging “experiential learning” and “critical thinking” (Devi and Chelvaraju, 2020). The establishment of a National Research Foundation to support excellent peer-reviewed work and effectively seed study at universities and colleges is one of the key highlights of the new education policy, which brings some fundamental changes to the current system. The primary goals of the policy are to raise the standard of Higher Education Institutions (HEIs) and position India as a centre for global education (Das, 2022). The focus is on providing an integrated curriculum with flexibility, enabling numerous undergraduate degree exit points, expediting research, increasing faculty support, and advancing globalization (Das & Barman, 2023). The proposed initiatives, such as the introduction of vocational courses, reduced board exam stress, and flexibility in subject choices, show promise in providing success for all stakeholders. The shift in focus from what the system provides to allowing students to learn based on their preferences is a positive transformation.

2. Review of Literature

Aithal and Aithal (2020) did the pioneer research on NEP and concluded that higher education plays a pivotal role in determining a country's economic, social status, technological advancement, and overall human behavior. The responsibility of the country's education department is to enhance Gross Enrollment Ratio (GER) by ensuring inclusive higher education opportunities for every citizen. NEP aims to realize its goals by 2030 by allowing private sector involvement with stringent quality controls, promoting merit-based admissions, offering scholarships, and encouraging research-based faculty, NEP-2020 aims. The transformation involves the conversion of affiliated colleges into multi-disciplinary autonomous colleges, granting degree-giving powers and establishing

an impartial National Research Foundation for funding priority research projects. The higher education system is set to become student-centric, providing freedom in subject choices, curriculum design, and evaluation methods.

Kalyani (2020) concluded that this is an ambitious proposal of the Indian government to enhance the country's education system is a significant undertaking. After a 34-year gap in the education system, the need for substantial change became evident, particularly in bridging the gap between academia and industry. This disparity resulted in the production of educated individuals who struggled to find suitable positions in the workforce, leading to unemployment or underemployment, causing frustration and mental health challenges. While the New Education Policy (NEP) 2020 is still in the proposal stage, there is recognition of the potential need for adjustments, either before implementation or based on practical outcomes.

Ross (2020) apprised that rise of technology-driven education is expected to replace traditional classroom instruction and influence NEP-2020 policies due to advancements in technology. In the twenty-first century, the vision is to lay the foundation for a hybrid education system that combines online and classroom-based learning, incorporating increased research components. Both elementary and higher education sectors, as per NEP-2020, will have a unified control and monitoring system. The implementation process consists of seven steps, with the first 10 years dedicated to implementation and the subsequent decade focused on operational aspects.

Kaurav et al. (2020) discussed that NEP 2020 presents a comprehensive framework aimed at advancing the educational system in India. It promotes critical thinking, experiential learning, and instruction in native languages. A key focus is on cultivating professionals across diverse fields, from agriculture to artificial intelligence, preparing India for future challenges. The policy introduces multi-disciplinary approaches, allowing students pursuing professional degrees to explore humanities, a freedom previously unavailable. Vocational skills and teacher training are paramount, offering flexibility through transferable credit banks to address high dropout rates. Prioritizing mother tongue/local language at the primary level minimizes dropouts and enhances learning capacities. NEP 2020 aims to equip students with essential skills, foreseeing a transformative impact on India's education landscape, potentially propelling it toward superpower status.

Sundaram (2020) discussed implementation of high-quality education holds the potential to unlock a myriad of opportunities in employment, business, entrepreneurship,

and teaching domains. NEP 2020 has the capacity to lift both individuals and communities from cycles of disadvantage. Students can now explore a diverse range of subjects in their courses, acquiring varied knowledge that empowers them to make productive career choices. The introduction of vocational courses has created avenues for self-employment, addressing the needs of the community and society at large. The policy places a particular emphasis on Sustainable Development Goals (SDGs), with SDG 4 specifically focusing on education. The policy envisions education as a catalyst to achieve other SDGs by 2030. Notably, NEP 2020 highlights music, arts, and instruments, offering new career opportunities for those with talent or an interest in these fields. Technological innovation in education presents new prospects for students aspiring to excel in software and hardware, both integral to the IT industry.

Verma and Kumar (2021) critically analysed the policy and suggested modifications to guarantee a smooth transition from its predecessor to current one, thus increasing its significance. The examination of the university level management practices and NEP 2020 requirements is presented in the current paper. There are suggestions for how NEPs should be created and implemented at the national and higher education levels (HEIs).

Choudhari (2022) advised that stakeholders need to actively engage with NEP 2020 to identify the skills necessary for effective participation in its implementation. It is crucial for stakeholders to proactively seek out and develop the skills essential for contributing to the economic growth facilitated by NEP 2020. Students, in particular, should assess their skills before selecting a course, as aligning their skills with their chosen course can expedite the achievement of their goals. Despite the broad potential for studying NEP 2020, there is a prevalent lack of awareness and understanding about its workings among the majority. Therefore, there is a pressing need for awareness campaigns and research efforts in this area to enhance knowledge among stakeholders. This increased understanding can accelerate the adoption of NEP 2020, contributing to the overall economic development.

Thakur (2022) concluded that Indian government has consistently crafted educational policies to maintain a high-quality and globally acknowledged education system. The impact of the previous two national educational policies has contributed to the development of India's educational landscape, setting the stage for the action plan under the third national educational policy. The effectiveness of this policy will be assessed by examining the outcomes derived from the current national education policy's action plan. Success of NEP hinges on the policy's ability to address

the root causes of prevailing challenges and issues.

Wani et al. (2023) offered a rejuvenating perspective to NEP, and concluded that policy incorporates flexibility and a hallmark of quality, shaping India into a vibrant society that resonates with its rich cultural heritage. The policy's focus on reducing the academic burden on students is pivotal for shaping the nation's future. However, its success hinges on uniform and transparent implementation across all levels, coupled with the equitable distribution of resources. Achieving this significant undertaking requires complete cooperation and collaboration among various stakeholders, supported by a robust institutional mechanism.

Yadav (2023) discussed that NEP 2020 promotes international collaboration and exchange initiatives to expose both students and educators to diverse global perspectives. The future prospects for NEP 2020 are very optimistic with its learner-centered approach, emphasis on comprehensive development, and integration of technology and skill enhancement, the policy holds the potential to bring about a transformative shift in India's education system. However, successful implementation necessitates committed efforts, collaboration among stakeholders, and ongoing assessments to ensure the attainment of desired outcomes.

Moreover studies are done in the context of opportunities, issues and challenges of NEP 2020. Few contributions are done to check impact of NEP 2020 on higher education of India in general perspective. But very scant contributions are done to take perspective of teachers about NEP 2020 and its impact. Present contribution has taken the perspective of teachers of higher education regarding sustainable impact of NEP 2020 on Indian education system on various dimensions. The focus is on examining NEP 2020 and the changes that have occurred in higher education. At these levels, emphasis was placed on practical approaches and job orientation, and the scope was expanded.

3.1 Objectives of the study

1. To know the features of NEP 2020 in context of higher education
2. To know the gender based perspective of teachers regarding impact of NEP 2020 with future prospects.

3.2. Hypothesis

H_0 : There is no significant difference of impact of NEP 2020 on Indian Education System between male and female teacher perspective.

4. Research Methodology

Both primary and secondary data has been taken to conduct the study. Primary data is collected from teachers of higher education. A sample of 100 teachers is collected

through questionnaire and convenient sampling technique is employed to define the sample. In a sample of 100 respondents, there were 56 men and 44 women. Secondary data is collected from the Ministry of Human Resource Development's NEP 2020 program. Independent sample t-test has been employed to analyze the data.

5.1. Features of NEP 2020

- The educational framework outlined in the NEP, structured as 5+3+3+4, is designed to offer students a more comprehensive and well-rounded learning experience, encompassing a diverse range of subjects and skills. This approach aims to enhance students' understanding of the world, equipping them to face the challenges of the 21st century effectively.
- The NEP underscores the importance of fostering critical thinking, creativity, and problem-solving skills. Through exposure to a broader array of subjects and skills, the revised curriculum intends to cultivate these vital abilities among students.
- The NEP introduces greater flexibility and choice in the curriculum, empowering students to customize their education based on individual needs and interests. This adaptability aims to nurture students' unique strengths and preferences, preparing them for their chosen career paths.
- Recognizing the significance of arts and humanities in shaping well-rounded individuals, the NEP advocates for an amplified emphasis on these disciplines. This approach seeks to provide students with a more holistic education, fostering a deeper understanding of the world and its diverse cultures.
- With the goal of enhancing students' readiness for the workforce, the NEP anticipates that the revised curriculum will contribute to achieving this objective. By exposing students to a broader spectrum of subjects and skills, coupled with an emphasis on critical thinking and problem-solving, the new curriculum is poised to equip students with the essential skills needed to excel in the contemporary workforce.
- Through the promotion of multilingual education, the NEP strives to foster a deeper appreciation and understanding of the diverse cultures and traditions within the country. This initiative is geared towards cultivating a more inclusive and respectful mindset towards different cultures among students, preparing them for the demands of an interconnected globalized world.
- Acknowledging the significance of proficiency in multiple languages, the NEP places importance on multilingual education to enhance students' communication skills. This focus is anticipated to enable students to communicate more effectively with individuals from diverse cultures, equipping them for the challenges posed by a globalized world.
- Proficiency in multiple languages is recognized as an advantageous skill in the job market, and the emphasis on multilingual education is projected to empower students with the language proficiency essential for success in their careers. This approach aims to open up a broader spectrum of job opportunities for students, aligning them with the demands of a globalized world.
- Drawing from research indicating the positive impact of multilingual education on cognitive development, the NEP's emphasis on multilingual education is poised to yield similar cognitive benefits. This emphasis seeks to enhance students' understanding of the intricacies of the world, better preparing them for the challenges characteristic of the 21st century.
- Through the broadening of vocational education, the NEP seeks to equip students with the necessary skills for success in the workforce. This initiative aims to enhance students' job readiness, better positioning them to tackle the challenges characteristic of the 21st century.
- The expansion of vocational education is anticipated to amplify access to skilled employment opportunities, particularly in sectors like manufacturing, construction, and information technology. This approach is designed to address the existing skills gap in the country, fostering a greater array of job prospects for students.
- The NEP endeavors to establish a stronger connection between education and the workforce, and the enlargement of vocational education is poised to contribute to this objective. By offering students practical, hands-on training in real-world skills, the expansion is anticipated to enhance students' understanding of workforce requirements, better preparing them for the challenges of the 21st century.
- The expansion of vocational education is expected to provide students with opportunities to cultivate skills in specific fields and gain practical, hands-on experience. This initiative is geared towards enabling students to develop the skills necessary for success in their chosen careers, effectively preparing them for the challenges of the 21st century.

5.2. Data Analysis

5.2.1. Descriptive Statistics

Table 1 provides statistical information based on the

responses of 100 participants, categorized by gender, to various statements related to the National Education Policy (NEP). In terms of gender distribution, the sample consists of 100 individuals, with an average of 1.24, a standard deviation of 0.429, and a variance of 0.184. Whereas, for the statement "NEP will improve and sustain quality in our educational institutions," the mean is 2.98 with a standard deviation of 1.110 and a variance of 1.232. Similarly, for the statement "NEP will bring complete literacy by 2050," the mean is 2.84, with a standard deviation of 0.950 and a variance of 0.903. The statement "NEP will bring profound changes in the employment requirement criteria of companies" has a mean of 3.61, a standard deviation of 1.270, and a variance of 1.614. Meanwhile, the statement "NEP will emphasize the promotion of vocational courses" has a mean of 3.55, a standard deviation of 1.167, and a variance of 1.361. Similarly, the statement "NEP will expand career opportunities through a multidisciplinary approach and bucket system" has a mean of 3.46, a standard deviation of 1.234, and a variance of 1.524. For the statement "NEP will improve the quality of teaching and learning," the mean is 3.12, with a standard deviation of 1.249 and a variance of 1.561. Lastly, the statement "NEP will improve overall governance on institutions" has a mean of 3.36, a standard deviation of 1.078, and a variance of 1.162. The data collectively reflects the

participants' responses, providing insights into their perceptions and attitudes towards different aspects of the National Education Policy.

SPSS Results

5.2.2 A Sustainable Impact of NEP 2020 on Indian Education System with Future Prospects

Table 2 provides a comprehensive analysis of gender-based perceptions regarding various aspects of the National Education Policy (NEP), as indicated by mean values and statistical measures. The t-values and associated p-values signify the significance of differences between male and female respondents.

Firstly, there is a statistically significant difference in the belief that the NEP will enhance and sustain the quality of educational institutions, with females expressing a higher mean score than males (3.167 vs. 2.921, $t = 5.402$, $p = 0.001$). Similarly, there is a significant gender-based difference in opinions about the NEP's potential to achieve complete literacy by 2050, where females exhibit a slightly lower mean score than males (2.792 vs. 2.855, $t = 4.634$, $p = 0.002$). Regarding employment criteria, the data reveals a significant gender-based distinction in the perception of whether the NEP will bring profound changes to the requirements of companies, with males showing a higher mean

Table 1 Descriptive Statistics

Variables	Mean	Std. Deviation	Variance
Gender	1.240	0.429	0.184
NEP will improve and sustain quality in our educational institutions	2.980	1.110	1.232
NEP will brings complete literacy by 2050	2.840	0.950	0.903
NEP will bring profound changes in the employment requirement criteria of companies	3.610	1.270	1.614
NEP will emphasize the promotion of vocation courses	3.550	1.167	1.361
NEP will expand career opportunities through a multidisciplinary approach and bucket system	3.460	1.234	1.524
NEP will improve the quality of teaching and learning	3.120	1.249	1.561
NEP will improve overall governance on institutions	3.360	1.078	1.162

score than females (3.645 vs. 3.500, $t = 2.378$, $p = 0.036$).

Moreover, there are significant gender differences in the belief that the NEP will emphasize the promotion of vocational courses, expand career opportunities through a multidisciplinary approach, and improve the quality of teaching and learning. Female respondents, on average, express higher levels of agreement with these statements compared to their male counterparts ($p < 0.001$). Additionally, both genders agree that the NEP will enhance overall governance in educational institutions, but females exhibit a higher mean score than males (3.625 vs. 3.276, $t = 7.496$, $p = 0.000$).

6. Conclusion

Gender-based perceptions on various aspects of the National Education Policy (NEP) reveals nuanced differences in attitudes. Female respondents generally express a more positive outlook, believing

that the NEP will significantly improve and sustain the quality of educational institutions, potentially achieve complete literacy by 2050, and bring about profound changes in employment criteria. Notably, there is a consistent trend where females exhibit higher mean scores across statements, emphasizing the importance of considering gender-specific perspectives in the evaluation of educational policies. The data suggests that females may hold a more optimistic view regarding the NEP's potential impact on vocational courses, career opportunities, and the quality of teaching and learning. Additionally, the agreement is observed on the NEP's positive influence on overall governance in educational institutions, with females again indicating a slightly more favorable perception than their male counterparts. These findings underscore the need for inclusive policy discussions that consider diverse perspectives to ensure effective and equitable implementation.

Table2 t-Test

Variables	Mean		t-value	Sig. p- value
	Male	Female		
NEP will improve and sustain quality in our educational institutions	2.921	3.167	5.402**	0.001
NEP will brings complete literacy by 2050	2.855	2.792	4.634**	0.002
NEP will bring profound changes in the employment requirement criteria of companies	3.645	3.500	2.378*	0.036
NEP will emphasize the promotion of vocation courses	3.513	3.667	7.240**	0.000
NEP will expand career opportunities through a multidisciplinary approach and bucket system	3.408	3.625	5.970**	0.001
NEP will improve the quality of teaching and learning	3.026	3.417	4.084**	0.006
NEP will improve overall governance on institutions	3.276	3.625	7.496**	0.000

****indicates significant at 1% and *indicates significant at 5%**

References

- ❑ Aithal, P.S. and Aithal, S. (2020). Implementation strategies of higher education part of national education policy 2020 of India towards achieving its objectives. *International Journal of Management, Technology, and Social Sciences*, 5(2), 283-325.
- ❑ Choudhari, D. D. (2022). A Study on National Education Policy – 2020 and its Impact on Stakeholders with respect to Higher Education Institutions of Nagpur City. *International Journal of Research Publication and Reviews*, 3(2), 390-394.
- ❑ Das, A.K. (2020). Understanding the changing perspectives of higher education in India. In *The Future of Higher Education in India* (pp. 226–228). <https://doi.org/10.5530/jscires.9.2.28>.
- ❑ Das, K., & Barman, A. (2021). Posits of workplace competencies in management education research- A review triangulation for discerning NEP-2020 (India)'s relevance. *Psychology and Education*, 58(5), 2271–2308. www.psychologyandeducation.net
- ❑ Das, P. (2022). National Education Policy 2020 : Role of information and communication technology (ICT) for implementing the modern education system.
- ❑ Das, P. (2023). Teacher education in the light of National Education Policy-2020. <https://doi.org/10.5281/zenodo.8332390>
- ❑ Das, P., & Barman, P. (2023). Does ICT Contribute Towards Sustainable Development in Education ? An Overview. *International Journal of Research Publication and Reviews*, 4(7), 544–548. <https://doi.org/10.5281/zenodo.8332286>
- ❑ Das, P., & Barman, P. (2023). Optimal Learning Environment for Higher Education Students in the Context of National Education Policy–2020 : An Analysis. <https://doi.org/10.5281/zenodo.8332322>
- ❑ Devi, L. and Cheluvaraju (2020). A study on awareness about the impact of national education policy-2020 among the stakeholder of commerce and management disciplinary. *European Journal of Business and Management Research*, 5(6), 1-5.
- ❑ Kalyani, P. (2020). An Empirical Study on NEP 2020 [National Education Policy] with Special Reference to the Future of Indian Education System and Its effects on the Stakeholders. *Journal of Management Engineering and Information Technology*, 7(5), 1-17.
- ❑ Kaurav, D. R. P. S., Suresh, P. K. G., Narula, D. S. and Baber, R. (2020). New education policy: qualitative (contents) analysis and twitter mining (sentiment analysis). *Journal of Content, Community & Communication*, 12(6), 4-13. [10.31620/JCCC.12.20/02](https://doi.org/10.31620/JCCC.12.20/02).
- ❑ "NEP 2020: A New Era in Indian Education," *The Pioneer*, August 5, 2020.
- ❑ National Education Policy 2020. https://www.mhrd.gov.in/sites/upload_files/mhrd/files/nep/NEP_Final_English.pdf. Accessed on 11/02/2023
- ❑ National Education Policy 2020. MHRD report https://www.education.gov.in/sites/upload_files/mhrd/files/NEP_Final_English_0.pdf. Accessed on 15/2/2023
- ❑ Reddy, D. P. N. (2021). National education policy 2020 - challenges and opportunities on the educational system. *International Journal of Science and Research*, 10(11), 927-930.
- ❑ Rose, A. (2020). National education policy 2020 and its impact on higher education India. *Journal of Commerce and Management*, 11(4), 351
- ❑ Smitha, S. (2020). National education policy (NEP) 2020 – opportunities and challenges in teacher education, *International Journal of Management*, 11(11), 1881-1886.

- ❑ Sundram, K. M. (2020). A Study on National Education Policy 2020 Concerning Career Opportunities. *Shanlax International Journal of Economics*, 9(1), 3–67.
- ❑ Thakur, P and Kumar, D. R. (2021). Educational Policies, Comparative Analysis of National Education Policies of India and Challenges. *International Journal of Multidisciplinary Educational Research*, 10(3), 13-16.
- ❑ Tiwari, D. R. (2022). National education policy: a vision for a new India. *Journal of Business and Management*, 24(8), 22-25.
- ❑ Verma, D. H. and Kumar, A. (2021). New Education Policy 2020 of India: A Theoretical Analysis. *International Journal of Business and Management Research*, 9(3), 302-306.
- ❑ Wani, A. A., Manhas, K. K. and Kumar, M. (2023). A theoretical analysis of national education policy 2020: Challenges and A way forward. *International Journal of Multidisciplinary Education and Research*, 8(1), 42-45.
- ❑ Yadav, S. (2023). A Comparative Study of Old and New Education Policy (NEP 2020) in India. *International Journal of Scientific Research in Science and Technology*, 10(4), 97-105.



REVIEW

Fork Index: A Quantitative Dermatoglyphic Marker for Human Sex Identification

Ms. Prerana Roy

*Department of Forensic Science, School of Basic and Applied Sciences,
Adamas University, Barasat, West Bengal 700126, India.*

Dr. Piyali Das

*Assistant Professor, Department of Anthropology, Dinabandhu Mahavidyalaya,
Bongaon, West Bengal 743235, India.*

Prof. Diptendu Chatterjee

*Professor, Department of Anthropology, University of Calcutta, 35 Ballygunge Circular Road,
Kolkata 700019, West Bengal, India.*

Dr. Biswarup Dey*

*Assistant Professor, Department of Forensic Science, School of Basic and Applied Sciences, Adamas
University, Barasat, West Bengal 700126, India*

**Corresponding Author*

Abstract:

Objectives. The current attempt uses the Fork Index to quantify the probabilities that fingerprint minutiae can be used to identify a person's sex.

Material and methods. The current study was carried out on the Adamas University campus in Barasat, North 24 Parganas district, West Bengal state, India. The sample was made up of 100 Bengali-speaking youth (students) from West Bengal, India (50 males and 50 females) to address this issue. All the bilateral fingerprints were collected using ink and roller techniques. All the collected prints were analyzed according to the standard classification and formula.

Results. The current study found that males have a substantially higher number of Forks and Minutiae in their fingertips than females. Furthermore, males score substantially higher mean on the Fork Index than females.

Conclusions. The Fork Index, like previous investigations, has demonstrated sexual dimorphism. Based on such sexual dimorphism, the current study concludes that the Fork Index has the potential to be a biomarker for human sex determination and is valuable for forensic purposes.

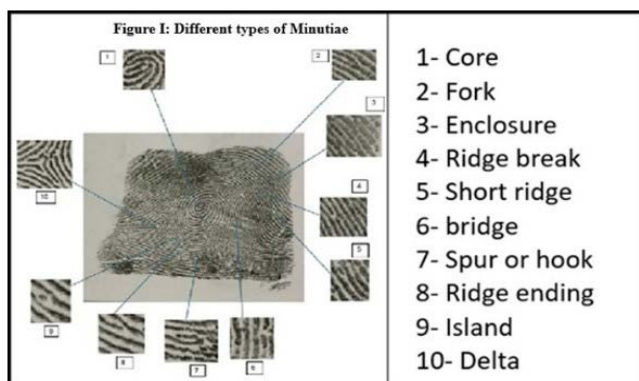
Keywords: Finger Dermatoglyphics, Minutiae, Fork, Fork Index, Sexual dimorphism, Bengali Population.

Introduction:

The scientific study of the cutaneous ridges on the fingers, palms, and soles that develop during the early stages of intrauterine life is known as dermatoglyphics [6]. Only genetic and environmental changes can affect the

development of epidermal ridges [1]. Through extensive investigation, Sir Francis Galton (1892) [5] established the durability of skin ridge patterns, significantly advancing the fingerprint recognition science. The basis for fingerprint identification in the modern period and the classification of physio-morphic features of the dermal ridges was well established [1].

The microscopic minute features of the friction ridge skin that enable the forensic application of fingerprint identification are known as fingerprint minutiae. Because fingerprints with the same number of arches, loops, and whorl patterns have different minutiae configurations, it is the most essential element for fingerprint recognition [2]. Ridge termination, ridge bifurcation, enclosure, short ridge, bridge, ridge crossing, hook, fork, and island are various minutiae points [3]. Sarkar (1980) stated that any



minutiae's quantity and location are biometric indicators of individualistic pattern formation [3]. Okajima (1970)[4] formulated the Fork Index [3]. Banerjee and Sarkar (1983) [3] studied the fork distribution in fingerprints and reported a comparatively higher distribution of FI among males than females. The present study aims to reinvestigate and find the utility of the Fork Index as a Forensic measure of human sex determination through finger dermatoglyphics.

Research methodology:

Research purpose and objectives

In the event of a Crime Scene investigation, the specialists discovered and traced many fingerprints. However, determining the sex of such prints is difficult because both males and females may have comparable patterns or ridge counts. The current study uses minutiae to determine the probable sex of lifted fingerprints. The fork is a distinct arrangement that can be easily traced among the various minutiae.

The objectives that guided this investigation were the following:

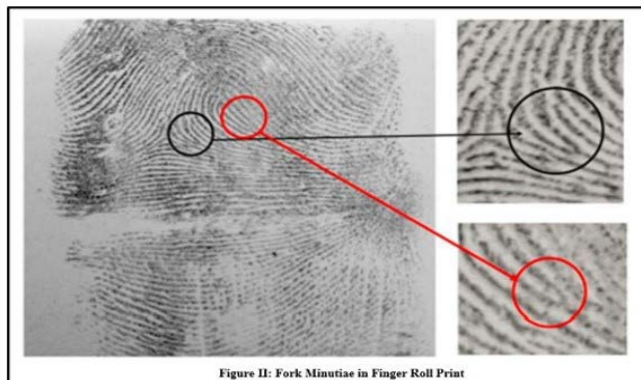


Figure II: Fork Minutiae in Finger Roll Print

The current study aims to assess the Fork Index's efficacy as a forensic measure of human sex determination utilising finger dermatoglyphics.

Research methods and instruments

All the bilateral fingerprints were collected according to the standard ink and roller method [6]. The minutiae classification and fork identification were done using the standard classification of Sarkar (2004) [7], and the fork index (FI) was computed using the formula proposed by Okajima (1970). The formula of FI is as follows:

$$\text{Fork Index (FI)} = \frac{\text{Total Number of Fork}}{\text{Total Number of Minutiae}} \times 100$$

Fork Index(FI)=(Total Number of Fork)/(Total Number of Minutiae)×100

All the data were interpreted in Microsoft Excel 2013, and all the statistical tests were performed in SPSS version 18.0. The cut-off was set at the 95% probability limit.

Participants

The present study was conducted within the campus of Adamas University, Barasat, North 24 Parganas, district, state of West Bengal, India. To solve this problem, the present study incorporated 100 (50 males;24.15±9.71 and 50 females 23.86±8.56) Bengali-speaking youth (students) from West Bengal, India. The purposive random sampling method was followed based on their availability at the time of their data collection.

Inclusion and Exclusion criteria

Healthy people without skin illness or dermatoglyphic abnormalities are included in the age group of 18 to 25 years. Furthermore, the subjects must be Bengali speakers who live in West Bengal, India.

Individuals with ridge disassociation and permanent scars on the finger ball (digital volar sac) due to injury, inflammation, surgery, or genetic alteration are excluded from the present paper. Further, polydactyl and monodactyls are also excluded.

Results:

Table 1 presents that the studied males have a significantly ($p<0.05$) higher prevalence of Forks in all ten fingers than the studied females. In the right hand, the Index finger (II), Ring finger (IV), and little finger (V) have shown the highest ($p=0.000$) sexual dimorphism in terms of the presence of the Forks. However, on the left hands, a similar type of higher prevalence of the forks was observed ($p=0.000$) within the finger balls of the Index finger (II), Ring finger (IV), and little finger (V). The box plot analysis revealed the distribution of the cumulative Fork Index values for each finger (F1–F5) on both hands, separated by sex (male and female). This suggests that males have a more significant ($p<0.05$) number of forks at their fingertips.

Table 2 revealed that the studied males have a significantly ($p<0.05$) higher prevalence of Minutiae in nine fingers among the ten fingers than the studied females. In the right hand, the Thumb (I) and Ring finger (IV) have shown the highest ($p=0.000$) sexual dimorphism regarding the presence of the Minutiae. However, the Index finger (II) never revealed any significant differences. Further, on the left hand, a similar type of higher prevalence ($p=0.000$) of the Minutiae was observed within the finger balls of the Thumb (I), Index finger (II), Middle Finger (III), and Ring finger (IV). The Box Plot revealed that the Right hand tends to show slightly larger values in females, notably for F2–F5. However, Males show less variability and higher means overall, reinforcing potential anatomical or functional differences. F3 (middle finger) seems to be the most reliable finger for distinguishing between sexes based

on these distributions. This suggests that males have a more significant ($p<0.05$) number of forks at their fingertips.

Table 3 resulted that the studied males have a significantly ($p<0.05$) higher value of FI in all ten fingers than the studied females. In the right hand, the Index finger (II), Ring finger (IV), and little finger (V) have shown the highest ($p=0.000$) sexual dimorphism in terms of the presence of the Forks. However, on the left hand, a similar type of higher value of the FI was observed ($p<0.05$) within the finger balls of the Index finger (II) and Ring finger (IV). The box plot demonstrates the distribution of finger measurements for males and females on both hands across five fingers (F1 to F5). Overall, male measurements consistently show higher median values and narrower interquartile ranges compared to females, suggesting more uniformity in their data. In contrast, female data displays greater variability, with wider boxes and more outliers, indicating a broader range of measurements. The difference is most pronounced in fingers F2 and F3, where the male measurements are not only higher but also more tightly clustered. This pattern suggests a consistent

anatomical difference in finger measurements between sexes, with males generally having larger and more consistently sized fingers than females. This suggests that males have a more significant ($p<0.05$) number of forks at their fingertips.

Discussion

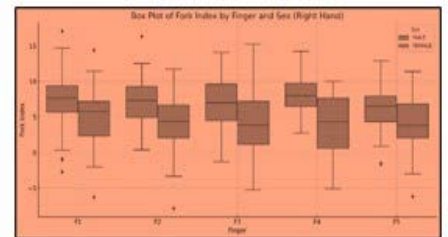
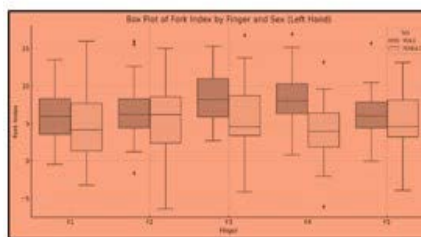
Sir Galton (1892) [5] described the valuable structural details of epidermal ridges as minutiae, and each person's quantity, type, shape, and position are distinct [1]. In forensic sciences, minutiae are a prominent biomarker for personal identification [1]. Loesch (1973) [8] and Steffens (1965) [9] made detailed categories, but the six-fold categorisation

Table 1: The bilateral distribution of Forks on the fingers of the studied males and females

Bilateral distribution of Fork				t Test		U Value
Side	Finger	Sex	N	Mean \pm SD	Std. Error Mean	
Right Hand	F1	MALE	50	7.32 \pm 3.41*	0.48	843*
		FEMALE	50	4.86 \pm 4.19	0.59	
	F2	MALE	50	7.48 \pm 3.30*	0.47	738.5*
		FEMALE	50	4.30 \pm 3.72	0.53	
	F3	MALE	50	7.84 \pm 3.39*	0.48	880*
		FEMALE	50	5.16 \pm 4.17	0.59	
	F4	MALE	50	7.98 \pm 2.99*	0.42	710*
		FEMALE	50	4.84 \pm 3.86	0.55	
	F5	MALE	50	6.68 \pm 2.74*	0.39	860*
		FEMALE	50	4.14 \pm 3.77	0.53	
Left Hand	F1	MALE	50	7.58 \pm 3.27*	0.46	876.5*
		FEMALE	50	5.00 \pm 4.61	0.65	
	F2	MALE	50	7.88 \pm 3.70*	0.52	765*
		FEMALE	50	4.98 \pm 4.33	0.61	
	F3	MALE	50	8.54 \pm 3.01*	0.43	698*
		FEMALE	50	5.06 \pm 4.17	0.59	
	F4	MALE	50	7.88 \pm 3.68*	0.52	732.5*
		FEMALE	50	4.56 \pm 3.97	0.56	
	F5	MALE	50	6.68 \pm 2.74*	1.47	860*
		FEMALE	50	4.14 \pm 3.77	2.82	

* $p<0.05$

Box Plot analysis of Table 1:



proposed by Penrose (1968) [10] and outlined by Cummins and Midlo (1961) [6] was widely accepted [1]. Okajima (1970) [4] introduced the fork index to express the number of forks concerning other minutiae. It was observed that the fork index showed finger-wise sex differences [3]. In continuation of Okajima's (1970) [4] work, Banerjee and Sarkar (1983) [3] reported a similar sexual dimorphism of FI. In that study, it was documented that the males have a higher value of FI than the females [3]. The IVth finger had the highest mean FI in men, while the Ist finger had the lowest. The order of the fingers based on the mean FI is IV > II > V > III > I (right hand) and II > III > IV > V > I (left hand). Females also exhibit the same pattern as males; the highest and lowest mean values in the IVth and Ist fingers,

respectively, were similar, but the order of the fingers differed slightly from that of the males. The order of the fingers based on the mean FI is IV > V > II > III > I (right hand), and III > IV > II > V > I (left hand) (Banerjee & Sarkar, 1983, p.279).

The present study also obtained a similar result, revealing that the males have significant ($p < 0.05$) higher Fork, Minutiae, and FI in both hands than the studied females. Among the males, the order of the fingers based on the highest to lowest mean FI is IV > V > II > III > I (right hand) and III > IV > II > V > I (left hand). However, among the females, the order of the fingers based on the highest to lowest mean FI is IV > III > V > II > I (right hand) and III > II > V > IV > I (left hand).

Conclusion

Based on the results, the current study may conclude that FI's sexually dimorphic character makes it a valuable forensic tool and can be utilised for primary sex identification from fingerprints quantitatively.

Acknowledgements

The authors are thankful to all the participants for their cooperation. Moreover, acknowledgement is also

owed to the Department of Forensic Science, SOBAS, Adamas University, for providing all the necessities for the present study.

References

- [1] Schaumann, B., & Alter, M. (1976) Dermatoglyphics in Medical Disorders. Springer-Verlag, New York
- [2] Wilder, H. H., & Wentworth, B. (1918). Personal Identification: Methods for the Identification of Individuals, Living or Dead. Richard G. Badger, The Gorham Press. Boston, USA.
- [3] Banerjee, A. R., & Sarkar, N. (1983). Distribution of Fork-Index Within the Area of Finger Ball Pattern. In I.J.s. Bansal (Eds.), Anthropology in Indian Context (pp. 25-29), Today and Tomorrow's Printers End Publishers, New Delhi, India.
- [4] Okajima, M. (1970). Frequency of forks in epidermal-ridge minutiae in the fingerprint. American Journal of Biological Anthropology, 32, (1):41-8. Retrieved January 1970. <https://doi.org/10.1002/ajpa.1330320106>
- [5] Galton, F. (1892). Finger Prints. [Reprint edition, 1965], Da Capo Press, New York. Retrieved from
- [6] Cummins, H., & Midlo, C. (1961). Finger Prints, Palms and Soles: An Introduction to Dermatoglyphics. Dover Publication, INC, New York.
- [7] Sarkar, N. (2004). Finger Ridge Minutiae: Classification,

Table 2: The bilateral distribution of total Minutiae on the fingers of the studied males and females

Bilateral distribution of Total Minutiae				t Test		U Value
Side	Finger	Sex	N	Mean±SD	SE	
Right Hand	F1	MALE	50	18.66±6.35*	0.90	698*
		FEMALE	50	12.76±7.01	0.99	
	F2	MALE	50	14.72±4.62	0.65	1054
		FEMALE	50	13.42±6.30	0.89	
	F3	MALE	50	15.14±3.74*	0.53	785.5*
		FEMALE	50	11.88±5.51	0.78	
	F4	MALE	50	14.10±3.69*	0.52	790*
		FEMALE	50	10.84±4.96	0.70	
	F5	MALE	50	12.64±3.53*	0.50	893.5*
		FEMALE	50	10.40±4.83	0.68	
Left Hand	F1	MALE	50	17.64±5.02*	0.71	701.5*
		FEMALE	50	11.84±7.05	1.00	
	F2	MALE	50	14.88±4.17*	0.59	767.5*
		FEMALE	50	11.46±4.53	0.64	
	F3	MALE	50	15.58±4.19*	0.59	654*
		FEMALE	50	10.24±5.12	0.72	
	F4	MALE	50	14.06±3.46*	0.49	778.5*
		FEMALE	50	10.58±4.73	0.67	
	F5	MALE	50	12.66±3.72*	0.53	887.5*
		FEMALE	50	10.10±4.53	0.64	

* $p < 0.05$

Box Plot analysis of Table 2:

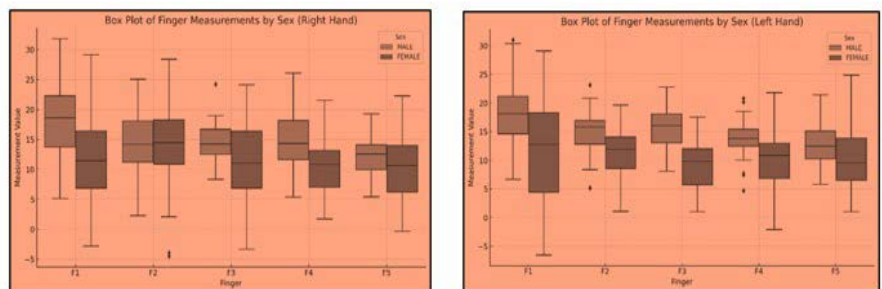
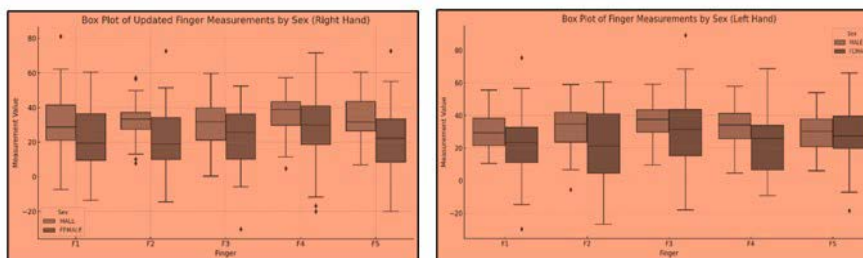


Table 3: The bilateral distribution of FI on the fingers of the studied males and females

Bilateral distribution of FI				t Test		U Value
Side	Finger	Sex	N	Mean±SD	SE	
Right Hand	F1	MALE	50	29.37±15.67*	2.22	821.5*
		FEMALE	50	20.99±17.98	2.54	
	F2	MALE	50	33.83±12.11*	1.71	735*
		FEMALE	50	21.01±18.31	2.59	
	F3	MALE	50	32.87±12.19*	1.72	870*
		FEMALE	50	24.55±18.19	2.57	
	F4	MALE	50	35.91±11.28*	1.60	892*
		FEMALE	50	27.00±19.36	2.74	
	F5	MALE	50	34.65±11.24*	1.59	748.5*
		FEMALE	50	21.80±18.67	2.64	
Left Hand	F1	MALE	50	29.50±11.80*	1.67	847*
		FEMALE	50	22.49±19.31	2.73	
	F2	MALE	50	34.37±12.04*	1.70	780.5*
		FEMALE	50	24.89±19.24	2.72	
	F3	MALE	50	35.05±10.18*	1.44	884*
		FEMALE	50	27.05±22.47	3.18	
	F4	MALE	50	34.97±10.41*	1.47	718*
		FEMALE	50	23.85±19.97	2.82	
	F5	MALE	50	33.09±11.20*	1.58	805.5*
		FEMALE	50	24.77±19.14	2.71	

*p<0.05

Box Plot analysis of Table 3:



Distribution and Genetics. Anthropological Survey of India, Ministry of Tourism and Culture, Government of India, Kolkata.

- [8] Loesch, D. (1973). Minutiae and clinical genetics. Journal of Mental Deficiency Research. 17: 97.
 [9] Steffens, C. (1965). Vergleichende Untersuchungen

- der Minutien der Fingerbeerenmuster bei Familien und eineiigenZwillingspaaren [Comparative studies of the minutiae of fingertip patterns in families and identical twin pairs]. Anthropologischer Anzeiger,29: 234.
 [10] Penrose, L. S. (1968). Memorandum on dermatoglyphic nomenclature. Birth Defects, 4(3):1.

Comparative Evaluation of Antioxidant and Free Radical Scavenging Activities of *Alocasia indica*, *Colocasia esculenta*, and *Amorphophallus campanulatus*

Rameshwar Mukhopadhyay*

Department of Biotechnology, School of Life
Science & Biotechnology,
Adamas University, Kolkata, India
<https://orcid.org/0000-0003-1007-2000>

Arpita Das

Department of Biotechnology, School of Life
Science & Biotechnology,
Adamas University, Kolkata, India
<https://orcid.org/0000-0002-8665-3074>

Swagata Roy Chowdhury*

Department of Biotechnology, School of Life
Science & Biotechnology,
Adamas University, Kolkata, India
<https://orcid.org/0009-0007-7183-5960>

Rajib Majumder#

Department of Biotechnology, School of Life
Science & Biotechnology,
Adamas University, Kolkata, India
<https://orcid.org/0000-0001-9069-2319>

Sanmitra Ghosh

Department of Biological Sciences, School of Life
Science & Biotechnology,
Adamas University, Kolkata, India
<https://orcid.org/0000-0001-7624-4595>

* Equal contribution

Corresponding author:

Rajib Majumder

Email: rajib.majumder@adamasuniversity.ac.in

Abstract

Oxidative stress, arising from the excessive production of reactive oxygen species (ROS), is a critical factor contributing to various chronic diseases such as cancer, atherosclerosis, cardiovascular disorders, aging, and inflammatory conditions. The search for natural antioxidants with therapeutic and cosmetic potential has intensified over the past decades. Plants rich in phytoconstituents like polyphenols, flavonoids, and carotenoids are recognized for their capacity to neutralize free radicals and protect biological macromolecules from oxidative damage. In this context, the present study aimed to evaluate and compare the antioxidant potential and free radical scavenging activities of aqueous and ethanolic extracts of *Alocasia indica* (giant taro), as well as a comparative analysis among ethanolic extracts of *Alocasia indica*, *Amorphophallus campanulatus* (elephant yam), and *Colocasia esculenta* (taro). These species, traditionally used in Indian and Ayurvedic medicine for various therapeutic purposes, were assessed using established antioxidant assays. The results demonstrated significant antioxidant activity in all tested extracts, with the ethanolic extract of *Alocasia indica* showing notably higher scavenging potential. Furthermore, when compared across the three species, variations in antioxidant efficiency were observed, suggesting species-specific phytochemical profiles. The findings validate the traditional uses of these plants and support their potential application as natural sources of antioxidants for pharmaceutical and nutraceutical development. This study emphasizes the relevance of utilizing indigenous plant resources in developing effective antioxidant therapies.

Keywords

Alocasia indica, Antioxidant, *Amorphophallus campanulatus*, *Colocasia esculenta*, ROS

INTRODUCTION

Oxidative stress is the production of reactive oxygen species (ROS) such as superoxide, hydroxyl, peroxy, and alkoxy radicals, and other free radicals that are produced during various physiological and biochemical reactions

within the human body. ROS is very harmful for the human body because it seeks stability through electron pairing with biological macromolecules such as proteins, lipids and DNA in healthy human cells and cause protein and DNA damage along with lipid peroxidation. These changes

contribute to cancer, atherosclerosis, cardiovascular diseases, ageing and inflammatory diseases [1]. The search for natural antioxidants of pharmaceutical & cosmetic use has become a major scientific & industrial challenge over the last two decades [2]. Several medicinal plants have been extensively investigated for the presence of polyphenols and other antioxidants [3]. The presence of wide range of phytoconstituents such as phenolics (flavonoids, phenolic acids and tocopherols), thiols & caretonoids in plants protect the human body against oxidative damage by free radicals [4]. Various active moieties present in the herbs are rich source of antioxidants and possess diverse medicinal values. They are being extracted and synthesized on large scale and are being widely used for more pronounced and marked effects than their crude forms [5]. WHO has estimated that 80% of the population of developing countries being unable to afford pharmaceutical drug relies on traditional medicines mainly plant based and plants are used in the treatment of various diseases from ancient times [6]. Herbal medicines are popularized due to their effectiveness, easy availability, low cost and comparatively being devoid of toxic effect [7]. In addition, antioxidants derived from plant sources are very effective and have reduced interference with body's ability to use free radicals constructively [8]. Therefore, the need for the search for antioxidants from natural origin has been greatly felt in the recent years.

Alocasia indica Schott. (family-Araceae) is a perennial herb found tropical and sub-tropical regions of India. *A. indica* (L.) schott, commonly known as giant taro (in bengali 'man kachu') up to 5m in height found wild and cultivated all over India. The species are widely cultivated for its tubers used as vegetable in Assam, West Bengal, Maharashtra and South India. The strain is normally used in inflammation and in diseases of abdomen and spleen. The leaves of the plant are reported to be used as digestive, anthelmintic, laxative, diuretic, astringent and the hydroalcoholic extract of the leaves of the plant have hepatoprotective activity [9].

Amorphophallus campanulatus and *Colocasia esculenta*, or elephant yam and taro in English, and 'ol kachu' and 'gathi kachu' in Bengali, are perennial rhizomatous herbs and are members of the family Araceae. Not only are the species grown on a large scale, but they also propagate in the wild all over India, especially in areas of East Asia, Malaysia, and along the Pacific coast. They are grown in large quantities in areas like Assam and Bengal as major food crops, with their underground stems being an integral part of the local food culture [10, 11]. The leaves and corms are highly valued for their nutritional content. In Ayurvedic medicine, the underground stems have been used for centuries to treat a range of ailments such as constipation, stomatitis, jaundice, abdominal ailments, spleen ailments, inflammation, hemorrhoids, hepato-splenopathies, and general debility.

The present study aims to carry out a comparative analysis of the antioxidant activities and free radical scavenging abilities of aqueous and ethanolic extracts of

Alocasia indica. Another observation was done to show a comparative study of free radical scavenging activity of ethanolic extract of *Alocasia indica*, *Amorphophallus campanulatus* and *Colocasia esculenta*.

II. MATERIALS AND METHODS

Chemicals

Ethylenediamine tetraacetic acid (EDTA), ascorbic acid, 2- deoxy-2-ribose, trichloroacetic acid (TCA), nitro blue tetrazolium (NBT), reduced nicotinamide adenine dinucleotide (NADH), phenazine methosulfate (PMS), sodium nitroprusside (SNP), sulfanilamide, naphthylethylenediamine dihydrochloride (NED), quercetin were obtained from Highmedia Research Laboratories Pvt. Ltd. Aluminium chloride (AlCl₃), ferric chloride, gallic acid, Ascorbic acid, Thiobarbituric acid (TBA), Sodium nitrite were obtained from Merck, India.

Plant material

The tuber part of *Alocasia indica* was collected from local market of Kolkata, West Bengal, India and authenticated through the Botany Dept. of Rammohan College, Kolkata, India. The plant material was chopped and dried at room temperature for 10 days and used as raw material. The dried tuber was finely powdered using a mechanical method and resulting powder was passed through the 40-micron sieve and stored in the airtight container.

Preparation of ethanolic extract (ETE)

The extraction was done by Soxhlet apparatus. An amount of 100 g of the dried and powdered tuber of *A. indica* was extracted in 500 mL of 80% ethanol (v/v) for 72 h. Then, the extract was centrifuged for 15 min at 4000 rpm. Supernatant was concentrated using a rotary evaporator to get semisolid residue which was dried under vacuum. The residue was kept at -20°C for future use.

For a comparative study ethanolic extraction was also done with another two strains *Amorphophallus campanulatus* and *Colocasia esculenta*. Preparation of ethanolic extract was done by the above method.

Preparation of aqueous extract (AQE)

Preparation of aqueous extract was done using water as solvent and then followed by the protocol was mentioned in preparation of ethanolic extract.

Estimation of dry extract weight (yield) protein and carbohydrate contents

The dried plant extract from ethanolic and aqueous method was estimated to measure the yield and then used for determining total protein and carbohydrate contents. Protein was assayed using coomassie blue (Bradford) protein assay reagent according to the technical instruction manual, with BSA as standard. The carbohydrate content of the enzyme preparations was determined by using the orcinol-sulphuric acid method [12] with glucose as the standard.

Phytochemical screening

A preliminary phytochemical screening of all these extracts of *A. indica* was carried out for detection of phytoconstituents like saponins, tannins, alkaloids, phlobatanins, glycosides etc. [13].

a.) Alkaloids- 1 ml of 1% HCl was added to 3 ml of the extract in a test tube. The mixture was then heated for 20 min, cooled and filtered about 2 drops of Mayer's reagent to 1 ml of the extract. A creamy precipitate was an indication of the presence of alkaloids.

b.) Tannins- 1 ml of freshly prepared 10% KOH was added to 1 ml of the extract. A dirty white precipitate showed the presence of tannins.

c.) Glycosides- 10 ml of 50% H₂SO₄ was added to 1 ml of the extract and the mixture heated in boiling water for about 15 min. 10ml of Fehling's solution was then added and the mixture boiled. A brick-red precipitate was confirmatory for the presence of glycosides.

d.) Saponins- Frothing test: 2 ml of the extract was vigorously shaken in the test tube for 2 min. Frothing means presence of saponins.

e.) Flavonoids- 1 ml of 10% NaOH was added to 3 ml of the extract. Yellow colouration in the reaction mixture indicates the presence of flavonoids.

f.) Steroids- Salkowski test: 5 drops of concentrated H₂SO₄ were added to 1 ml of the extract in a test tube. Red colouration indicates the presence of steroids.

g.) Phlobatanins- 1 ml of the extract was added to 1% HCl. Red precipitate indicates positive results.

h.) Triterpenes- 1 ml of the extract was added to 5 drops of Acetic anhydride and a drop of concentrated H₂SO₄ added. The mixture was then steamed for 1 h and neutralized with NaOH followed by the addition of chloroform. Absence of blue-green colour indicates the absence of triterpenes.

Determination of total phenolic content

The total phenolic content was determined by using the Folin- Ciocalteu reagent [14]. About 1ml of plant extract was mixed with 5 ml of Folin-ciocalteu reagent (1:10) followed by 4 ml of Na₂CO₃ (0.7 M). Subsequently, the mixture was shaken for 1 h at room temperature and absorbance measured at 760 nm. All tests were performed in triplicate. The concentration of total phenolic compounds was determined as µg gallic acid equivalents.

Determination of total flavonoid content

The total flavonoid content was determined by aluminium chloride (AlCl₃) according to a known method [15]. The tuber extract (0.1 ml) was added to 0.3 ml distilled water followed by NaNO₂ (0.03 ml, 5%). After 5 min at 25°C, AlCl₃ (0.03 ml, 10%) was added. After a further 5 min, the reaction mixture was treated with 0.2 ml 1 mM NaOH. Finally, the reaction mixture was diluted to 1 ml with water and the absorbance was measured at 510 nm. All tests were performed six times. The flavonoid content was calculated from a quercetin standard curve.

Total antioxidant activity

Total antioxidant activities of ethanolic and aqueous extract were determined as described by Badrinathan et al., 2011 [16]. In brief, 0.3 ml of sample was mixed with 3.0 ml reagent solution prepared by 0.6 M sulfuric acid, 28 mM sodium phosphate and 4 mM ammonium molybdate. Reaction mixture was incubated at 95°C for 90 min under water bath and absorbance was measured at 695 nm. All tests were performed in triplicate. Total antioxidant activity was expressed as the number of equivalents of ascorbic acid in milligram.

DPPH radical scavenging activity

50 µl of 0.16 mM 2, 2-Diphenyl-1-picrylhydrazyl (DPPH) solution in methanol were added to 50 µl aliquot of test sample or standard ascorbic acid. The mixture was vortexed for 1 min and kept at room temperature for 30 min in the dark. The absorbance of all the sample solutions was measured at 517 nm with respective blank [16]. All tests were performed in triplicate. The scavenging effect (%) was calculated by the following equation:

$$\text{Scavenging activity (\%)} = \frac{[(\text{Abs control} - \text{Abs sample})]}{(\text{Abs control})} \times 100$$

Hydroxyl radical scavenging

The scavenging capacity for hydroxyl radical was measured according to the modified method of Saumya & Mahaboob basha, 2011 [14]. Stock solutions of EDTA (1 mM), FeCl₃ (10 mM), ascorbic acid (1mM), H₂O₂ (10 mM) and deoxyribose (10 mM) were prepared in distilled deionized water. The assay was performed by adding 0.1 ml of EDTA 0.01 ml of FeCl₃, 0.1 ml of H₂O₂, 0.36 ml of deoxyribose, 1.0 ml of plant extract or ascorbic acid as standard (1-10 µg/ml), 0.33 ml of phosphate buffer (50 mM, pH 7.4) and 0.1ml of ascorbic acid in sequence. The mixture was then incubated at 37°C for 1 hr. About 1.0 ml portion of the incubated mixture was mixed with 1.0 ml of 10% TCA and 1.0 ml of 0.5% TBA to develop the pink chromogen, measured at 532 nm. Decreasing value of absorbance of reaction mixture indicates increasing Hydroxyl scavenging activity. All tests were performed in triplicate. Percentage scavenging activity was calculated using the formula given above.

Nitric oxide radical scavenging

The extent of nitric oxide generation was studied using Griess reagent method [14]. 4 ml extract (1-50 µg/ml) was added with 1 ml of sodium nitroprusside solution (5 mM) and incubated for 2 h at 27°C. An aliquot (2 ml) of the incubation solution was removed and diluted with 1.2 ml of Griess reagent (1% sulfanilamide in 5% H₃PO₄ and 0.1% naphthylethylene diamine dihydrochloride). The absorbance of the chromophore was read immediately at 550 nm and compared with standard, ascorbic acid. All tests were performed in triplicate. Percentage Nitric oxide radical scavenging activity was calculated using the formula given above.

Reducing power

Reducing power was measured by the reaction mixture containing 1.0 ml of different concentration of sample mixed with 2.5 ml of phosphate buffer (0.2 M, pH 6.6) and 2.5 ml potassium ferricyanide (1%). Reaction mixture was incubated at 50°C for 20 min. After incubation, 2.5 ml of TCA (10%) was added and centrifuged (650 g) for 10 min. From the upper layer, 2.5 ml solution was mixed with 2.5 ml distilled water and 0.5 ml FeCl3 (0.1%) and absorbance was measured at 695 nm [16]. Increased absorbance indicates increased reducing power. The results were expressed in ascorbic acid equivalents. All tests were performed in triplicate.

Superoxide radical scavenging and superoxide dismutase activity (SOD)

The reaction mixture contained 1 ml of NBT solution (156 µM prepared in phosphate buffer, pH 7.4), 1 ml of NADH solution (468 µM prepared in phosphate buffer, pH 7.4) and different fractions of the diluted extracts were added. Finally, reaction was accelerated by adding 100 µl PMS solution (60 µM prepared in phosphate buffer, pH 7.4) to the mixture. The reaction mixture was shaken and incubated at 25°C for 5 min and absorbance at 560 nm was measured against blank sample. Ascorbic acid and (10 -50 µg/ml) were taken as standard. Decreasing value of absorbance of reaction mixture indicates increasing superoxide-anion-scavenging activity. All tests were performed in triplicate. Percentage scavenging activity was calculated using the formula given above as described earlier [17]. SOD activity was expressed as nKat/ min/ mg of protein.

Catalase activity

Catalase activity was determined by measuring the decrease in absorbance at 240 nm [18]. The reaction mixture contained 0.5 ml of enzyme extract and 2.0 ml of 0.1 M sodium phosphate buffer (pH 6.8) and the reaction was started by the addition of 0.5 ml of 10 mM hydrogen peroxide. The decrease in absorbance was recorded. Decrease of absorbance was recorded in every 15 sec up to 3 min. Catalase activity was expressed as nKat/ min/ mg of protein.

Statistical analysis

All data are given as the mean ± SD of four measurements. An IC50 was calculated as the concentration which brought about a 50% reduction in absorbance compared to blank. Ascorbic acid was used as standard.

III. RESULTS

A) Comparative study of in vitro antioxidant activity of the ethanolic and aqueous extract of *A. indica*

Estimation of yield and biochemical composition of extract of *A. indica*

Biologically active molecules for general screening of bioactivity need various solvents for extraction methods.

In this study soxhlet extraction was done using ethanol and water for extraction of tuber of *A. indica*. The yields of the extracts obtained by two extraction methods are given in Tables 1. Water extraction (AQE) of the material showed 1.9 times higher yield than that of the ethanolic extraction (ETE) method.

The biochemical contents like protein and carbohydrate were quantified in crude extract powder. *A. indica* extracted in water medium (AQE) has approximately 4.15 mg/gm of plant material (0.42 %) and 109 mg/g of plant material (10.9 %) of protein and carbohydrate respectively. In ethanolic extraction (ETE) the protein and carbohydrate contents were found to be 2.21 times and 1.32 times higher respectively (Tables 1). Protein and carbohydrate compositions have been indicated to be variable by season and species. The intracellular and cell wall polysaccharides influence carbohydrate composition while the presence of various enzymes and pigments influence protein composition.

Table 1: Estimation of dry extract weight, protein and carbohydrate content of different extraction method of *A. indica*. ETE- ethanolic extraction; AQE- Water (aqueous) extraction.

Parameter	ETE	AQE
Dry extract weight (mg/ g dry wt of <i>A. indica</i> tuber)	0.94	1.79
Carbohydrate (mg/g dry extract)	144	109
Protein (mg/g dry extract)	9.16	4.15

Phytochemical study

Preliminary phytochemical screening revealed the presence of various phytochemical given in the following Table 2.

Table 2: Phytochemical screening of ethanolic (ETE) and water (AQE) extracts of *A.indica*.

Parameter	ETE	AQE
Alkaloids	+	+
Tannins		
Glycosides	+	+
Saponins	+	+
Flavonoids	+	+
Steroids		
Phlobatanins		
Triterpenes		

Determination of total phenolic content

Phenolic compounds may contribute directly to antioxidative action. The total phenolic content of ETE and AQE were 123.66±12.09 mg and 94.71±7.83 mg gallic acid equivalent per g of plant extract respectively (Fig 1).

Figure 1

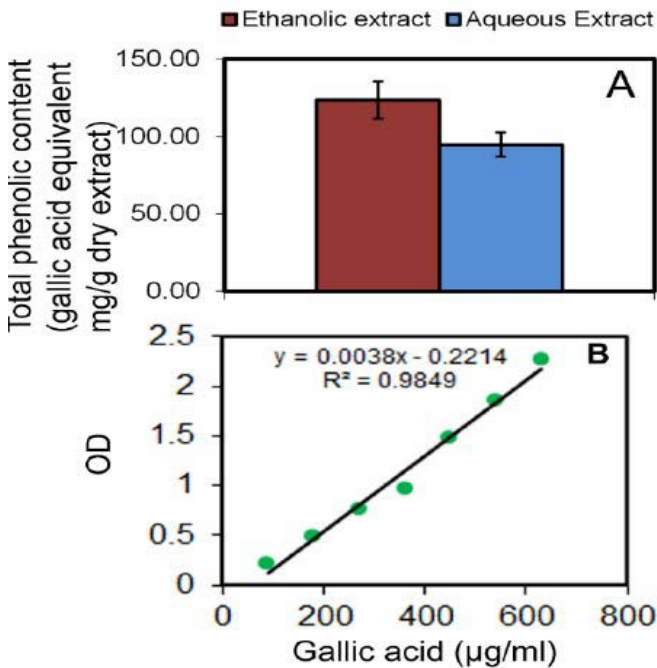


Figure 1: Total phenolic content of ethanolic (ETE) and aqueous (AQE) extract (mg/g dry extract) of *A. indica* (1A) with gallic acid standard (µg/ml) (1B).

Determination of total flavonoid content

The total flavonoid content of the 80% ETE and AQE of *A. indica* was 6.47 ± 0.35 mg and 1.04 ± 0.39 mg quercetin equivalent per g of plant extract respectively (Fig 2).

Figure 2

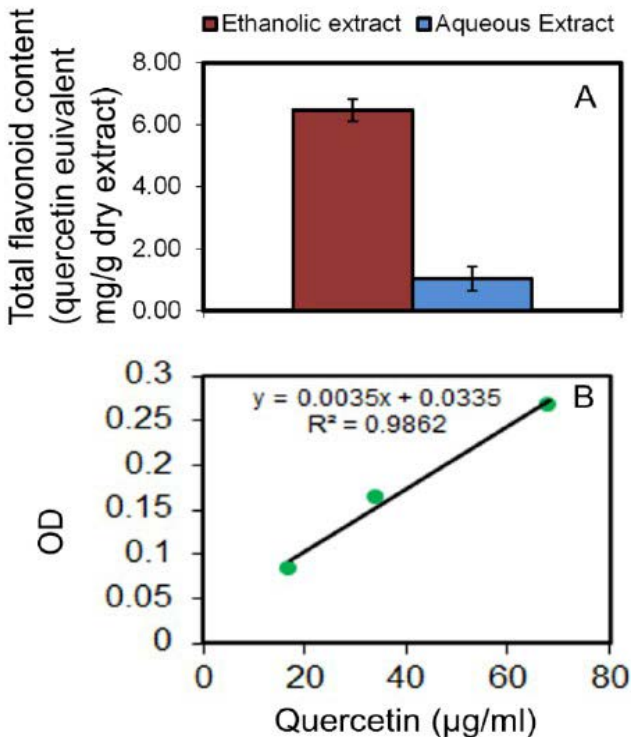


Figure 2: Total flavonoid content of ethanolic (ETE) and

aqueous (AQE) extract (mg/g dry extract) of *A. indica* (2A) with quercetin standard (µg/ml) (2B)

Total antioxidant activity

Soxhlet extraction with ethanol demonstrated moderately increased total antioxidant activity compared with water extraction (Fig 3). ETE showed highest antioxidant activity (729.69 ± 77.48 mg ascorbic acid equivalent/g dry extract) than AQE (369.78 ± 10.76 mg ascorbic acid equivalent/g dry extract).

Figure: 3

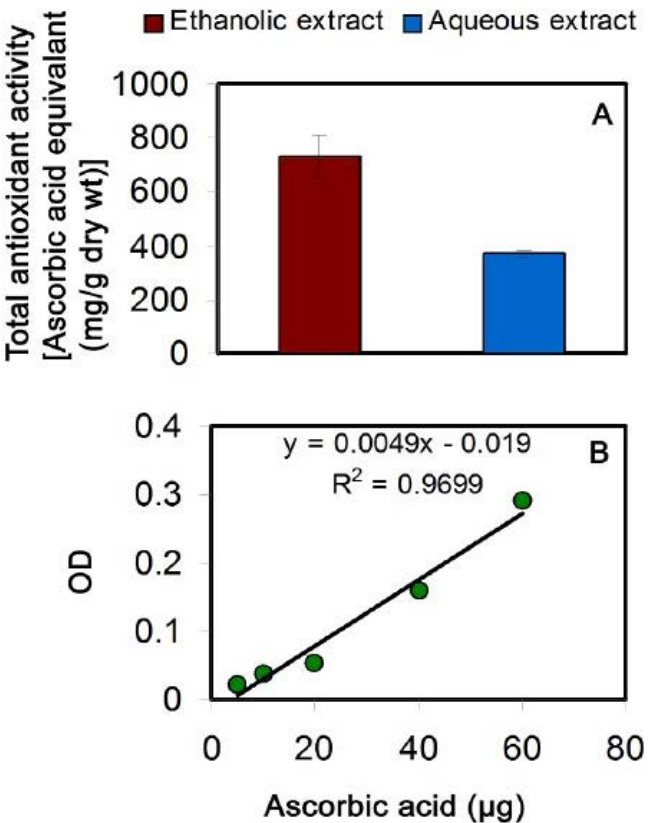


Figure 3: Total antioxidant activity of ethanolic (ETE) and aqueous (AQE) extract (mg/g dry extract) of *A. indica* was measured by ascorbic acid equivalent (3A) with ascorbic acid standard (µg/ml) (3B).

DPPH radical scavenging assay

Radical scavenging effect of natural antioxidants could be evaluated using DPPH, a free radical donor under in vitro conditions [19]. Ethanolic and water extracts of *A. indica* were used for assessing its free radical quenching activity using DPPH. It was observed that in 0.5 mg/ml concentration ETE of *A. indica* tuber had 32.28 % higher activity for scavenging DPPH than that of AQE (Fig 4). The IC₅₀ values of ethanolic and water extracts were found to be 1.31mg/ml, and 3.32 mg/ml respectively.

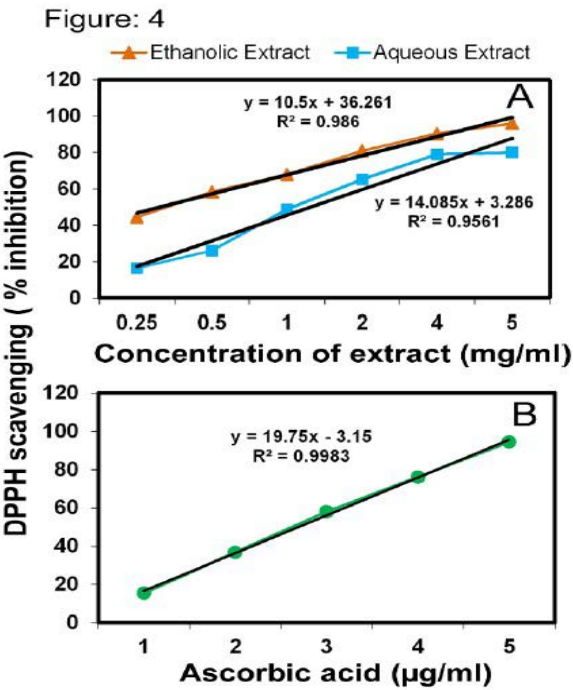


Figure 4: DPPH radical scavenging assay of ethanolic (ETE) and aqueous (AQE) extract of *A. indica* (4A) with ascorbic acid standard (µg/ml) (4B). The percentage inhibition was plotted against the concentration of samples. Hydroxyl radical scavenging assay shows the ability of the extracts and standard BHT to inhibit hydroxyl radical-mediated deoxyribose degradation in a Fe³⁺-EDTA-ascorbic acid and H₂O₂ reaction mixture. ETE showed 3.5 times higher % inhibition than AQE in 0.5mg/ml of the extract (Fig 5). The IC₅₀ values of ETE, AQE and standard in this assay were 3.09 mg/ml, 3.71 mg/ml and 2.85 µg/ml, respectively. The IC₅₀ value of the ETE and AQE were higher than that of standard showing more ability in hydroxyl radical scavenging.

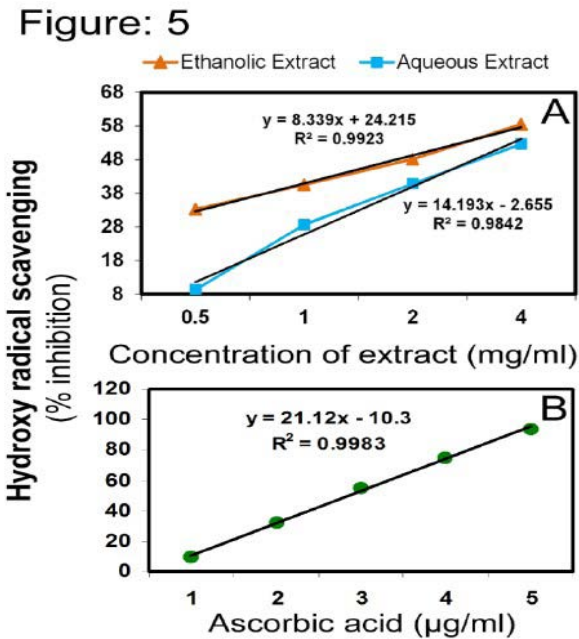


Figure 5: Hydroxyl radical scavenging assay of ethanolic (ETE) and aqueous (AQE) extract of *A. indica* (5A) with ascorbic acid standard (µg/ml) (5B). The percentage inhibition was plotted against the concentration of samples. Nitric oxide radical scavenging In this method, nitrite produced by sodium nitroprusside in standard phosphate buffer was reduced by antioxidant present in the extracts, which compete with oxygen to react with nitric oxide there by inhibiting the generation of nitrite. *A. indica* extract caused a moderate dose-dependent inhibition of nitric oxide. Ascorbic acid was used as a standard and 4.77 µg/ml ascorbic acid was needed for 50% inhibition (Fig 6). The IC₅₀ value of the ETE and AQE were 13.97 mg/ml and 19.95 mg/ml respectively, which were lower than that of the standard. At 1 mg/ml, the percentage inhibition of the ETE and AQE was 17.92 % and 2.05 % whereas at 200 µg/ml the percent inhibition of ascorbic acid was 47.8%.

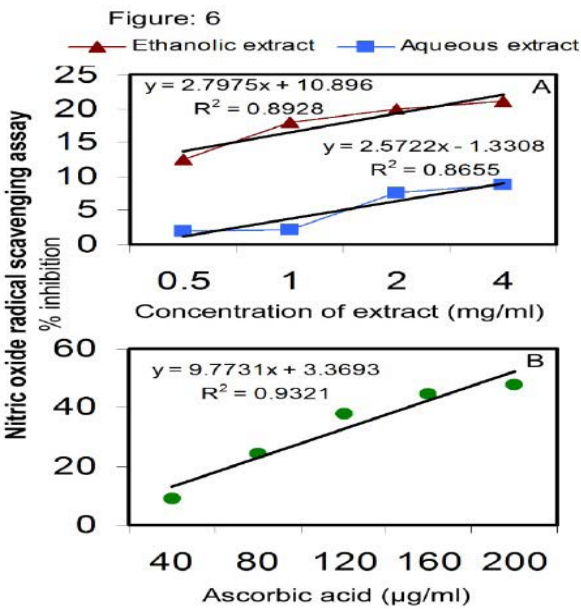


Figure 6: Nitric oxide radical scavenging assay of ethanolic (ETE) and aqueous (AQE) extract of *A. indica* (6A) with ascorbic acid standard (µg/ml) (6B). The percentage inhibition was plotted against the concentration of samples. B) Comparative study of in vitro antioxidant activity of the ethanolic extract of *Alocasia indica*, *Amorphophallus campanulatus*, *Colocasia esculenta*.

IC50 of % inhibition	<i>Alocasia indica</i>	<i>Amorphophallus campanulatus</i>	<i>Colocasia esculenta</i>	Standard
DPPH radical scavenging	1.31 mg/ml	0.68 mg/ml	1.34 mg/ml	2.69 µg/ml
Hydroxyl radical scavenging	3.09 mg/ml	0.66 mg/ml	1.05 mg/ml	2.85 µg/ml

IV. DISCUSSION AND CONCLUSION

Natural antioxidants that are present in herbs are responsible for inhibiting or preventing the deleterious consequences of oxidative stress. Herbs contain free radical scavengers like polyphenols, flavonoids and phenolic compounds. In the present study, we have evaluated the antioxidant potential of ethanolic and aqueous extracts of tuber of *Alocasia indica* in vivo. Results of the present study revealed that though the yield of dry extract was higher in water extract of *A. indica*, the protein and carbohydrate content was higher in ethanolic extract (Table 1). Phytoconstituents analysis showed same composition in both extracts (Table 2) as well as significant level of phenolic compounds is also present in both extracts of *A. indica*. The ethanolic extract had a higher concentration of total phenolic compounds than the aqueous extract (Fig. 1). The difference in their phenolic compounds may be due to their respective polarities. Flavonoids are a group of polyphenolic compounds with known properties which include free radical scavenging, inhibition of hydrolytic and oxidative enzymes and anti-inflammatory action. Results of this study revealed that the flavonoid contents in terms of quercetin equivalent are much higher in ethanolic extract than the aqueous extract of *A. indica* (Fig. 2). So, flavonoids present in the ethanolic and aqueous extract of *A. indica* may help provide protection against different diseases by contributing along with antioxidant vitamins and enzymes, to the total antioxidant defense system of the human body. Our results showed total antioxidant activity was higher in ethanolic extract than the water extract (Fig. 3).

Free radicals are involved in many disorders like neurodegenerative diseases, cancer and AIDS. Antioxidants through their scavenging power are useful for the management of those diseases. Both, the aqueous and ethanolic extracts of *A. indica* were found to possess DPPH scavenging activity (Fig. 4). This suggests that the tuber of *A. indica* contains compounds that are capable of donating hydrogen to a free radical to remove odd electrons which is responsible for radical's reactivity. Hydroxyl radical is the most reactive among the ROS. The ethanolic extract of *A. indica* extracts showed higher hydroxyl radical scavenging activity when compared to the water extracts (Fig. 5). Nitric oxide is a free radical produced in mammalian cells, involved in the regulation of various physiological processes. However, excess production of NO is associated with several diseases. The results revealed that the ethanolic extract exhibited maximum inhibition as compared to aqueous extract (Fig. 6).

This research is a comparative analysis of the antioxidant activity contained in ethanolic extracts of *Amorphophallus campanulatus*, *Alocasia indica*, and *Colocasia esculenta*. The analysis was done according to their capacity to scavenge DPPH radicals and other reactive oxygen species including hydroxyl and superoxide radicals. The ethanolic

extract of *Amorphophallus campanulatus* was the most active in scavenging free radicals among the three extracts and thus indicates its antioxidant activity indirectly.

Because all three tuber species are commonly eaten as a food crop, their robust antioxidant properties present a promising field for future pharmacognostic research. These findings could be part of the process of creating therapeutic agents to be employed in the treatment of lifestyle-induced oxidative stress diseases.

ACKNOWLEDGEMENT

The authors are really indebted to Prof. (Dr.) Samit Ray Chancellor, Adamas University, Kolkata, India for basic research infrastructure facilities. Special thanks to Dean, School of Life Science & Biotechnology, Adamas University, Kolkata, India for his technical support and valuable suggestions.

REFERENCES

- [1] Hazra B, Biswas S, Mandal N. (2008). Antioxidant and free radical scavenging activity of *Spondias pinnata*. BMC Comp Alt Med, 8, 63.
- [2] Ali S, Kasoju N, Luthra A, Singh A, Sharanabasava H. (2008). Indian medicinal herbs as source of antioxidants. Food Res Int, 41, 1-15.
- [3] Pilarski R, Zieliński H, Ciesiołka D, Gulewicz K. (2006). Antioxidant activity of ethanolic and aqueous extracts of *Uncaria tomentosa* (Willd.) DC. J Ethnopharm, 104, 18-23.
- [4] Abu Bakar MF, Mohammad M, Rahmat, Fry J. (2009). Phytochemicals and antioxidant activity of different parts of bambangan (*Magnifera pajang*) and tarap (*Artocarpus odoratissimus*). Food Chem, 113, 479-483.
- [5] Tanwar V, Sachdeva J, Kishore K, Mittal R, Nag TC, Ray R, Kumari S, Arya DS. (2010). Dose-dependent actions of curcumin in experimentally induced myocardial necrosis: a biochemical, histopathological, and electron microscopic evidence. Cell Biochem Funct, 28, 74-82.
- [6] Evans WC, Trease GE, Evans D. (2002). Text book of Pharmacognosy. 15th edition. China: Elsevier limited.
- [7] Ali M. (1998). Text book of Pharmacognosy. 2nd edition. New Delhi: CBS Publisher & Distributor.
- [8] Wolfe K, Xianzhong WU, Liu RH. (2003). Antioxidant activity of apple peels. J Agric Food Chem, 51, 609-614.
- [9] Mulla WA, Salunkhe VR, Kuchekar SB, Qureshi N. (2009). Free radical scavenging activity of leaves of

- Alocasia indica* (Linn). Indian J Pharm Sci, 71, 303–307.
- [10] Singh SK, Rajasekar N, Raj NAV, Paramaguru R. (2011). Hepatoprotective and antioxidant effects of *amorphophallus campanulatus* against acetaminopheninduced hepatotoxicity in rats. Int J Pharm Pharm Sci, 3, 202-205.
- [11] Patil BR, Ageely HM. (2011). Antihepatotoxic activity of *colocasia esculenta* leaf juice. Int J Adv Biotech Res, 2, 296-304.
- [12] Brown W, Anderson O. (1971). Preparation of xylodextrins and their separation by gel chromatography. J Chromatogr, 57, 255-263.
- [13] Abalaka ME, Mann A, Adeyemo SO. (2011). Studies on in-vitro antioxidant and free radical scavenging potential and phytochemical screening of leaves of *Ziziphus mauritiana* L. and *Ziziphus spinachristi* L. compared with ascorbic acid. J Med Gen Genom, 3, 28 – 34.
- [14] Saumya SM, Mahaboob basha P. (2011). In vitro evaluation of free radical scavenging activities of *Panax ginseng* and *lagerstroemia speciosa*: a comparative analysis. Int J Pharm Pharm Sci, 3, 165-169.
- [15] Zhishen J, Mengcheng T, Jianming W. (1999). The determination of flavonoid content in mulberry and their scavenging effects on superoxide radicals. Food Chem, 64, 555-559.
- [16] Badrinathan S, Suneeva SC, Shiju TM, Girish Kumar CP, Pragasa V. (2011). Exploration of a novel hydroxyl radical scavenger from *Sargassum myriocystum*. J Med Plant Res, 5, 1997-2005.
- [17] Mandal P, Misra TK, Singh ID, Das JK, Bhunia M. (2009). Free-radical-scavenging activity in the inflorescence of European Nettle/*Sisnu* (*Urtica dioica* L.) J young pharm, 1, 129-135.
- [18] Rout JR, Kanungo S, Das R, Sahoo SL. (2010). In Vivo Protein Profiling and Catalase Activity of *Plumbago zeylanica* L. Nat Sci, 8, 87-90.
- [19] Weydert CJ, Cullen JJ. (2010). Measurement of superoxide dismutase, catalase, and Glutathione peroxidase in cultured cells and tissue. Nat Protoc, 5, 51–66.



INFORMATIVE


Student Research Initiative



A dynamic cross-disciplinary team at Adamas University bringing together 21 talented students from eight different academic programs to drive innovation through collaborative research. Our initiative harnesses the power of diverse perspectives⁴from agriculture to artificial intelligence⁴to tackle real-world challenges and create meaningful impact in our communities.

Student Multidisciplinary Team Innovation thrives at the intersection of diverse expertise. Our research initiative brings together students from across campus, creating a rich ecosystem where agricultural insights meet engineering precision, business acumen fuels technological advancement, and scientific rigor drives creative solutions. Agriculture 7 students bringing expertise in sustainable farming, crop science, and agricultural technology Computer Science & Engineering 3 CSE students developing innovative software solutions and data systems AI & Robotics 2 students pioneering intelligent automation and machine learning applications Mechanical Engineering 3 students designing and optimizing mechanical systems and hardware Electronics & Communication 2 EC students creating connected systems and communication networks Pharmacy 2 students exploring applications in healthcare and agricultural sciences Business 2 students developing strategies for commercialization and market impact Biotechnology 2 students applying biological innovation to solve complex challenges

Students successes we have reached final state for the projects AI genesis A project focused on developing innovative techniques for successfully growing saffron in lowland regions, emphasizing methods that are environmentally friendly and sustainable. Sustainable saffron farming techniques Lowland soil adaptation strategies Water management practices for saffron Organic cultivation practices ideal-one health regional hackathon A project aimed at promoting and implementing sustainable farming methods in lowlands for saffron saffron cultivation in lowlands Sustainable pest management solutions Soil conservation techniques industrial scale production of saffron.



Adamas Knowledge City, Barasat - Barrackpore Road,
Jagannathpur, Kolkata, West Bengal 700126